“DESIGN AND SYNTHESIS OF NOVEL HYDROGELS FOR DRUG DELIVERY AND TISSUE ENGINEERING APPLICATIONS”

A THESIS SUBMITTED TO

SAVITRIBAI PHULE PUNE UNIVERSITY

FOR AWARD OF DEGREE OF

DOCTOR OF PHILOSOPHY (Ph.D.)

IN

CHEMICAL ENGINEERING

SUBMITTED BY

ANUMON V. D.

UNDER THE GUIDANCE OF

Dr. MANOHAR V. BADIGER

POLYMER SCIENCE & ENGINEERING DIVISION

CSIR – NATIONAL CHEMICAL LABORATORY

PUNE – 411008, INDIA

JUNE 2016

CERTIFICATE

CERTIFIED that the work incorporated in the thesis entitled "**Design and Synthesis of Novel Hydrogels for Drug Delivery and Tissue Engineering Applications**" Submitted by **Mr. Anumon V. D.** was carried out by the candidate under my supervision/guidance. Such material has been obtained from other sources has been duly acknowledged in the thesis.

Date :

Place : Pune

Dr. Manohar V. Badiger
(Research Guide)
CSIR-NCL, Pune

DECLARATION

I declare that the thesis entitled "**Design and synthesis of Novel Hydrogels for Drug Delivery and Tissue Engineering Applications**" submitted by me for the degree of Doctor of Philosophy is the record of work carried out by me during the period from **02-08-2011** to **20-05-2016** under the guidance of **Dr Manohar V. Badiger** and has not formed the basis for the award of any degree, diploma, associateship, fellowship, titles in this or any other University or other institution of Higher learning.

I further declare that the material obtained from other sources has been duly acknowledged in the thesis.

Date :

Place : Pune

Anumon V. D.

(Research Student)

CSIR-NCL, Pune

Acknowledgement

Completing my PhD degree is probably the most challenging activity of my life. The best and worst moments of my doctoral journey have been shared with many people. It has been a great privilege to spend a few years in the Polymer Science and Engineering Division of the CSIR-National Chemical Laboratory and its members will always remain dear to me.

My first debt of gratitude must go to my advisor, ***Dr. Manohar V. Badiger.*** *He patiently provided the vision, encouragement and advice necessary for me to proceed through the doctoral program and complete my dissertation. His mentorship was paramount in providing a well-rounded experience consistent with my long-term career goals. He encouraged me not only to grow as an experimentalist and a chemist but also as an instructor and an independent thinker.*

I wish to thank the ***Director****, CSIR- NCL for providing me all the required facilities to work in NCL.*

I also owe my gratitude to ***Dr. Prakash P. Wadgaonkar, Dr Rajmohanan, Dr Ashish K. Lele, Dr B.L.V Prasad, Dr Sreekumar, Dr Ashok Giri*** *who have inspired me in my research with stimulating discussions and conversations.*

Special thanks to my Ph.D. committee ***Dr. Prakash P. Wadgaonkar, Dr. Vaishali S. Shinde, Dr. Rajan****,* ***Dr. Shubangi Nair, Dr. Ravi kumar, Dr M. Jayakanan*** *for their support, guidance and helpful suggestions.*

I would like to thank ***Dr Mohan G. Kulkarni*** *not only as former 'Head' of the Polymer Science and Engineering Division but also for allowing me to be a part of his group activities and promoted a stimulating and welcoming academic and social environment.*

Additionally, I am very grateful for the friendship of the entire members of his research group, ***Dr. Santhosh, Dr. Prerna, Dr. Ramesh, Dr. Ujjwal, Dr. Hemant, Dr. Jiten, Dr. Sachin, Dr. Satish, Dr. Sameera, Neelam, Arpita, Muntazim, Vrushali, Pavan*** *with whom I worked closely and puzzled over many of the same problems.*

In addition, I would like to thank my colleagues ***Dr. Shubhangi, Dr. Aarti, Dr. Vivek, Dr. Nivika, Suresha, Manjusha, Rajeshwari, Ashwini, Neha, Yogesh, Sanoop.***

A special thanks to ***Dr Vilas, Arun Torris, Lal B Azad, Sachin S. Surwase, Priyanka, Sarath Kanadambat, Leena, Prajitha, Maya, Anuja*** *for carrying out few experimental studies relating to my thesis work in their labs.*

I also wish to thank to ***Dr. Neelima, Dr. Anuya Nisal, Dr. Suresh Bhatt, Dr. Avadhani, Dr. Nilakshi, Dr. GVN Rathna, Naresh, Bhagyashree, Nidhi****,* ***Amarnath****,* ***Pratiksh, Lokanadhan.***

I also wish to thank the Student Academic Office staff, ***Mrs Puranik, Mrs Kolhe, Mr Pavithran, and Mr Iyer*** *for their extended help.*

Special gratitude to ***Dr. Jijo, Reji, Reny, Rahul, Jijil, Dr. Beena, Dr. Rajesh, Dr. Bindu, Dr. Sreekuttan, Dr. Bihag, Priya Sarate, Dr. Yojana, Ketan, Spinvin, Giju Skaria, Anusha, Sandeep*** *for making my life in NCL more wonderful and homely.*

I would like to thank ***Dr Hari Krishna, Dr Shijo, Dr Eldho, Dr Suresh, , Reji, Dr. Vijaydas, Dr. Roshna, Dr. Hari, Dr. Anu, Dr. Priya, Hilda, Remya, Anjali, Dr. Unnikrishnan, Anjali Krishnankutty, Athira, Dr. Nishamol, Dr. Nishakumari, Dr. Jaya, Gino, Pranav, Rejith, Vidyanand, Shibin, Munaver, Rashid, Renjish, Sarath, Shabeeb, Abdul Kayum, Tony, Vipin, Alson, Anish, Jithesh, Dr. Govind, Vyshak, Sunil, Minu.***

My special regards and heartfelt thanks to my childhood friend ***Sunil Paul*** *for all his extended help and support without whom this journey would be meaningless.*

I would like to thank administrative and technical staff members ***Mr. U.V. Dhavale****,* ***Mr. Mahajan****,* ***Mr. Bharati*** *who have been kind enough to advise and help in their respective roles.*

I am also grateful to some people from early days of my college; ***Dr. Unnikrishnan, Dr. Sabu Thomas, Dr. K.E. George, Dr. Sunil K. Narayanankutty, Dr. Roy Joseph, Dr. P. Ramesh*** *and all my* ***teachers*** *were among those who kept me going at the beginning.*

I wish to thank the wonderful lady in the academic section in the Pune University office, ***Mrs Chavan****, who with an ever smiling face answered all my queries whenever I went to her.*

I acknowledge the ***CSIR-SRF, UGC-RGNF*** *for providing fellowships to pursue doctoral studies and* ***DBT*** *for providing travel to Japan for the International conference.*

And last, but definitely not the least, ***my family****. As you know, work is not my (entire) life. I really like working, but you are far more important to me.*

I thank my parents, ***Father*** *and* ***Mother****, for their faith in me and allowing me to be as ambitious as I wanted. It was under their watchful eye that I gained so much drive and an ability to tackle challenges head on. My mother, a strong and a gentle soul who taught me to trust in God, believe in hard work and that so much could be done with little. She has always been my role model, and she is probably the strongest and most resilient person I know for countless words of wisdom over the years. She is sadly missed, and I wish that she could have seen me finish this degree.*

*I would like to thank **Divya** and **Arun Kumar** (my sister and brother) and entire family just for being there for me, no matter what. I hope that this work makes you proud.....*

*Last but not the least my deepest heartfelt gratitude to my lovely wife **Deepasree** for her faith in me and my beloved daughter **Rishima** for being such a wonderful girl and always cheering me up. Without their continuous support and tireless efforts this journey would never have been so successful.*

Anumon

TABLE OF CONTENTS

Abstract

Design and Synthesis of Novel Hydrogels for Drug Delivery and Tissue Engineering Applications

The aim of this thesis was to design and synthesize novel polyurethane hydrogels for drug delivery and tissue engineering applications. Hydrogels are becoming increasingly important materials in these areas due to their soft 3-Dimensional structure and compatibility to the cell matrix. Hydrogels are basically 3-D network of hydrophilic polymers which are capable of absorbing copious amount of water without loosing their structural integrity. Hydrogels have wide range of applications such as, scaffolds/implants in tissue engineering, vehicles for drug delivery, synthetic extra cellular matrix, sensors, actuators, enzyme immobilization, stimuli-responsive materials etc. However, many of the hydrogels used/or proposed in tissue engineering and drug delivery applications exhibit weak mechanical strength and are unsuitable to sustain dynamic environment. Therefore, there is a great scope for designing and developing novel hydrogel system with improved mechanical properties coupled with good biological properties (e.g. biocompatibility, biodegradability) and controlled pore structure.

In this context, the work was undertaken to design and synthesize novel polyurethane (PEG-PU) based hydrogels by solvent free, one-pot method. PEG-PU hydrogels were prepared using PEG-4000 as a soft segment, H_{12}MDI as a hard segment and Hexanetriol (HT) as a crosslinker. The reaction was catalysed by Dibutyl tin dilaurate (DBTDL). PEG-PU hydrogels with different crosslink densities were obtained using different contents of HT. The hydrogels could be prepared into any intricate shapes and sizes depending on the shapes and sizes of the moulds. Different types of hydrophilic/hydrophobic diols such as Polycaprolactone diol (PCL), Polycarbonate diol (PCD), Tetraol (FTL) were used in combination with PEG to obtain PU hydrogels with tunable properties. Further, with the focus on synthesizing hydrogels for drug delivery and tissue engineering applications, curcumin incorporated PU hydrogels were prepared. Curcumin with reactive –OH groups and having anti-bacterial properties could be easily incorporated into PU hydrogels. The

porous structure in the hydrogel was created by cryogenic treatment followed by lyophilization.

All the synthesized hydrogels were characterized in terms of their structure/microstructure, swelling, mechanical properties (e.g. tensile strength, compressive strength, % elongation etc.), biological properties (cytotoxicity, MTT assay, anti-bacterial etc.) using FTIR, Solid-state NMR, WAXD, SAXS, DMA, UTM, SEM, μ-CT and biological tests.

In PEG-PU hydrogels, the swelling property which is the most important parameter for drug delivery and tissue engineering applications could be controlled by the amount of HT in the hydrogel. In the case of PU hydrogels with different diols, apart from the HT content, the hydrophobicity of the diol dictated the degree of swelling. In curcumin incorporated hydrogels, curcumin was found to exist in both chemically linked and physically entrapped form in the hydrogel structure. The degree of swelling could be controlled by the amount of curcumin in the hydrogel. The WAXD and SAXS studies revealed the crystalline lamellar structure of the gel originated from the soft segments of the diols. The porous structure of all the hydrogels was evidenced by SEM and μ-CT results. The pore sizes were in the range of 2-20μm with the interconnectivity of the pores. All the hydrogels showed good mechanical strength at moderate swelling. Interestingly, when curcumin was incorporated into hydrogels, the compressive strength of the hydrogel increased significantly. The compressive strengths at break were in the range of 1.5-4.5 MPa with nearly 90% compression. This remarkable increase in compressive strength was explained on the basis of heterogeneity in the hydrogel structure and easy dissipation of energy under deformation. Finally, the cytotoxicity studies of the hydrogels showed the continuous growth of the cells, indicating the non-toxic nature of the hydrogels. The in vitro drug release study with an anti-cancer drug doxorubicin hydrochloride from the hydrogels containing different diols was performed and the release rates were correlated with the hydrophobicity/swelling of gels. All the obtained hydrogels with the detailed characterization show great promise in controlled drug delivery and tissue engineering applications.

LIST OF SCHEMES

LIST OF TABLES

LIST OF FIGURES

ABBREVATIONS AND SYMBOLS

A-549	Adenocarcinomic human alveolar basal epithelial cells
CUR	Curcumin
DBTDL	Dibutyltin dilaurate
Dox.HCl	Doxorubicin hydrochloride
DMEM	Dulbecco's modified eagle medium
DMA	Dynamic mechanical analyser
DMSO	Dimethyl sulfoxide
DN	Double network
DPBS	Dulbecco's phosphate buffer solution
DRS	Diffuse reflectance spectroscopy
DSC	Differential scanning calorimetry
ECM	Extracellular matrix
FBS	Fetel bovine serum
FTIR	Fourier transform infra red spectroscopy
FTL	Tetraol
E′	Storage modulus
HA	Hyaluronic acid
HASE	Hydrophobically alkali swellable emusion
HDI	Hexamethylene diisocyanate
HEUR	Hydrophobically modified ethoxylated urethane
H_{12}MDI	4,4' methylenebis (cyclohexyl isocyanate)
HR-MS	High resolution Mass spectroscopy
HT	Hexanetriol
LCST	Lower critical solution temperature
LDI	Lysine diisocyanate
MCF-7	Breast cancer cell line
Micro-CT	Microcomputed Tomography
MPa	MegaPascal
MTT	3-(4,5-Dimethylthiazol-2-yl)-2,5-Diphenyltetrazolium Bromide

NC	Nanocomposite
NMR	Nuclear Magnetic Resonance
OD	Oxygen demand
PCD	Poly hexamethylene carbonate diol
PEG	Polyethylene glycol
PEO	Poly ethylene oxide
PEU	Polyethylene urethane
PGA	Poly glycolic acid
PHEMA	Poly (2, hydroxyl ethyl methyacrylate)
PLGA	Poly lactic glycolic acid
PLDLA	Poly lactic-d-lactic acid
PLLA	Poly L, lactic acid
PMMA	Poly methyl metacrylate
POSS	Polyhedral oligosil sesquioxanes
PPG	Polypropylene glycol
PPO	Polypropylene oxide
PU	Polyurethane
PU-CUR	Curcumin incorporated Polyurethane
PU-FTL	Tetraol incorporated Polyurethane
PU-PCD	Polycarbonate diol incorporated Polyurethane
PU-PCL	Polycaprolactone diol incorporated Polyurethane
SAP	Super absorbent polymers
SAXS	Small-angle X-ray scattering
SEM	Scanning electron microscopy
THF	Tetrahydrofuran
T_g	Glass Transition Temperature
WAXD	Wide-angle X-ray diffraction

Introduction

Chapter – I

In the first chapter, a detailed literature survey was done on hydrogels in terms of their classification, synthesis, properties, advantages and disadvantages and applications for drug delivery and tissue engineering. Literature survey on the state-of-the-art of polyurethane (PU) hydrogels is given. The characterization techniques such as WAXD, SAXS, UTM, μ-CT, biological tests etc., used for studying the micro-structural, surface morphology, mechanical behaviour and cytotoxicity of the hydrogels were briefly explained.

1.1 Introduction

Polymeric hydrogels are becoming increasingly important in recent years due to their special physico-chemical properties, such as softness, bio-compatibility, stimuli-responsiveness, water permeability, self-healing etc.[1-9] Therefore, they find wide applications as scaffolds/implants in tissue engineering,[10-14] vehicles for drug delivery,[15-16] synthetic extra cellular matrix,[17] sensors,[18] actuators,[19] enzyme immobilization,[20] robotics[21] etc. The existence of hydrogels dates back to 1960, when Wichterle and Lim first proposed the use of a synthetic hydrogel, Poly (2-hydroxy ethyl methacrylate) (PHEMA) for contact lens application.[22] Since then the use of hydrogels has been rigorously extended to various biomedical, controlled release, pharmaceutical applications.[15, 23-24]

Hydrogels are basically three-dimensional (3D) hydrophilic polymeric networks with physical or chemical crosslinks and are capable of absorbing large quantities of water or biological fluids. The amount of water in the fully swollen state (or equilibrium swelling) is a balance between thermodynamic force of mixing and elastic retractive force of 3D polymeric network. The mixing force mainly arises from the hydrophilic nature of the polymer backbone which is characterized by the interaction between the polymer and the solvent. Whereas, the retractive force strongly depends on the interconnectivity (degree of crosslinking) of the network structure. Consequently, there is a wide scope in designing hydrogels with different swelling capacities by modulating the contribution of these individual forces.

1.1.1 Classification of hydrogels

Hydrogels can be classified based on their sources: natural or synthetic; on the nature of crosslinking: covalently crosslinked or physically crosslinked; on the type of network: homo polymer networks, co-polymeric networks, interpenetrating networks; on the effect of micro-organism: degradable and non-degradable; on functional groups: ionic and non-ionic hydrogels.

A wide variety of synthetic and naturally obtained materials have been used to form hydrogels for drug delivery and tissue engineering applications. The most commonly used synthetic polymers include poly (ethylene oxide) [PEO], poly (vinyl alcohol) [PVA], poly (acrylic acid) [PAA], copolymers of PEO and PPO [Pluronics],

and some of the poly peptides. Whereas, naturally derived polymers include agarose, alginates, chitosan, collagen, fibrin, gelatin and hyaluronic acid.

1.1.2 Hydrogel synthesis

In general, hydrogels are prepared by polymerising hydrophilic monomers, in the presence of a crosslinker and an initiator. In order to control the heat of polymerization and the final hydrogel properties, some diluents such as water and other aqueous solutions are invariably used. Subsequently, the isolation of pure hydrogel involves treating of formed hydrogel with water to remove unreacted monomers, crosslinker, initiator and some unwanted by-products. One can modulate the properties of hydrogels by varying the reaction conditions and using different types of monomers, crosslinkers, initiators, crosslinker-to-monomer ratios, and the monomer concentration.

Synthetic hydrogels are generally prepared via bulk, solution and inverse suspension polymerization technique. The bulk and solution polymerizations are done in a homogeneous medium in which the monomer (s), initiators and crosslinkers (s) are easily soluble in water. Using these techniques the hydrogels can be prepared in any shape and size depending on the mould in which the polymerization takes place. Further, the solution polymerization is more preferred due to better control of the heat of polymerization. Hydrogels can also be prepared in micron sizes (called as microgels) by inverse suspension polymerization technique based on the dispersed and continuous phase. The monomer is usually dissolved in the dispersed phase, and a surfactant is dissolved in a continuous phase. The surfactant enables uniform dispersion of the monomer and other reactants in the continuous phase. Inverse suspension polymerization is more suitable for highly hydrophilic monomers, such as salts of acrylic and methacrylic acids, as well as acrylamide.

1.1.3 Chemically and physically cross-linked hydrogels

Covalent bond formation and reversible non-covalent interactions (physical interactions) constitute two important approaches to form three-dimensional networks in polymer gels. Accordingly, the polymer gels obtained can be defined as chemical gels or physical gels respectively.[10-11] The chemical gels can undergo volume-phase transitions in response to external stimuli such as**,** temperature, pH, solvent –

nonsolvent etc.[25] Whereas physical gels can exhibit reversible sol-gel transitions in response to external stimuli. Traditionally, the covalently crosslinked hydrogels are prepared by crosslinking co-polymerization, crosslinking of polymer precursors (post-crosslinking) and crosslinking via polymer-polymer interactions through functional groups. These approaches with undesirable side reactions may yield hydrogels with some defects. Further, if the monomer is hydrophilic and the crosslinking agent is hydrophobic, then the aqueous polymerization can give rise to hydrogels with random distributions of crosslinks in the network structure. Variety of monomers and crosslinking agents have been used for the synthesis of hydrogels with a wide range of chemical compositions. A few examples of typical monomers and crosslinking agents are listed in **Table 1.1.**

Table 1.1 *Examples of Monomers and crosslinking agents for the synthesis of hydrogels*

Monomers	
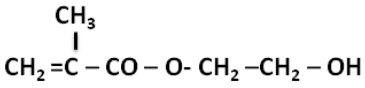	2-Hydroxyethyl methacrylate
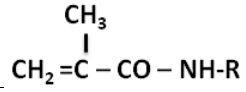	*N*-alkylmethacrylamides
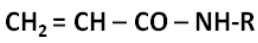	*N*-alkylacrylamides
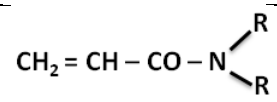	*N*,*N*-dialkylacrylamides
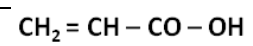	Acrylic acid
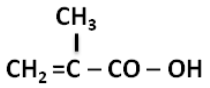	Methacrylic acid
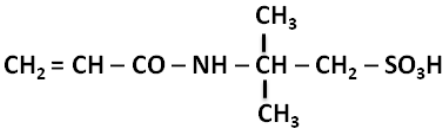	2-Acrylamido-2-methyl propane sulfonic acid
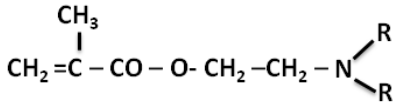	*N*,*N*-dialkylaminoethyl methacrylate
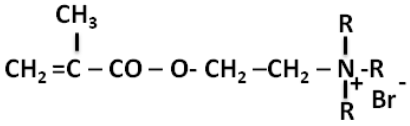	Methacryloyloxy ethyl tri alkyl ammonium bromide
Crosslinking Agents	
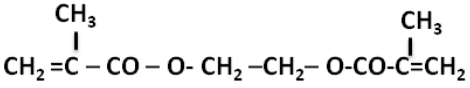	Ethylene dimethacrylate
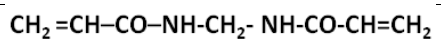	Methylenebisacrylamide

In physically crosslinked hydrogels, the network structure is formed by physical (non-covalent) interactions such as columbic, van-der waals, dipole-dipole, hydrogen bonding, and hydrophobic interactions etc. Hydrophobic interaction in some of the hydrophobically modified water-soluble polymers can self-assemble into hydrogels and exhibit reversible sol-gel transitions.[26-29] Some of the examples of hydrophobically associating polymers include hydrophobically modified alkali-swellable emulsions (HASE), hydrophobically modified polyacrylamides[30-32] and hydrophobically modified ethoxylated urethane (HEUR).[33-42] Thermo-reversible polymers (based on LCST polymers) exhibiting interesting reversible sol-gel transition in response to temperature are also becoming extremely important as smart injectable in controlled release technology.[43] The sol-gel transition in thermo-reversible polymers occur due to reversible hydrophobic associations trigged by small changes in temperature.

1.1.4 Drawbacks of conventional hydrogels and new structural attributes

Although there are large number of application of hydrogels in tissue engineering and controlled drug delivery, they suffer from certain drawbacks such as poor mechanical strengths, non-porous nature, limited self-healing property etc. Therefore, major research efforts are being made in designing and developing novel molecular architectures in hydrogels which include nano-composite gels,[44-47] double-network hydrogels,[48-51] slide-ring gels,[52-53] topological gels,[54] and self-healing[8-9] hydrogels.

Haraguchi and co-workers[44] have reported on the novel nanocomposite hydrogels based on NIPAm monomer with clay, hectorite as a multifunctional crosslinking agent. The exfoliated clay in the hydrogel matrix exhibited enhanced mechanical strength to the hydrogels. Osada and Gong[48] reported on the double network (DN) hydrogels which contain two independently crosslinked networks, the first one consisting of highly crosslinked and the second one with slightly crosslinked structure. These hydrogels were found to exhibit excellent mechanical strength when the molar ratio of second network to the first network is higher than 10 or more. The enhanced mechanical properties of these DN hydrogels is believed to happen due to the dissipation of energy by the loosely crosslinked networks. This phenomenon was demonstrated for DN hydrogels consisting of highly crosslinked poly (2-acrylamido-

2-methyl propane sulfonic acid) and the lightly crosslinked polyacrylamide. Now efforts are being made to develop other DN hydrogels based on cellulose.[55]

A new topological networks consisting of novel sliding ring crosslinking mode was reported by Okumura and Ito.[52, 54, 56] In these systems, the linear polymers such as PEGs were pierced through cyclodextrin molecules and end capped with bulky groups like adamantine to prevent the slipping away from the cyclodextrins. Then the cyclodextrins were connected together to obtain mobile crosslinks with a figure of eight (8). These sliding ring gels exhibited a "pulley effect" where the sliding motions tend to equalize the stresses in the network structure co-operatively resulting into enhanced mechanical properties.

An excellent review on novel molecular architectures for hydrogels with improved mechanical strengths and toughness are reported in the literature by Mark and co-workers and Peak etal.[57-58] Recently, conducting hydrogels are also becoming more and more important in neural networks,[59] electrochemical biosensors,[60] electro stimulated drug release.[61] Electrical conductivity can be induced in hydrogels by incorporating various conducting materials such as conducting polymers (eg: polyaniline, polypyrrole, polythiophene), carbon, metal nanoparticles etc., into the hydrogel matrix.

1.1.5 Hydrogels for controlled release applications

Hydrogels are very upcoming classes of materials in controlled release of drugs. Particularly, swelling-controlled and stimuli-responsive hydrogels are becoming extremely important in controlled drug delivery. In general, hydrogels in drug delivery are divided into 'matrix' and 'reservoir' types. Hydrogels can be made into various shapes and sizes and the design of hydrogel dosage forms depends on the routes of administration of drug which include: per - oral route – spherical, cylindrical, discs; implants route – disc shape, drum shaped; rectal route – tubes, rods; vaginal – cylindrical etc.

The release of drug from hydrogel involves simultaneous absorption of water/body fluids and release of drug via a swelling controlled mechanism. The most common release mechanism is diffusion. The diffusion of the drug can occur through a reservoir in which the drug core is surrounded by a polymer film or the drug can be

released from the matrix where in the drug is uniformly distributed in the hydrogel matrix. The matrix system tend to follow a Higuchi's model where in the drug release is proportional to square root of time 't' ($t^{1/2}$). This may not give uniform release rates. On the other hand the reservoir system can give near-constant release rates. The most important parameters of hydrogels for controlled drug delivery applications include degree of crosslinking and mechanical strength, network pore size, drug distribution in the hydrogel, and diffusion of drug.

Hydrogels can exhibit dramatic changes in their swelling in response to various stimuli such as, pH, temperature, electric field, magnetic field, ultrasonic radiation, glucose, urea etc. These hydrogels have been termed as "stimuli-responsive" or "smart hydrogels" or "Intelligent gels". Some of the examples of hydrogels with the stimuli and the drug for the applications in controlled drug delivery are given in **Table 1.2.**

Table 1.2 *Examples of stimuli-responsive hydrogels in drug delivery*

Hydrogels	**Stimuli**	**Drug**	**Ref**
PHEMA	pH	Salicylic acid	62
Chitosan – PEO	pH	Amoxicillin, Metronidazole	63
Gelatin - PEO	pH	Riboflavin	64
Poly (N-isopropyl acrylamide) [PNIPAM]	Temperature	Heparin	65
PNIPAM-co-butyl methacrylate-co-AA	pH & Temperature	Calcitonin	66
Ethylene-co-vinyl acetate [EVAc]	Magnetic field	Insulin	67
EVAc	Glucose	Insulin	68
PHEMA	Electric field	Proprandol hydrocloride	69
EVAc	Ultrasonic radiation	Insulin	70-71

Drugs can also be covalently conjugated to the hydrogel matrix and the release of the drug can be effected by the rate of chemical or enzymatic cleavage of the polymer-drug bond. For example, dexamethasone was conjugated to a photo reactive PEG by a degradable lactide bond.[72]

1.1.6 Hydrogels for Tissue Engineering

Tissue Engineering has become an important field to treat patients who suffer from the loss or failure of an organ due to accident or diseases. In general, tissue or organ transplantations are a common approach/therapy to replace damaged tissues or organs. However, because of the lack of donors, this approach has encountered/ severe limitations. In this context, hydrogels have emerged as promising materials in tissue engineering where they are used as scaffolds/implants to mimic many roles of extracellular matrices and to generate new tissues. However, there is a significant challenge in the design and manufacture of hydrogel scaffold that has good mechanical strength and possess both highly porous structure and the ability to control the release kinetics of growth factors during the tissue regeneration. Hydrogel scaffolds/implants for tissue engineering require the following characteristics:

- Should be non-toxic and biocompatible
- Should mimic the extra cellular matrix (ECM)
- Should have good mechanical strength
- Should have a porous structure with interconnected pores
- Should support cell adhesion and proliferation, facilitating cell-cell contact and cell migration
- Preferably biodegradable and bioadsorbable at pre-determined time-period, and the space initially occupied by the scaffold should be replaced by growth tissue.

The average pore size of the hydrogel greatly affects the growth and penetration of the cells in the 3-D structure of the hydrogel. There are various techniques used for creating porous structure in the polymer scaffolds/implants. These include, solvent casting,[73-74] particle leaching,[75-76] freeze-drying,[77-78] gas foaming,[79] by using porogens,[80] electrospinning[81] etc. The optimum pore sizes of scaffolds in tissue engineering have been shown to be 5 µm for neovascularisation, 20-125 µm for regeneration of adult mammalian skin, and 100-350 µm for regeneration of bone. Besides these, the micro-architecture of the scaffold also plays an important role in tissue regeneration.[82-83]

A wide variety of synthetic and natural polymers have been used to form hydrogels for tissue engineering scaffolds/implants. Synthetic polymers include aliphatic polyesters,[84-85] poly anhydrides,[86-87] poly orthoesters,[88] polyethylene oxide (PEO),[89-93] polyvinyl alcohol (PVA),[94-95] poly acrylic acid,[96-97] polypeptides.[98-100] The naturally derived polymers include chitosan,[101-102] collagen,[103-104] agarose,[105-106] alginates,[107-108] fibrin,[109] gelatin[110-111] and hyaluronic acid[112-113] etc. All these materials are generally used in the form of foams, sponges and films.

Hydrogels have been used for tissue engineering of cartilage,[114] bone,[115] neural tissue,[116] vocal matrix,[117] ligaments,[118] heart valves,[119] skeletal muscles,[120] hair follicles,[121] trachea,[122] lungs[123] etc. Scaffolds based on terpolymer of gelatin-co-chitosan-co-hyaluronic acid have been reported to mimic natural cartilage.[124] Combination of HA with alginate and poly-L-lysine have been used to develop scaffolds for variety of tissue engineering applications.[125] Hydrogels have also been used to culture fibroblast,[126] pre-adipocytes,[127] bone-marrow stromal cells,[128] pancreatic islet cell,[129] human umbilical vein endothelial cells,[130] hepatocytes,[131] osteoblasts[132] etc. Some of the polymers used commercially for making scaffolds are mentioned in the **Table 1.3** below:

Table 1.3 *Examples of commercial polymers used for making scaffolds in tissue engineering applications.*

Polymer	Application	Commercial name
PGA	Biodegradable synthetic suture	Dexor
PLGA	Skin graft	Vicryl Mesh
PLDLA	Bioresorbable Implant	Resomer
PLGA-Collagen	Tissue regeneration membrane	Cytoplast Resorb
PEU	Tissue engineering	Degrapol
Collagen	Bioengineered skin equivalent	Transcyte
HA	Bone graft	OSSIGEL
Polyanhydride	Chemo-therapeutic application	Gliadel

1.1.7 Polyurethanes for biomedical applications

Recent years have witnessed a great interest in polyurethane based hydrogels because of their excellent biocompatibility, chemical versatility and superior mechanical properties.[133-135] Besides other applications in adhesives, coatings,

synthetic leather etc. PUs have been extensively investigated for biomedical applications including cardiovascular devices such as vascular prostheses, intra-aortic balloons, cardiac valves, membranes for dialysis, craniofacial reconstruction, breast implants etc.[136-141] Biodegradable PUs having degradable poly-ε-caprolatone segments are used as implants in tissue engineering.[142]

PUs are prepared by the reaction between isocyanate and diols to obtain polymers with urethane linkages (-NH-COO-) in their main chain. The chemical and physical properties of PUs can be tailored to their target applications by selecting different types of diols/polyols (based on PEG, caprolactone etc.) and aliphatic (hexamethylene diisocyanate, cyclohexyldiisocyanate) and aromatic (TDI, MDI, LDI etc.) diisocyanates. When difunctional isocyanates and polyols are used, the resulting polymers are linear PUs. Crosslinked PUs are obtained when tri-(or higher) functional monomers/crosslinker are used. Therefore, the chemical structures of diols/polyols and diisocyantes as well as chain extenders play an important role in determining the properties of PUs.

PU hydrogels obtained from UV-curable urethane prepolymer were synthesized and their properties were evaluated for contact lenses application;[143] Physically crosslinked PU-block-poly (glycerol methacrlyate) hydrogels have been reported for tissue engineering applications;[144] Petrini et al., have reported on the synthesis of porous PU hydrogel by one-step bulk polymerization technique for tissue engineering applications.[145]

Graham and McNeil[146-148] have reported on the prolonged delivery of prostaglandin E_2, caffeine and melatonin from PU hydrogels. Biomedical applications of PUs have been reported by Zdrahala and Zdrahala.[149] Transparent PU hydrogels were obtained by using the combinations of PEG and PPG diols.[150] A review article has been published which summarizes on the synthesis of biodegradable PUs as scaffolds for regenerative medicine.[151] These biomaterials are designed to undergo controlled degradation in-vivo and promote in growth of new tissue. Thermo-responsive polyurethane hydrogels based on PEG and polycaprolactone for biomedical application have been reported recently.[152] Son et al., have published a review in which they have described the preparation of polyurethane with their merits and demerits as scaffolds in tissue engineering applications.[153]

1.1.8 Characterization techniques used in this work

1.1.8.1 Wide-Angle X-ray Diffraction (WAXD)

X-ray diffraction is a non-destructive analytical technique used extensively in solid-state chemistry and material science. Particularly, in the crystalline materials the diffraction depends on the crystal structure and the wavelength. Since the wavelength of X-ray is comparable to the size of atoms, the intensities of the diffracted X-ray can be used to probe the structural arrangement of atoms and molecules in a wide variety of materials.

Bragg's law in X-ray diffraction relates the wavelength of X-rays (λ), to the angle of incidence (θ) and the interatomic distance (d) with the following equation.

$$n\lambda = 2d \sin \theta \qquad (1)$$

Where, 'λ' is the wave length of the X-rays, 'd' is *d*-spacing between atomic planes (interplanar distances) in the crystal, 'n' is an integral denoting the order of diffraction peaks.

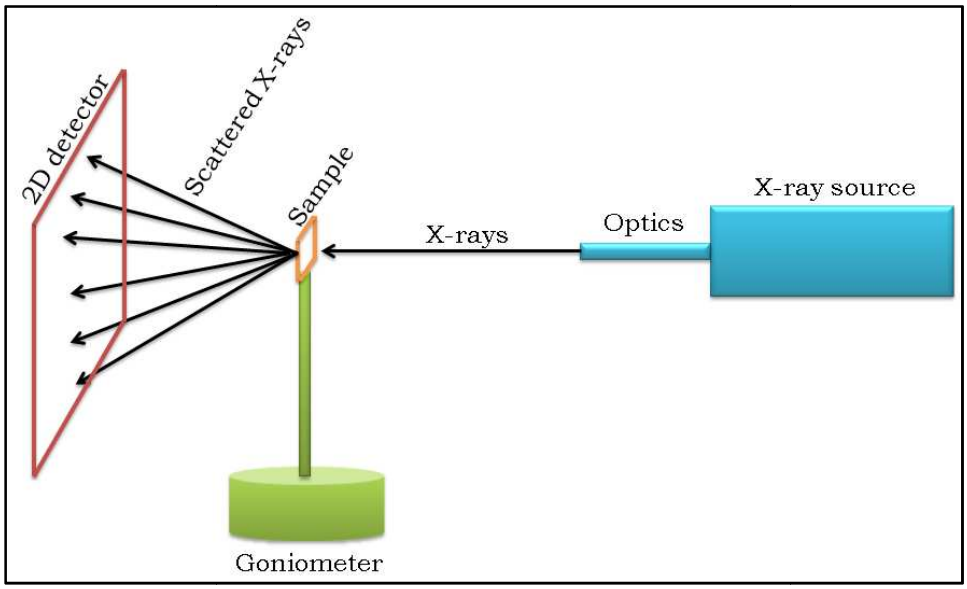

Figure 1.1: *Schematic of WAXD instrument*
[Redrawn and modified according to (© Rice University, Houston)]

X-rays are produced by collision of high speed electrons with a metal target and have the wavelength in the range of 0.5-2.5 Å. An X-ray diffractometer contains three main components namely, (i) X-ray tube generator, (ii) sample holder and (iii) detector. X-ray tube has an evacuated tube containing a cathode and an anode (target).

A high voltage is applied across the electrodes for accelerating the emitted electrons to the target. X-rays preliminary interact with electrons in atoms and an XRD spectrum is obtained by measuring the diffracted intensity as a function of diffracted angles, 2θ (angle between incident and diffracted beams) and orientation of the specimen. The peaks in X-ray diffraction pattern are directly related to the atomic distance by Bragg's law. In our study, we have used XRD to investigate the microstructure of PU based xerogels.[154]

1.1.8.2 Small-Angle X-ray Scattering (SAXS)

SAXS is an analytical method to determine microscale and nanoscale structure of particle systems in solid, liquid and gaseous states. Unlike the WAXD ($10\text{-}90^0$) the SAXS offers scanning at an angle between $0\text{-}10^0$. SAXS has been extensively used in studying the particle size and morphology of semi-crystalline polymers, microphase separation in block copolymers, polymer blends etc. This technique is also used in understanding the microstructures in metals, cement, oils, proteins, foods and pharmaceuticals.

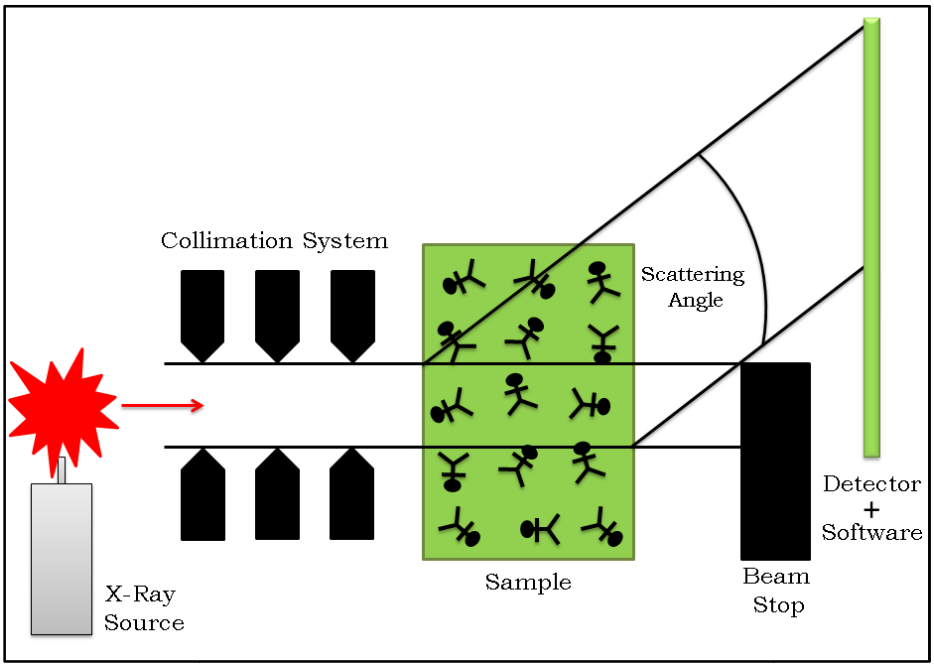

Figure 1.2: *Schematic of SAXS instrument*
[Redrawn and modified according to (© Anton Paar GmbH, Austria)]

When a monochromatic beam of X-rays hit the sample, some are absorbed, some are transmitted without any interaction and some are scattered from the sample.

The scattered X-ray form a scattering pattern that is detected by a detector situated behind the sample perpendicular to the primary X-ray beam. The scattering pattern contains the information on the structure of the samples.

The basic components of all SAXS instruments consist of a source, a collimation system, a sample holder, a beam stop and a detection system (Figure 1.2). The collimation system makes the beam narrow and defines the zero-angle position. The beam stop prevents the intensive incident beam hitting the detector, which would otherwise overshadow the relatively weak scattering of the sample and can destroy some of the detectors.[155]

The relation between scattering vector (q) and scattering angle (θ) is given by,

$$q = \frac{4\pi}{\lambda} \sin \frac{\theta}{2} \qquad (2)$$

Where 'λ' is the X-ray wavelength (Cu Kα = 1.5418 Å). The average distance'd' between domains can be estimated by the peak position using a well established equation as follows:

$$d = \frac{2\pi}{q_{max}} \qquad (3)$$

Where, q_{max} is a scattering vector at maximum intensity of the correlation peak.

We have used SAXS technique in our study to demonstrate the presence of lamellar microstructure in PU xerogels.

1.1.8.3 Scanning Electron Microscopy (SEM)

SEM is an electron microscopy technique which produces images of samples upon scanning with beam of high energy electrons. The electrons interact with atoms in the samples and produce signals that contain information about the surface morphology.

The images of the specimen can be captured in high and low vacuum, in dry and wet (in environmental SEM) conditions and at wide range of temperatures. The resolution of the images can be better than 1.0 nm. The magnification of images can be obtained from 10 to 500,000 times. The scanning electron microscope consists of

an electron gun, column in which electrons travel through electromagnetic lenses, sample chamber, detectors, vacuum system and data output device. The schematic of SEM is shown in **Figure 1.3**.

When the electrons hit the sample with high energy, they produce secondary electrons, backscattered electrons and characteristic X-rays. If the sample contains conducting material, its image can be obtained directly. For the non-conducting samples, the surface is coated with metallic film by sputtering. These signals are then collected by detectors to form images on the computer display.

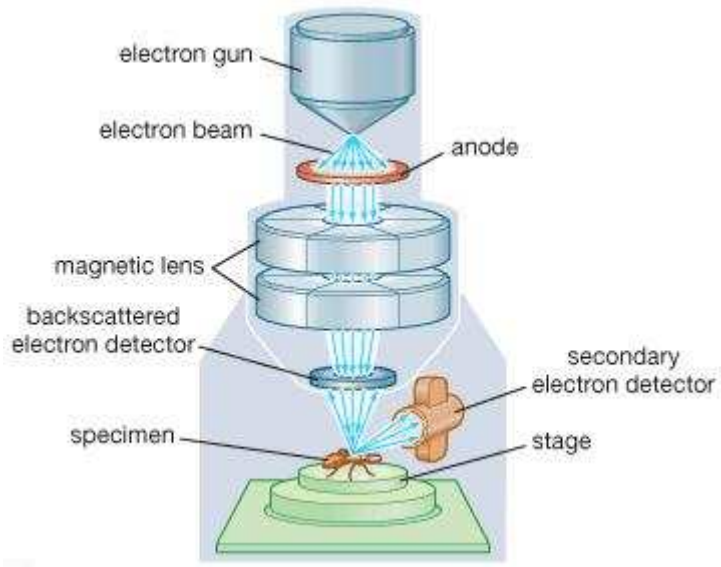

Figure 1.3: *Schematic of a SEM instrument*
(© Encyclopædia Britannica, Inc.)

The SEM is widely used to investigate the microstructure of wide range of materials.[156]

1.1.8.4 Microcomputed Tomography (µ-CT)

Microcomputed Tomography (µ-CT) is a non-invasive, high resolution X-ray scanning technique that allows unique possibilities for precise 3-dimentional imaging and quantification of micro-architectural, morphological, and stereological parameters of materials including ceramics, polymers, metal forms, composites and mineralized tissues.[157] µ-CT combines micro-focal spot X-ray projections rotated through multiple viewing directions to produce 3-D reconstructed images of materials. The tomographic reconstruction can be based on a cone-beam convolution-

back projection algorithm. Combined with 3-D simulations and analyses that are capable of handling the complexity of microstructures in materials, µ-CT has emerged as a powerful tool that provides clear insights into the link between materials processing and properties.

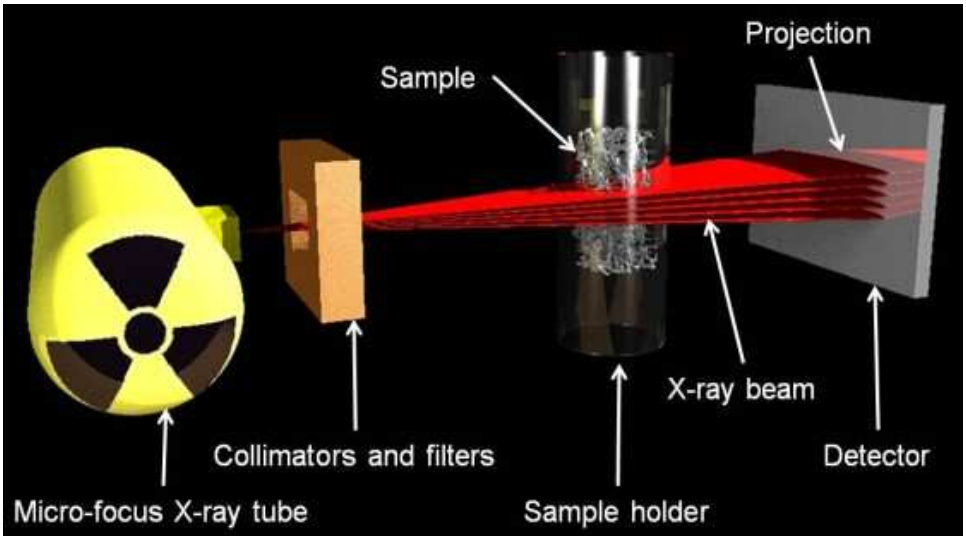

Figure 1.4: *Main components and working principle of a µ-CT scanner.*
(© Queen Mary University of London)

The µ-CT units consists of an X-ray source, a specimen that is to be imaged, an X-ray to – electronic signal – converting imaging array, and a device that either rotates the specimen or rotates the scanner around the stationary specimens **(Figure 1.4)**.

The method of providing high resolution images falls into one of the three approaches: (i) cone-beam (ii) optical magnification and (iii) Bragg's diffraction. µ-CT can be used to investigate micro structural characterization of wide range of materials which includes cellular metallic heterogeneous structure, electronic components, dental materials, polymer scaffolds for tissue engineering and drug delivery, trabecular bone, bio-ceramics etc. In our work, we have used µ-CT technique to investigate the pore structure and flow simulation in PU xerogels.[158]

1.1.8.5 Universal Testing Machine (UTM)

UTM is a device which is used to study the mechanical properties such as tensile, compressive, flexural strength, modulus, strain etc., of a wide range of materials including plastics, elastomers, metals, glass, paper etc. In UTM, a load or

deformation is applied to a standard sample of a specific size and dimension and the natural resistance of the material to this applied load or deformation is accurately sensed by a well calibrated load-cell. The signal from the load cell is appropriately converted to the mechanical parameters with the help of a suitable transducer and a computer.

The UTM consists of transducer, load-cell, sample fixture (grips) and a cross-head for moving (pull or press the sample) the fixture in appropriate direction (**Figure 1.5**). The movement of the cross-head, and hence the fixture, is accurately measured by means of another transducer of LVDT (linear variable differential transducer) type, which gives the strain value accurately.[159]

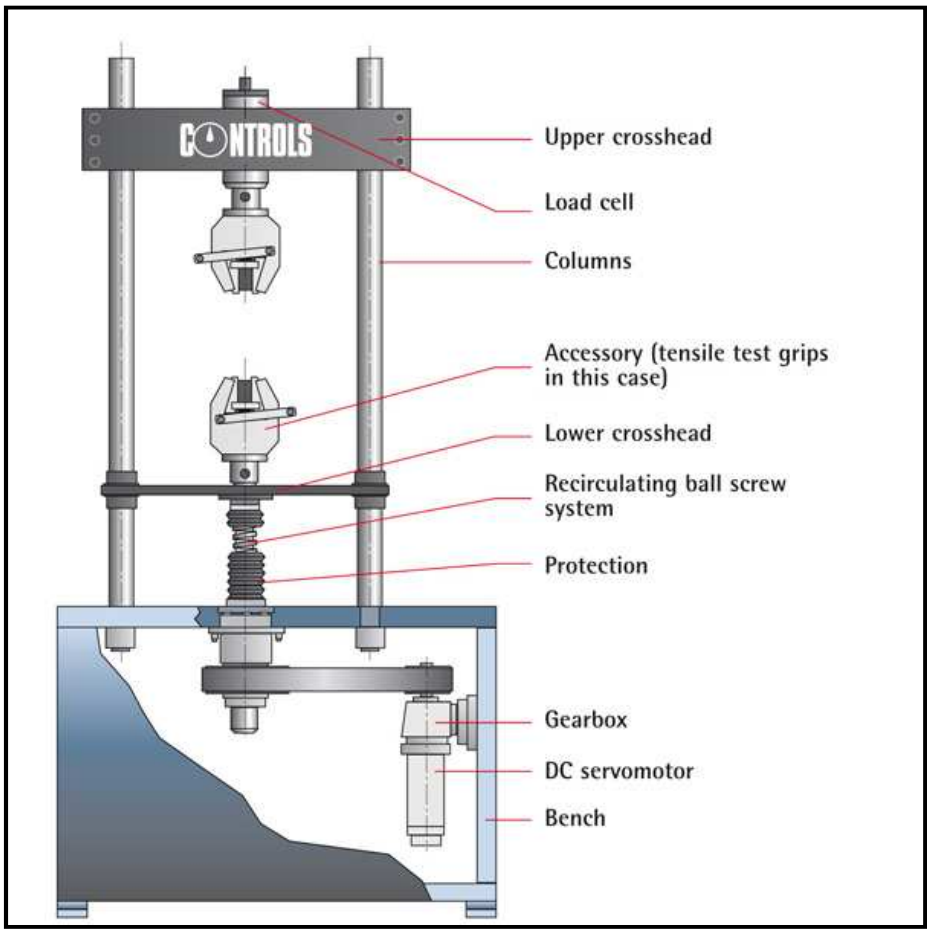

Figure 1.5: *Schematic of UTM*
(© Instron Illinois Tool works Inc)

A typical stress v/s strain curve contains various regimes of mechanical property analysis (**Figure 1.6**). The initial linear region is also called the Hookean region is the elastic regime. Then, beyond yield point, the regime is called the region

of plastic deformation.[160] The slope of this elastic region will give the elastic modulus or generally termed as Young's modulus of the material. At the end of this regime is called the yield point, which demarcates between the region of reversible and non-reversible deformation. Further, the highest value of the stress obtained from a material is called its ultimate strength or tensile strength (if it is a tensile mode of testing).

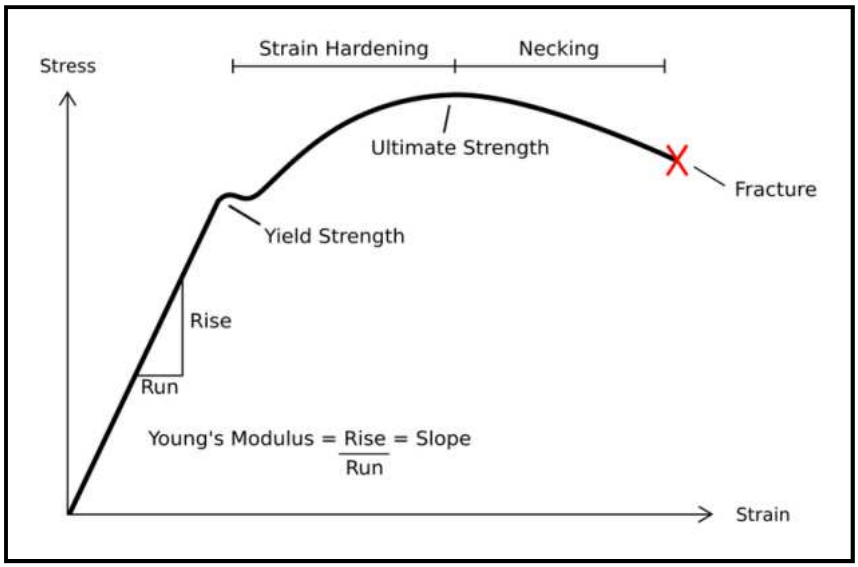

Figure 1.6: *A typical stress v/s strain graph*

We have extensively used UTM in our work to study the mechanical properties of PU hydrogels.

1.1.8.6 MTT Assay

A tetrazolium-based colorimetric assay (MTT - 3-(4,5-dimethylthiazol-2yl)-2,5,diphenyl tetrazolium bromide) is often used to evaluate polymer cytotoxicity, or more precisely the metabolic activity of cells in contact with the material. The MTT assay is simple, reproducible, and denotes cell viability. MTT, when in contact with the live cells, produces a formazan product that has an absorbance maximum at 490 nm. Here the MTT are tested with both control cell line (L929) and cancerous cell lines (A549, MCF7). These cells are incubated at 37±2 ^{0}C in air with 5% $C0_2$ for a minimum of 24hrs. Cytotoxicity was qualitatively evaluated using phase contrast microscope for general morphology, vacuolization, detachment of cells and cell lysis. Sub confluent monolayers of cells were trypsinize. With a multi channel pipette added 100 µL of the cell suspension to each well of the 10 central column of multi well plate

containing 0.5 – 1 x 10^3 cells / well. Growth medium is added and incubated till attaining sub confluency. Medium is removed and the plate is fed with 200 μL of fresh medium and 50 μL of MTT. Wells were incubated from 4 hrs to overnight in humidified atmosphere. Medium and MTT were removed from the wells and the MTT formazan crystals were dissolved by adding 200 μL of DMSO / Propanol. Absorbance at 570nm was recorded immediately, since the product is unstable.[161]

1.2 Summary

This introductory Chapter-I gives a comprehensive review of the literature on hydrogels, classification of hydrogels, synthesis of hydrogels, properties of hydrogels and draw backs of conventional hydrogels and new structural attributes that cover the application of hydrogels in all areas. The emphasis is given on the application of hydrogels in drug delivery and tissue engineering. It includes, currently used hydrogels with their advantages and drawbacks and scope for newly developed hydrogels. Background on polyurethane hydrogels and their further scope in drug delivery and tissue engineering applications is discussed.

The characterization techniques such as WAXD, SAXS, SEM, μ-CT and UTM used in this work have been briefly described. Relevant references are given at the end of the chapter.

1.3 References

1. Yang, C.-Y.; Song, B.; Ao, Y.; Nowak, A. P.; Abelowitz, R. B.; Korsak, R. A.; Havton, L. A.; Deming, T. J.; Sofroniew, M. V., Biocompatibility of amphiphilic diblock copolypeptide hydrogels in the central nervous system. *Biomaterials* **2009,** 30, (15), 2881-2898.
2. Darnell, M. C.; Sun, J.-Y.; Mehta, M.; Johnson, C.; Arany, P. R.; Suo, Z.; Mooney, D. J., Performance and biocompatibility of extremely tough alginate/polyacrylamide hydrogels. *Biomaterials* **2013,** 34, (33), 8042-8048.
3. Alexander, C., Stimuli-responsive hydrogels: Drugs take control. *Nature Materials* **2008,** 7, (10), 767-768.
4. Koetting, M. C.; Peters, J. T.; Steichen, S. D.; Peppas, N. A., Stimulus-responsive hydrogels: Theory, modern advances, and applications. *Materials Science and Engineering: R: Reports* **2015,** 93, 1-49.
5. Sood, N.; Bhardwaj, A.; Mehta, S.; Mehta, A., Stimuli-responsive hydrogels in drug delivery and tissue engineering. *Drug Delivery* **2016,** 23, (3), 758-780.
6. Hoch, G.; Chauhan, A.; Radke, C. J., Permeability and diffusivity for water transport through hydrogel membranes. *Journal of Membrane Science* **2003,** 214, (2), 199-209.
7. Tuncaboylu, D. C.; Sari, M.; Oppermann, W.; Okay, O., Tough and Self-Healing Hydrogels Formed via Hydrophobic Interactions. *Macromolecules* **2011,** 44, (12), 4997-5005.
8. Gulyuz, U.; Okay, O., Self-Healing Poly(acrylic acid) Hydrogels with Shape Memory Behavior of High Mechanical Strength. *Macromolecules* **2014,** 47, (19), 6889-6899.
9. Jacob, R. S.; Ghosh, D.; Singh, P. K.; Basu, S. K.; Jha, N. N.; Das, S.; Sukul, P. K.; Patil, S.; Sathaye, S.; Kumar, A.; Chowdhury, A.; Malik, S.; Sen, S.; Maji, S. K., Self healing hydrogels composed of amyloid nano fibrils for cell culture and stem cell differentiation. *Biomaterials* **2015,** 54, 97-105.
10. Lee, K. Y.; Mooney, D. J., Hydrogels for tissue engineering. *Chemical Reviews* **2001,** 101, (7), 1869-1879.
11. Hoffman, A. S., Hydrogels for biomedical applications. *Advanced Drug Delivery Reviews* **2002,** 54, (1), 3-12.

12. Zhu, J., Bioactive modification of poly(ethylene glycol) hydrogels for tissue engineering. *Biomaterials* **2010,** 31, (17), 4639-4656.
13. Van Vlierberghe, S.; Dubruel, P.; Schacht, E., Biopolymer-Based Hydrogels As Scaffolds for Tissue Engineering Applications: A Review. *Biomacromolecules* **2011,** 12, (5), 1387-1408.
14. Hunt, J. A.; Chen, R.; van Veen, T.; Bryan, N., Hydrogels for tissue engineering and regenerative medicine. *Journal of Materials Chemistry B* **2014,** 2, (33), 5319-5338.
15. Hoare, T. R.; Kohane, D. S., Hydrogels in drug delivery: Progress and challenges. *Polymer* **2008,** 49, (8), 1993-2007.
16. Zhang, H.; Patel, A.; Gaharwar, A. K.; Mihaila, S. M.; Iviglia, G.; Mukundan, S.; Bae, H.; Yang, H.; Khademhosseini, A., Hyperbranched Polyester Hydrogels with Controlled Drug Release and Cell Adhesion Properties. *Biomacromolecules* **2013,** 14, (5), 1299-1310.
17. Tibbitt, M. W.; Anseth, K. S., Hydrogels as extracellular matrix mimics for 3D cell culture. *Biotechnology and Bioengineering* **2009,** 103, (4), 655-663.
18. Buenger, D.; Topuz, F.; Groll, J., Hydrogels in sensing applications. *Progress in Polymer Science* **2012,** 37, (12), 1678-1719.
19. Ionov, L., Hydrogel-based actuators: possibilities and limitations. *Materials Today* **2014,** 17, (10), 494-503.
20. Kim, B.; Lee, Y.; Lee, K.; Koh, W.-G., Immobilization of enzymes within hydrogel microparticles to create optical biosensors for the detection of organophosphorus compounds. *Current Applied Physics* **2009,** 9, (4, Supplement), e225-e228.
21. Higashi, K.; Miki, N., A self-swimming microbial robot using microfabricated nanofibrous hydrogel. *Sensors and Actuators B: Chemical* **2014,** 202, 301-306.
22. Wichterle, O.; Lim, D., Hydrophilic Gels for Biological Use. *Nature* **1960,** 185, (4706), 117-118.
23. Caló, E.; Khutoryanskiy, V. V., Biomedical applications of hydrogels: A review of patents and commercial products. *European Polymer Journal* **2015,** 65, 252-267.
24. Kashyap, N.; Kumar, N.; Kumar, M. N. V. R., Hydrogels for Pharmaceutical and Biomedical Applications. **2005,** 22, (2), 107-150.

25. Conley, G. M.; Nöjd, S.; Braibanti, M.; Schurtenberger, P.; Scheffold, F., Superresolution microscopy of the volume phase transition of pNIPAM microgels. *Colloids and Surfaces A: Physicochemical and Engineering Aspects* **2016,** 499, 18-23.
26. Philippova, O. E.; Hourdet, D.; Audebert, R.; Khokhlov, A. R., Interaction of Hydrophobically Modified Poly(acrylic acid) Hydrogels with Ionic Surfactants. *Macromolecules* **1996,** 29, (8), 2822-2830.
27. Karakasyan, C.; Lack, S.; Brunel, F.; Maingault, P.; Hourdet, D., Synthesis and Rheological Properties of Responsive Thickeners Based on Polysaccharide Architectures. *Biomacromolecules* **2008,** 9, (9), 2419-2429.
28. Hu, J.; Ge, Z.; Zhou, Y.; Zhang, Y.; Liu, S., Unique Thermo-Induced Sequential Gel−Sol−Gel Transition of Responsive Multiblock Copolymer-Based Hydrogels. *Macromolecules* **2010,** 43, (12), 5184-5187.
29. Brassinne, J.; Stevens, A. M.; Van Ruymbeke, E.; Gohy, J.-F.; Fustin, C.-A., Hydrogels with Dual Relaxation and Two-Step Gel–Sol Transition from Heterotelechelic Polymers. *Macromolecules* **2013,** 46, (22), 9134-9143.
30. Yang, Q.; Song, C.; Chen, Q.; Zhang, P.; Wang, P., Synthesis and aqueous solution properties of hydrophobically modified anionic acrylamide copolymers. *Journal of Polymer Science Part B: Polymer Physics* **2008,** 46, (22), 2465-2474.
31. Shashkina, Y. A.; Zaroslov, Y. D.; Smirnov, V. A.; Philippova, O. E.; Khokhlov, A. R.; Pryakhina, T. A.; Churochkina, N. A., Hydrophobic aggregation in aqueous solutions of hydrophobically modified polyacrylamide in the vicinity of overlap concentration. *Polymer* **2003,** 44, (8), 2289-2293.
32. Al-Sabagh, A. M.; Kandile, N. G.; El-Ghazawy, R. A.; Noor El-Din, M. R.; El-sharaky, E. A., Synthesis and characterization of high molecular weight hydrophobically modified polyacrylamide nanolatexes using novel nonionic polymerizable surfactants. *Egyptian Journal of Petroleum* **2013,** 22, (4), 531-538.
33. Karunasena, A.; Brown, R. G.; Glass, J. E., Hydrophobically Modified Ethoxylated Urethane Architecture. In *Polymers in Aqueous Media*, American Chemical Society: **1989**; Vol. 223, pp 495-525.

34. Shay, G. D., Alkali-Swellable and Alkali-Soluble Thickener Technology. In *Polymers in Aqueous Media*, American Chemical Society: **1989**; Vol. 223, pp 457-494.

35. Shay, G. D.; Kravitz, F. K.; Brizgys, P. V., Effects of Process Variables on the Emulsion and Solution Properties of Hydrophobically Modified Alkali-Swellable Emulsion Thickeners. In *Polymers as Rheology Modifiers*, American Chemical Society: **1991**; Vol. 462, pp 121-141.

36. Siu, H.; Duhamel, J., Associations between a Pyrene-Labeled Hydrophobically Modified Alkali Swellable Emulsion Copolymer and Sodium Dodecyl Sulfate Probed by Fluorescence, Surface Tension, and Viscometry. *Macromolecules* **1991,** 39, (3), 1144-1155.

37. English, R. J.; Jenkins, R. D.; Bassett, D. R.; Khan, S. A., Rheology of a HASE Associative Polymer and Its Interaction with Non-Ionic Surfactants. In *Associative Polymers in Aqueous Media*, American Chemical Society: **2000**; Vol. 765, pp 369-380.

38. English, R. J.; Laurer, J. H.; Spontak, R. J.; Khan, S. A., Hydrophobically Modified Associative Polymer Solutions: Rheology and Microstructure in the Presence of Nonionic Surfactants. *Industrial & Engineering Chemistry Research* **2000,** 41, (25), 6425-6435.

39. Miller, C. M.; Olesen, K. R.; Shay, G. D., Determination of the Thickening Mechanism of a Hydrophobically Modified Alkali Soluble Emulsion Using Dynamic Viscosity Measurements. In *Associative Polymers in Aqueous Media*, American Chemical Society: **2000**; Vol. 765, pp 338-350.

40. Suzuki, S.; Uneyama, T.; Watanabe, H., Concentration Dependence of Nonlinear Rheological Properties of Hydrophobically Modified Ethoxylated Urethane Aqueous Solutions. *Macromolecules* **1989,** 46, (9), 3497-3504.

41. Kaczmarski, J. P.; Glass, J. E., Synthesis and Characterization of Step Growth Hydrophobically-Modified Ethoxylated Urethane Associative Thickeners. *Langmuir* **2000,** 10, (9), 3035-3042.

42. Ma, Z.; Glass, J. E., Complexations of Beta-Cyclodextrin with Surfactants and Hydrophobically Modified Ethoxylated Urethanes. In *Associative Polymers in Aqueous Media*, American Chemical Society: **2000**; Vol. 765, pp 254-270.

43. Gandhi, A.; Paul, A.; Sen, S. O.; Sen, K. K., Studies on thermoresponsive polymers: Phase behaviour, drug delivery and biomedical applications. *Asian Journal of Pharmaceutical Sciences* **2015,** 10, (2), 99-107.

44. Haraguchi, K.; Takehisa, T., Nanocomposite hydrogels: A unique organic-inorganic network structure with extraordinary mechanical, optical, and swelling/de-swelling properties. *Advanced Materials* **2002,** 14, (16), 1120-1124.

45. Schexnailder, P.; Schmidt, G., Nanocomposite polymer hydrogels. *Colloid and Polymer Science* **2009,** 287, (1), 1-11.

46. Wang, Q.; Mynar, J. L.; Yoshida, M.; Lee, E.; Lee, M.; Okuro, K.; Kinbara, K.; Aida, T., High-water-content mouldable hydrogels by mixing clay and a dendritic molecular binder. *Nature* **2010,** 463, (7279), 339-343.

47. Gaharwar, A. K.; Peppas, N. A.; Khademhosseini, A., Nanocomposite hydrogels for biomedical applications. *Biotechnology and Bioengineering* **2014,** 111, (3), 441-453.

48. Gong, J. P.; Katsuyama, Y.; Kurokawa, T.; Osada, Y., Double-network hydrogels with extremely high mechanical strength. *Advanced Materials* **2003,** 15, (14), 1155-58.

49. Brown, H. R., A Model of the Fracture of Double Network Gels. *Macromolecules* **2007,** 40, (10), 3815-3818.

50. Webber, R. E.; Creton, C.; Brown, H. R.; Gong, J. P., Large Strain Hysteresis and Mullins Effect of Tough Double-Network Hydrogels. *Macromolecules* **2007,** 40, (8), 2919-2927.

51. Yu, Q. M.; Tanaka, Y.; Furukawa, H.; Kurokawa, T.; Gong, J. P., Direct Observation of Damage Zone around Crack Tips in Double-Network Gels. *Macromolecules* **2009,** 42, (12), 3852-3855.

52. Kato, K.; Inoue, K.; Kidowaki, M.; Ito, K., Organic−Inorganic Hybrid Slide-Ring Gels: Polyrotaxanes Consisting of Poly(dimethylsiloxane) and γ-Cyclodextrin and Subsequent Topological Cross-Linking. *Macromolecules* **2009,** 42, (18), 7129-7136.

53. Bin Imran, A.; Esaki, K.; Gotoh, H.; Seki, T.; Ito, K.; Sakai, Y.; Takeoka, Y., Extremely stretchable thermosensitive hydrogels by introducing slide-ring polyrotaxane cross-linkers and ionic groups into the polymer network. *Nat Commun* **2014,** 5.

54. Okumura, Y.; Ito, K., The Polyrotaxane Gel: A Topological Gel by Figure-of-Eight Cross-links. *Advanced Materials* **2001,** 13, (7), 485-487.

55. Nakayama, A.; Kakugo, A.; Gong, J. P.; Osada, Y.; Takai, M.; Erata, T.; Kawano, S., High Mechanical Strength Double-Network Hydrogel with Bacterial Cellulose. *Advanced Functional Materials* **2004,** 14, (11), 1124-1128.

56. Ito, K., Novel Cross-Linking Concept of Polymer Network: Synthesis, Structure, and Properties of Slide-Ring Gels with Freely Movable Junctions. *Polym. J* **2007,** 39, (6), 489-499.

57. Johnson, J. A.; Turro, N. J.; Koberstein, J. T.; Mark, J. E., Some hydrogels having novel molecular structures. *Progress in Polymer Science* **2010,** 35, (3), 332-337.

58. Peak, C. W.; Wilker, J. J.; Schmidt, G., A review on tough and sticky hydrogels. *Colloid and Polymer Science* **2013,** 291, (9), 2031-2047.

59. Nyberg, T.; Inganäs, O.; Jerregård, H., Polymer Hydrogel Microelectrodes for Neural Communication. *Biomedical Microdevices* 4, (1), 43-52.

60. Brahim, S.; Narinesingh, D.; Guiseppi-Elie, A., Polypyrrole-hydrogel composites for the construction of clinically important biosensors. *Biosensors and Bioelectronics* **2002,** 17, (1–2), 53-59.

61. Murdan, S., Electro-responsive drug delivery from hydrogels. *Journal of Controlled Release* **2003,** 92, (1–2), 1-17.

62. Ferreira, L.; Vidal, M. M.; Gil, M. H., Evaluation of poly(2-hydroxyethyl methacrylate) gels as drug delivery systems at different pH values. *International Journal of Pharmaceutics* **2000,** 194, (2), 169-180.

63. Patel, V. R.; Amiji, M. M., Preparation and characterization of freeze-dried chitosan-poly (ethylene oxide) hydrogels for site-specific antibiotic delivery in the stomach. *Pharmaceutical Research* **1996,** 13, (4), 588-593.

64. Amiji, M.; Tailor, R.; Ly, M.-K.; Goreham, J., Gelatin-Poly(Ethylene Oxide) Semi-interpenetrating Polymer Network with pH-Sensitive Swelling and Enzyme-Degradable Properties for Oral Drug Delivery. *Drug Development and Industrial Pharmacy* **1997,** 23, (6), 575-582.

65. Gutowska, A.; Bae, Y. H.; Feijen, J.; Kim, S. W., Heparin release from thermosensitive hydrogels. *Journal of Controlled Release* **1992,** 22, (2), 95-104.

66. Serres, A.; Baudyš, M.; Kim, S. W., Temperature and pH-sensitive Polymers for Human Calcitonin Delivery. *Pharmaceutical Research* 13, (2), 196-201.

67. Creque, H. M.; Langer, R.; Folkman, J., One Month of Sustained Release of Insulin from a Polymer Implant. *Diabetes* **1980,** 29, (1), 37-40.

68. Brown, L. R.; Edelman, E. R.; Fischel-Ghodsian, F.; Langer, R., Characterization of glucose-mediated insulin release from implantable polymers. *Journal of Pharmaceutical Sciences* **1996,** 85, (12), 1341-1345.

69. D'Emanuele, A.; Staniforth, J. N., An electrically modulated drug delivery device: I. *Pharmaceutical Research* **1991,** 8, (7), 913-918.

70. Mathiowitz, E., *Encyclopedia of controlled drug delivery*. Wiley-Interscience: 1999; Vol. 2.

71. Lee, V. H., Encyclopedia of Controlled Drug Delivery, Volume 1 and 2: Edith Mathiowitz, editor. John Wiley & Sons, Inc., New York, 1999, 1057 pp. *Journal of Controlled Release* **2001,** 71, (3), 353-354.

72. Nuttelman, C. R.; Tripodi, M. C.; Anseth, K. S., Dexamethasone-functionalized gels induce osteogenic differentiation of encapsulated hMSCs. *Journal of Biomedical Materials Research Part A* **2006,** 76A, (1), 183-195.

73. Sheridan, M. H.; Shea, L. D.; Peters, M. C.; Mooney, D. J., Bioadsorbable polymer scaffolds for tissue engineering capable of sustained growth factor delivery. *Journal of Controlled Release* **2000,** 64, (1-3), 91-102.

74. Quirk, R. A.; France, R. M.; Shakesheff, K. M.; Howdle, S. M., Supercritical fluid technologies and tissue engineering scaffolds. *Current Opinion in Solid State & Materials Science* **2004,** 8, (3-4), 313-321.

75. Suh, S. W.; Shin, J. Y.; Kim, J. H.; Kim, J. G.; Beak, C. H.; Kim, D. I.; Kim, S. J.; Jeon, S. S.; Choo, I. W., Effect of different particles on cell proliferation in polymer scaffolds using a solvent-casting and particulate leaching technique. *Asaio Journal* **2002,** 48, (5), 460-464.

76. Zhang, J. C.; Wu, L. B.; Jing, D. Y.; Ding, J. D., A comparative study of porous scaffolds with cubic and spherical macropores. *Polymer* **2005,** 46, (13), 4979-4985.

77. Lin, W.-C.; Yu, D.-G.; Yang, M.-C., Blood compatibility of novel poly(γ-glutamic acid)/polyvinyl alcohol hydrogels. *Colloids and Surfaces B: Biointerfaces* **2006,** 47, (1), 43-49.

78. Lee, M.; Wu, B. M.; Dunn, J. C. Y., Effect of scaffold architecture and pore size on smooth muscle cell growth. *Journal of Biomedical Materials Research Part A* **2008,** 87A, (4), 1010-1016.

79. Lips, P. A. M.; Velthoen, I. W.; Dijkstra, P. J.; Wessling, M.; Feijen, J., Gas foaming of segmented poly(ester amide) films. *Polymer* **2005,** 46, (22), 9396-9403.

80. Badiger, M. V.; McNeill, M. E.; Graham, N. B., Porogens in the preparation of microporous hydrogels based on poly(ethylene oxides). *Biomaterials* **1993,** 14, (14), 1059-1063.

81. Dhandayuthapani, B.; Anila, M.; Ravindran Girija, A.; Yutaka, N.; Venugopal, K.; Yasuhiko, Y.; Toru, M.; Sakthikumar, D., Hybrid fluorescent curcumin loaded zein electrospun nanofibrous scaffold for biomedical applications. *Biomedical Materials* **2012,** 7, (4), 045001.

82. Annabi, N.; Nichol, J. W.; Zhong, X.; Ji, C.; Koshy, S.; Khademhosseini, A.; Dehghani, F., Controlling the Porosity and Microarchitecture of Hydrogels for Tissue Engineering. *Tissue Engineering. Part B, Reviews* **2010,** 16, (4), 371-383.

83. Mata, A.; Kim, E. J.; Boehm, C. A.; Fleischman, A. J.; Muschler, G. F.; Roy, S., A three-dimensional scaffold with precise micro-architecture and surface micro-textures. *Biomaterials* **2009,** 30, (27), 4610-4617.

84. Thomson, R. C.; Mikos, A. G.; Beahm, E.; Lemon, J. C.; Satterfield, W. C.; Aufdemorte, T. B.; Miller, M. J., Guided tissue fabrication from periosteum using preformed biodegradable polymer scaffolds. *Biomaterials* **1999,** 20, (21), 2007-2018.

85. Shalaby, W. S., Bioabsorbable Polymers. In *Encyclopedia of Pharmaceutical Technology, Third Edition*, Taylor & Francis: **2013**; Vol. null, pp 155-163.

86. Ashammakhi, N.; Rokkanen, P., Absorbable polyglycolide devices in trauma and bone surgery. *Biomaterials* **1997,** 18, (1), 3-9.

87. Burkoth, A. K.; Anseth, K. S., A review of photocrosslinked polyanhydrides:: in situ forming degradable networks. *Biomaterials* **2000,** 21, (23), 2395-2404.

88. Andriano, K. P.; Tabata, Y.; Ikada, Y.; Heller, J., In vitro and in vivo comparison of bulk and surface hydrolysis in absorbable polymer scaffolds for tissue engineering. *Journal of Biomedical Materials Research* **1999,** 48, (5), 602-612.

89. Zalipsky, S., Synthesis of an end-group functionalized polyethylene glycol-lipid conjugate for preparation of polymer-grafted liposomes. *Bioconjugate Chemistry* **1993,** 4, (4), 296-299.

90. Zalipsky, S., Functionalized Poly(ethylene glycols) for Preparation of Biologically Relevant Conjugates. *Bioconjugate Chemistry* **1995,** 6, (2), 150-165.

91. Gombotz, W. R.; Pettit, D. K., Biodegradable Polymers for Protein and Peptide Drug Delivery. *Bioconjugate Chemistry* **1995,** 6, (4), 332-351.

92. West, J. L.; Hubbell, J. A., Polymeric Biomaterials with Degradation Sites for Proteases Involved in Cell Migration. *Macromolecules* **1999,** 32, (1), 241-244.

93. Andreopoulos, F. M.; Deible, C. R.; Stauffer, M. T.; Weber, S. G.; Wagner, W. R.; Beckman, E. J.; Russell, A. J., Photoscissable Hydrogel Synthesis via Rapid Photopolymerization of Novel PEG-Based Polymers in the Absence of Photoinitiators. *Journal of the American Chemical Society* **1996,** 118, (26), 6235-6240.

94. Peppas, N. A.; Stauffer, S. R., Reinforced uncrosslinked poly (vinyl alcohol) gels produced by cyclic freezing-thawing processes: a short review. *Journal of Controlled Release* **1991,** 16, (3), 305-310.

95. Burczak, K.; Gamian, E.; Kochman, A., Long-term in vivo performance and biocompatibility of poly(vinyl alcohol) hydrogel macrocapsules for hybrid-type artificial pancreas. *Biomaterials* **1996,** 17, (24), 2351-2356.

96. Stile, R. A.; Healy, K. E., Poly (N-isopropylacrylamide)-based semi-interpenetrating polymer networks for tissue engineering applications. 1. Effects of linear poly (acrylic acid) chains on phase behavior. *Biomacromolecules* **2002,** 3, (3), 591-600.

97. Lu, Y.; Wang, D.; Li, T.; Zhao, X.; Cao, Y.; Yang, H.; Duan, Y. Y., Poly (vinyl alcohol)/poly (acrylic acid) hydrogel coatings for improving electrode–neural tissue interface. *Biomaterials* **2009,** 30, (25), 4143-4151.

98. Deming, T. J., Facile synthesis of block copolypeptides of defined architecture. *Nature* **1997,** 390, (6658), 386-389.

99. Urry, D. W., Molecular Machines: How Motion and Other Functions of Living Organisms Can Result from Reversible Chemical Changes. *Angewandte Chemie International Edition in English* **1993,** 32, (6), 819-841.

100. Panitch, A.; Yamaoka, T.; Fournier, M. J.; Mason, T. L.; Tirrell, D. A., Design and Biosynthesis of Elastin-like Artificial Extracellular Matrix Proteins Containing Periodically Spaced Fibronectin CS5 Domains. *Macromolecules* **1999,** 32, (5), 1701-1703.

101. Chenite, A.; Chaput, C.; Wang, D.; Combes, C.; Buschmann, M. D.; Hoemann, C. D.; Leroux, J. C.; Atkinson, B. L.; Binette, F.; Selmani, A., Novel injectable neutral solutions of chitosan form biodegradable gels in situ. *Biomaterials* **2000,** 21, (21), 2155-2161.

102. Muzzarelli, R. A. A.; Zucchini, C.; Ilari, P.; Pugnaloni, A.; Mattioli Belmonte, M.; Biagini, G.; Castaldini, C., Osteoconductive properties of methylpyrrolidinone chitosan in an animal model. *Biomaterials* **1993,** 14, (12), 925-929.

103. Rault, I.; Frei, V.; Herbage, D.; Abdul-Malak, N.; Huc, A., Evaluation of different chemical methods for cros-linking collagen gel, films and sponges. *Journal of Materials Science: Materials in Medicine* **1996,** 7, (4), 215-221.

104. Srivastava, S.; Gorham, S. D.; Courtney, J. M., The attachment and growth of an established cell line on collagen, chemically modified collagen, and collagen composite surfaces. *Biomaterials* **1990,** 11, (3), 162-168.

105. Dillon, G. P.; Xiaojun, Y.; Sridharan, A.; Ranieri, J. P.; Bellamkonda, R. V., The influence of physical structure and charge on neurite extension in a 3D hydrogel scaffold. *Journal of Biomaterials Science, Polymer Edition* **1998,** 9, (10), 1049-1069.

106. Borkenhagen, M.; Clémence, J. F.; Sigrist, H.; Aebischer, P., Three-dimensional extracellular matrix engineering in the nervous system. *Journal of Biomedical Materials Research* **1998,** 40, (3), 392-400.

107. Uludag, H.; De Vos, P.; Tresco, P. A., Technology of mammalian cell encapsulation. *Advanced Drug Delivery Reviews* **2000,** 42, (1–2), 29-64.

108. Klöck, G.; Pfeffermann, A.; Ryser, C.; Gröhn, P.; Kuttler, B.; Hahn, H.-J.; Zimmermann, U., Biocompatibility of mannuronic acid-rich alginates. *Biomaterials* **1997,** 18, (10), 707-713.

109. Schense, J. C.; Hubbell, J. A., Cross-Linking Exogenous Bifunctional Peptides into Fibrin Gels with Factor XIIIa. *Bioconjugate Chemistry* **1999,** 10, (1), 75-81.

110. Kuijpers, A. J.; Engbers, G. H. M.; Feijen, J.; De Smedt, S. C.; Meyvis, T. K. L.; Demeester, J.; Krijgsveld, J.; Zaat, S. A. J.; Dankert, J., Characterization of the Network Structure of Carbodiimide Cross-Linked Gelatin Gels. *Macromolecules* **1999,** 32, (10), 3325-3333.

111. Choi, Y. S.; Hong, S. R.; Lee, Y. M.; Song, K. W.; Park, M. H.; Nam, Y. S., Study on gelatin-containing artificial skin: I. Preparation and characteristics of novel gelatin-alginate sponge. *Biomaterials* **1999,** 20, (5), 409-417.

112. Vercruysse, K. P.; Marecak, D. M.; Marecek, J. F.; Prestwich, G. D., Synthesis and in Vitro Degradation of New Polyvalent Hydrazide Cross-Linked Hydrogels of Hyaluronic Acid. *Bioconjugate Chemistry* **1997,** 8, (5), 686-694.

113. Liu, L.-S.; Thompson, A. Y.; Heidaran, M. A.; Poser, J. W.; Spiro, R. C., An osteoconductive collagen/hyaluronate matrix for bone regeneration. *Biomaterials* **1999,** 20, (12), 1097-1108.

114. Kim, I. L.; Mauck, R. L.; Burdick, J. A., Hydrogel design for cartilage tissue engineering: A case study with hyaluronic acid. *Biomaterials* **2011,** 32, (34), 8771-8782.

115. Xavier, J. R.; Thakur, T.; Desai, P.; Jaiswal, M. K.; Sears, N.; Cosgriff-Hernandez, E.; Kaunas, R.; Gaharwar, A. K., Bioactive Nanoengineered Hydrogels for Bone Tissue Engineering: A Growth-Factor-Free Approach. *Acs Nano* **2015,** 9, (3), 3109-3118.

116. Aurand, E. R.; Lampe, K. J.; Bjugstad, K. B., Defining and designing polymers and hydrogels for neural tissue engineering. *Neuroscience Research* **2012,** 72, (3), 199-213.

117. Hammond, T. H.; Zhou, R.; Hammond, E. H.; Pawlak, A.; Gray, S. D., The intermediate layer: A morphologic study of the elastin and hyaluronic acid constituents of normal human vocal folds. *Journal of Voice* **1997,** 11, (1), 59-66.

118. Vavken, P., Tissue Engineering of Ligaments and Tendons. In *Fundamentals of Tissue Engineering and Regenerative Medicine*, Meyer, U.; Handschel, J.; Wiesmann, P. H.; Meyer, T., Eds. Springer Berlin Heidelberg: Berlin, Heidelberg, **2009**; pp 317-327.

119. Puperi, D. S.; O'Connell, R. W.; Punske, Z. E.; Wu, Y.; West, J. L.; Grande-Allen, K. J., Hyaluronan Hydrogels for a Biomimetic Spongiosa Layer of Tissue Engineered Heart Valve Scaffolds. *Biomacromolecules* **2016**.

120. Caseiro, A. R.; Pereira, T.; Bártolo, P. J.; Santos, J. D.; Luís, A. L.; Maurício, A. C., Mesenchymal Stem Cells and Biomaterials Systems – Perspectives for Skeletal Muscle Tissue Repair and Regeneration. *Procedia Engineering* **2015,** 110, 90-97.

121. Yoo, B.-Y.; Shin, Y.-H.; Yoon, H.-H.; Seo, Y.-K.; Park, J.-K., Hair follicular cell/organ culture in tissue engineering and regenerative medicine. *Biochemical Engineering Journal* **2010,** 48, (3), 323-331.

122. He, X.; Fu, W.; Zheng, J., Cell sources for trachea tissue engineering: past, present and future. *Regenerative medicine* **2012,** 7, (6), 851-863.

123. Dunphy, S. E.; Bratt, J. A. J.; Akram, K. M.; Forsyth, N. R.; El Haj, A. J., Hydrogels for lung tissue engineering: Biomechanical properties of thin collagen–elastin constructs. *Journal of the Mechanical Behavior of Biomedical Materials* **2014,** 38, 251-259.

124. Tan, H.; Gong, Y.; Lao, L.; Mao, Z.; Gao, C., Gelatin/chitosan/hyaluronan ternary complex scaffold containing basic fibroblast growth factor for cartilage tissue engineering. *Journal of Materials Science: Materials in Medicine* **2007,** 18, (10), 1961-1968.

125. Mjahed, H.; Porcel, C.; Senger, B.; Chassepot, A.; Netter, P.; Gillet, P.; Decher, G.; Voegel, J.-C.; Schaaf, P.; Benkirane-Jessel, N.; Boulmedais, F., Micro-stratified architectures based on successive stacking of alginate gel layers and poly(l-lysine)-hyaluronic acid multilayer films aimed at tissue engineering. *Soft Matter* **2008,** 4, (7), 1422-1429.

126. Smithmyer, M. E.; Sawicki, L. A.; Kloxin, A. M., Hydrogel scaffolds as in vitro models to study fibroblast activation in wound healing and disease. *Biomaterials Science* **2014,** 2, (5), 634-650.

127. Combellack, E. J.; Jessop, Z. M.; Naderi, N.; Griffin, M.; Dobbs, T.; Ibrahim, A.; Evans, S.; Burnell, S.; Doak, S. H.; Whitaker, I. S., Adipose regeneration and implications for breast reconstruction: update and the future. *Gland Surgery* **2016,** 5, (2), 227-241.

128. Betz, M. W.; Modi, P. C.; Caccamese, J. F.; Coletti, D. P.; Sauk, J. J.; Fisher, J. P., Cyclic acetal hydrogel system for bone marrow stromal cell encapsulation and osteodifferentiation. *Journal of Biomedical Materials Research Part A* **2008,** 86A, (3), 662-670.

129. Su, J.; Hu, B.-H.; Lowe Jr, W. L.; Kaufman, D. B.; Messersmith, P. B., Anti-inflammatory peptide-functionalized hydrogels for insulin-secreting cell encapsulation. *Biomaterials* **2010,** 31, (2), 308-314.

130. Saunders, R. L.; Hammer, D. A., Assembly of Human Umbilical Vein Endothelial Cells on Compliant Hydrogels. *Cellular and Molecular Bioengineering* **2010,** 3, (1), 60-67.

131. Motoyama, W.; Sayo, K.; Mihara, H.; Aoki, S.; Kojima, N., Induction of hepatic tissues in multicellular spheroids composed of murine fetal hepatic cells and embedded hydrogel beads. *Regenerative Therapy* **2016,** 3, 7-10.

132. Neufurth, M.; Wang, X.; Schröder, H. C.; Feng, Q.; Diehl-Seifert, B.; Ziebart, T.; Steffen, R.; Wang, S.; Müller, W. E. G., Engineering a morphogenetically active hydrogel for bioprinting of bioartificial tissue derived from human osteoblast-like SaOS-2 cells. *Biomaterials* **2014,** 35, (31), 8810-8819.

133. Chattopadhyay, D. K.; Raju, K. V. S. N., Structural engineering of polyurethane coatings for high performance applications. *Progress in Polymer Science* **2007,** 32, (3), 352-418.

134. Sardon, H.; Engler, A. C.; Chan, J. M. W.; García, J. M.; Coady, D. J.; Pascual, A.; Mecerreyes, D.; Jones, G. O.; Rice, J. E.; Horn, H. W.; Hedrick, J. L., Organic Acid-Catalyzed Polyurethane Formation via a Dual-Activated Mechanism: Unexpected Preference of N-Activation over O-Activation of Isocyanates. *Journal of the American Chemical Society* **2013,** 135, (43), 16235-16241.

135. Engels, H.-W.; Pirkl, H.-G.; Albers, R.; Albach, R. W.; Krause, J.; Hoffmann, A.; Casselmann, H.; Dormish, J., Polyurethanes: Versatile Materials and Sustainable Problem Solvers for Today's Challenges. *Angewandte Chemie International Edition* **2013,** 52, (36), 9422-9441.

136. Zhang, C.; Zhang, N.; Wen, X., Synthesis and characterization of biocompatible, degradable, light-curable, polyurethane-based elastic hydrogels. *Journal of Biomedical Materials Research Part A* **2007,** 82A, (3), 637-650.

137. Guidoin, R.; Sigot, M.; King, M.; Sigot-Luizard, M.-F., Biocompatibility of the Vascugraft ®: evaluation of a novel polyester methane vascular substitute by an organotypic culture technique. *Biomaterials* **1992,** 13, (5), 281-288.

138. Stokes, K.; Cobian, K., Polyether polyurethanes for implantable pacemaker leads. *Biomaterials* **1982,** 3, (4), 225-231.

139. Eberhart, A.; Zhang, Z.; Guidoin, R.; Laroche, G.; Guay, L.; De La Faye, D.; Batt, M.; King, M. W., A new generation of polyurethane vascular prostheses: Rara Avis or Ignis Fatuus? *Journal of Biomedical Materials Research* **1999,** 48, (4), 546-558.

140. Liu, S. Q.; Kodama, M., Porous polyurethane vascular prostheses with variable compliances. *Journal of Biomedical Materials Research* **1992,** 26, (11), 1489-1502.

141. Martz, H.; Beaudoin, G.; Paynter, R.; King, M.; Marceau, D.; Guidoin, R., Physicochemical characterization of a hydrophilic microporous polyurethane vascular graft. *Journal of Biomedical Materials Research* **1987,** 21, (3), 399-412.

142. Sun, X.; Gao, H.; Wu, G.; Wang, Y.; Fan, Y.; Ma, J., Biodegradable and temperature-responsive polyurethanes for adriamycin delivery. *International Journal of Pharmaceutics* **2011,** 412, (1–2), 52-58.

143. Lai, Y.-C.; Baccei, L. J., Novel polyurethane hydrogels for biomedical applications. *Journal of Applied Polymer Science* **1991,** 42, (12), 3173-3179.

144. Mequanint, K.; Patel, A.; Bezuidenhout, D., Synthesis, Swelling Behavior, and Biocompatibility of Novel Physically Cross-Linked Polyurethane-block-Poly(glycerol methacrylate) Hydrogels. *Biomacromolecules* **2006,** 7, (3), 883-891.

145. Petrini, P.; Fare, S.; Piva, A.; Tanzi, M., Design, synthesis and properties of polyurethane hydrogels for tissue engineering. *Journal of Materials Science: Materials in Medicine* **2003,** 14, (8), 683-686.

146. McNeill, M. E.; Graham, N. B., Vaginal pessaries from crystalline/rubbery hydrogels for the delivery of prostaglandin E2. *Journal of Controlled Release* **1984,** 1, (2), 99-117.

147. Graham, N. B.; McNeill, M. E., Morphology of poly(ethylene oxide)-based hydrogels in relation to controlled drug delivery. *Makromolekulare Chemie. Macromolecular Symposia* **1988,** 19, (1), 255-273.

148. Graham, N. B.; McNeill, M. E., Hydrogels for controlled drug delivery. *Biomaterials* **1984,** 5, (1), 27-36.

149. Zdrahala, R. J.; Zdrahala, I. J., Biomedical Applications of Polyurethanes: A Review of Past Promises, Present Realities, and a Vibrant Future. *Journal of Biomaterials Applications* **1999,** 14, (1), 67-90.

150. Haschke, E.; Sendijarevic, V.; Wong, S.; Frisch, K. C.; Hill, G., Clear Nonionic Polyurethane Hydrogels for Biomedical Applications. *Journal of Elastomers and Plastics* **1994,** 26, (1), 41-57.

151. Guelcher, S. A., Biodegradable Polyurethanes: Synthesis and Applications in Regenerative Medicine. *Tissue Engineering Part B: Reviews* **2008,** 14, (1), 3-17.

152. Polo Fonseca, L.; Bergamo Trinca, R.; Isabel Felisberti, M., Thermo-responsive polyurethane hydrogels based on poly(ethylene glycol) and poly(caprolactone): Physico-chemical and mechanical properties. *Journal of Applied Polymer Science* **2016,** 133, (25), n/a-n/a.

153. Son, J. S.; Lee, S. H.; Lee, B.; Kim, H. J.; Ko, J. H.; Park, Y. H.; Chun, H. J.; Kim, C. H.; Kim, J. H.; Kim, M. S., Polyurethanes for biomedical application. *Tissue Engineering and Regenerative Medicine* **2009,** 6, (4-11), 427-431.

154. Shih, K., *X-Ray Diffraction: Structure, Principles and Applications*. Nova Science Publishers, Incorporated: **2013**.

155. Guinier, A.; Fournet, G., *Small-angle scattering of X-rays*. Wiley: **1955**.

156. Hayat, M. A., *Principles and techniques of scanning electron microscopy*. Van Nostrand Reinhold Co.: **1978**.

157. Stock, S. R., *MicroComputed Tomography: Methodology and Applications*. CRC Press: **2008**.

158. Ho, S. T.; Hutmacher, D. W., A comparison of micro CT with other techniques used in the characterization of scaffolds. *Biomaterials* **2006,** 27, (8), 1362-1376.

159. Monroe, R. J., *Measuring the Mechanical Response of Swollen Hydrogels*. Michigan State University. Mechanical Engineering: **2008**.

160. Yanagioka, M.; Engineering, S. U. D. o. C., *Analysis of the structure-mechanical property relationships of nanoparticle-filled hydrogels*. Stanford University: **2009**.

161. Berthiaume, F.; Morgan, J. R., *Methods in Bioengineering: 3D Tissue Engineering*. Artech House: **2010**.

Scope and Objectives

Chapter – II

In the second chapter, we have discussed the scope and objectives of thesis work.

Most of the hydrogels used /or proposed in tissue engineering applications exhibit weak mechanical strength and hence invariably are unsuitable for application under load. The fracture energy of typical hydrogels fall in the range of 10^{-1} - 10^{0} J/m^2, which is much smaller than the fracture energy of usual rubbers.[1] Therefore, major research efforts are underway in designing and developing novel hydrogels with improved mechanical properties. These include double network gels,[2] nanocomposite gels,[3] slide ring gels/ topological gels.[4] Recently, Jeong Yun Sun et al.,[5] have reported on the highly stretchable and tough hydrogels made by the combination of alginates and poly(acrylamides). The toughness in the hydrogel was introduced by recoverable energy dissipating mechanisms.

Besides good mechanical strength of the hydrogels, the porosity of hydrogels plays an important role in designing scaffolds and implants in tissue engineering. The scaffold allows cells to enter in it, proliferate and secrete their own extra cellular matrix (ECM), leading to a complete and natural tissue replacement in the long run. The porosity, pore size and pore structure of the scaffold is vital for nutrient supply of cells. The diffusion rate of nutrients increases with the presence of an open interconnected porous network in the scaffold. Different techniques have been used to fabricate porous scaffolds which include porogen leaching,[6-8] phase separation,[9] emulsion freeze-drying,[10-11] solvent evaporation[12-13] and gas foaming[14] etc.

Lately, Polyurethanes (PUs) are becoming increasingly important synthetic elastomers in variety of medical implants (like cardiac pace makers, vascular grafts etc.) because of their excellent mechanical properties and good biocompatibility. PUs are also designed to have chemical linkage that are degradable in biological environments.[15] However, a major drawback has been the toxicity of degradation products, particularly those derived from the diisocyanate component[16-17] of PUs. Accordingly, to address these issues in designing degradable PUs, diisocyanates such as lysine diisocyanate (LDI) [2,6-diisocyanatohexanoate] and other aliphatic diisocyanates like hexamethylene diisocyanate (HDI) and 1, 4-butane diisocyanate have been used, which yield non-toxic degradation products.

The advantage with PU polymers/hydrogels is that the polyethylene glycols (PEGs) component used for making PUs can impart soft flexible nature to the final structure. The combination of hard (diisocyanate) and soft (PEGs) segments in the

hydrogel structure can be varied and crosslinking can be affected to obtain hydrogels with desired properties. The diisocyanate and PEG components provide both hydrophobic and hydrophilic nature to the obtained hydrogels. The hydrophilic/hydrophobic balance of the resultant system can be optimized with the control of PEG segments (with different MWs of PEGs), and accordingly the lipophilic/hydrophilic therapeutic agents can be incorporated into PU hydrogels matrices. PU hydrogels can be prepared by one-pot solvent free method by the reaction between neat PEGs and diisocyanates in the presence of a crosslinking agent such as hexanetriol (HT). The products can be prepared in any shape and size depending on the mould used. The porous structure in the hydrogels can be induced by simple cryogenic and lyophilization technique. Such a benign and prudent approach is a most desirable strategy for the synthesis of polymers for biomedical applications. Further, the use of diols such as polycaprolactone diols (PCL) and polycarbonate diols (PCD) can result into degradable PU hydrogels. By employing PCL and PCD-diols, the modulus as well as the hydrophobicity of the resultant PU hydrogels can be tailored to suit end applications. Due to versatile chemical reaction of making PU hydrogels with the reactive functional groups in PEGs and diisocyanate, simple biological molecules can be incorporated chemically (covalently linked) and/or physically dispersed in the PU gel matrix. From a few studies reported in the literature[18-19] on the covalently linked molecules to PU chains, it can be realized that, there is a good scope in designing and synthesizing new drug conjugated PU hydrogels system for drug delivery and tissue engineering applications.

Although there are reports on natural and synthetic hydrogels for scaffolds and implants applications in tissue engineering, their technological development is still in infancy. Therefore, there is a great scope for designing and developing new hydrogel system with good biological properties (e.g., biocompatibility, biodegradability), having controlled pore structure and having good mechanical properties.

The objectives of the thesis are:

- To design and synthesize PEG-PU hydrogels by one-pot method using PEG-4000 as a soft segment and 4,4′-methylenebis cyclohexyl isocyanate (H_{12}MDI) as a hard segment with hexanetriol (HT) as a crosslinker.

- To induce porous structure in the obtained PEG-PU hydrogels by simple cryogenic and lyophilization technique.
- Characterization of PEG-PU hydrogels by FTIR, Solid-State NMR, WAXD, SAXS, Swelling, mechanical strength by DMA and UTM. Analysis of porous structure by SEM and microcomputed tomography (μ-CT).
- To incorporate bio-molecules such as Curcumin into PEG-PU hydrogels to obtain mechanically strong hydrogels and to correlate the structure with properties.
- To study the biological properties of the obtained PU hydrogels in terms of Cytotoxicity, MTT Assay, antimicrobial and antibacterial activities.
- To demonstrate the potential use of the above studied new PU hydrogels for drug delivery and tissue engineering applications.

References

1. Lake, G. J., Fatigue and Fracture of Elastomers. *Rubber Chemistry and Technology* **1995,** 68, (3), 435-460.
2. Gong, J. P.; Katsuyama, Y.; Kurokawa, T.; Osada, Y., Double-network hydrogels with extremely high mechanical strength. *Advanced Materials* **2003,** 15, (14), 1155-58.
3. Haraguchi, K.; Takehisa, T., Nanocomposite hydrogels: A unique organic-inorganic network structure with extraordinary mechanical, optical, and swelling/de-swelling properties. *Advanced Materials* **2002,** 14, (16), 1120-1124.
4. Okumura, Y.; Ito, K., The Polyrotaxane Gel: A Topological Gel by Figure-of-Eight Cross-links. *Advanced Materials* **2001,** 13, (7), 485-487.
5. Sun, J. Y.; Zhao, X. H.; Illeperuma, W. R. K.; Chaudhuri, O.; Oh, K. H.; Mooney, D. J.; Vlassak, J. J.; Suo, Z. G., Highly stretchable and tough hydrogels. *Nature* **2012,** 489, (7414), 133-136.
6. Badiger, M. V.; McNeill, M. E.; Graham, N. B., Porogens in the preparation of microporous hydrogels based on poly(ethylene oxides). *Biomaterials* **1993,** 14, (14), 1059-1063.
7. Suh, S. W.; Shin, J. Y.; Kim, J. H.; Kim, J. G.; Beak, C. H.; Kim, D. I.; Kim, S. J.; Jeon, S. S.; Choo, I. W., Effect of different particles on cell proliferation in polymer scaffolds using a solvent-casting and particulate leaching technique. *Asaio Journal* **2002,** 48, (5), 460-464.
8. Zhang, J.; Wu, L.; Jing, D.; Ding, J., A comparative study of porous scaffolds with cubic and spherical macropores. *Polymer* **2005,** 46, (13), 4979-4985.
9. Ricciardi, R.; D'Errico, G.; Auriemma, F.; Ducouret, G.; Tedeschi, A. M.; De Rosa, C.; Laupretre, F.; Lafuma, F., Short time dynamics of solvent molecules and supramolecular organization of poly (vinyl alcohol) hydrogels obtained by freeze/thaw techniques. *Macromolecules* **2005,** 38, (15), 6629-6639.
10. Lin, W.-C.; Yu, D.-G.; Yang, M.-C., Blood compatibility of novel poly(γ-glutamic acid)/polyvinyl alcohol hydrogels. *Colloids and Surfaces B: Biointerfaces* **2006,** 47, (1), 43-49.

11. Lee, M.; Wu, B. M.; Dunn, J. C. Y., Effect of scaffold architecture and pore size on smooth muscle cell growth. *Journal of Biomedical Materials Research Part A* **2008,** 87A, (4), 1010-1016.
12. Sheridan, M. H.; Shea, L. D.; Peters, M. C.; Mooney, D. J., Bioadsorbable polymer scaffolds for tissue engineering capable of sustained growth factor delivery. *Journal of Controlled Release* **2000,** 64, (1-3), 91-102.
13. Quirk, R. A.; France, R. M.; Shakesheff, K. M.; Howdle, S. M., Supercritical fluid technologies and tissue engineering scaffolds. *Current Opinion in Solid State & Materials Science* **2004,** 8, (3-4), 313-321.
14. Lips, P. A. M.; Velthoen, I. W.; Dijkstra, P. J.; Wessling, M.; Feijen, J., Gas foaming of segmented poly(ester amide) films. *Polymer* **2005,** 46, (22), 9396-9403.
15. Soeda, Y.; Toshima, K.; Matsumura, S., Synthesis and Chemical Recycling of Novel Poly(ester-urethane)s Using an Enzyme. *Macromolecular Bioscience* **2005,** 5, (4), 277-288.
16. Gogolewski, S.; Pennings, A. J., Biodegradable materials of polylactides, 4. Porous biomedical materials based on mixtures of polylactides and polyurethanes. *Die Makromolekulare Chemie, Rapid Communications* **1982,** 3, (12), 839-845.
17. Lai, Y.-C.; Baccei, L. J., Novel polyurethane hydrogels for biomedical applications. *Journal of Applied Polymer Science* **1991,** 42, (12), 3173-3179.
18. Abraham, G. A.; de Queiroz, A. A. A.; Román, J. S., Immobilization of a nonsteroidal antiinflammatory drug onto commercial segmented polyurethane surface to improve haemocompatibility properties. *Biomaterials* **2002,** 23, (7), 1625-1638.
19. Sivak, W. N.; Zhang, J.; Petoud, S.; Beckman, E. J., Simultaneous drug release at different rates from biodegradable polyurethane foams. *Acta Biomaterialia* **2009,** 5, (7), 2398-2408.

Design, synthesis and characterization of polyethylene glycol – polyurethane hydrogels

Chapter – III

In the third chapter, we report the synthesis of porous poly (ethylene glycol)–polyurethane (PEG-PU) hydrogels using PEG-4000 as a soft segment and 4,4′ methylenebis (cyclohexyl isocyanate) as a hard segment. The degree of swelling in the hydrogels could be controlled by varying the amount of crosslinking agent, namely 1,2,6-hexanetriol. The characterization techniques such as Solid-state ^{13}C NMR, FTIR, WAXD, SAXS, SEM, DMA, μ-CT, biological tests etc., used for studying the structural, micro-structural, surface morphology, mechanical behaviour and cytotoxicity of the hydrogels were briefly explained.

Polymer International. 2015; 64: 397-404

3.1 Introduction

Polyurethane based hydrogels are attracting increasing attention lately in bio-medical applications because of their flexible nature and versatility in the synthesis.[1-5] Guan et al., have reported on the porous, biodegradable polyurethane scaffolds for soft tissue applications.[6] Graham and Mc Neil have reported on the controlled release of prostaglandin E_2, caffeine and melatonin from PU based hydrogels.[7-8] Badiger et al., have reported on the porogens for the preparation of PU hydrogels for controlled drug delivery application.[9] Polyurethane based materials have been used for immobilization of enzyme and cells.[10] Wu et al., have synthesized PEG-POSS multi block polyurethane hydrogels using Polyhedral oligosil sesquioxanes (POSS) nanocrystals as physical crosslinks.[11] Although there are a few reports on PU hydrogels, their detailed investigation in terms of mechanical strength and porosity is not fully explored.

In this chapter, we report on the synthesis of porous polyethylene glycol-polyurethane (PEG-PU) hydrogels using PEG-4000 as a soft segment and 4, 4'-methylenebis (cyclohexyl isocyanate) as a hard segment. Hexanetriol (HT) was used as a crosslinker and dibutyltin dilaurate (DBTDL) was used as a catalyst. The structural characterization of hydrogels was performed using FTIR and ^{13}C solid-state NMR spectroscopy. The micro structure of the hydrogels was investigated by wide-angle X-ray diffraction (WAXD), small angle X-ray scattering (SAXS), scanning electron microscopy (SEM) and X-ray microcomputed tomography (X-ray µ-CT). The mechanical strength of the hydrogels was evaluated using Dynamic Mechanical Analyser (DMA). The desired porosity in the hydrogels was created by cryogenic treatment of chemically crosslinked PEG-PU hydrogels, followed by removal of frozen water crystals in the hydrogel matrix through lyophilization. Preliminary in vitro cytotoxicity test was performed on PEG-PU hydrogels.

3.2 Experimental

3.2.1 Materials

PEG (MW~4000g/mol) and dibutyltin dilaurate (DBTDL) were obtained from Merck India; 4, 4' methylenebis (cyclohexyl isocyanate) (H_{12}MDI) was purchased from Sigma Aldrich, USA; 1,2,6 hexanetriol (HT) was obtained from Fluka USA.

Dulbecco's Modified Eagle Medium (DMEM) and Fetal Bovine Serum (FBS) was purchased from Invitrogen USA; Dulbecco's Phosphate buffered saline (DPBS) was obtained from HiMedia India. All the chemicals were of analytical grade and used as received.

3.2.2 Synthesis of PEG-PU Hydrogels

Polyethylene glycol [MW~4000g/mol] was dried at 60 ^{0}C for 6 hours in a rotary evaporator to remove any residual moisture and stored molten in a sealed flask in an oven at 70 ^{0}C until use. To 0.335g of HT in a 50ml glass beaker, 5mg of dibutyltin dilaurate (DBTDL) was added and stirred immediately using a glass rod. The mixture was then placed in an oven at 95 ^{0}C and 10g of molten dry PEG 4000 was added, mixed well and left in the oven to attain equilibrium temperature. To this mixture, 1.5ml of 4,4' methylenebis (cyclohexyl isocyanate) was added using a 5ml glass syringe under nitrogen atmosphere and mixed using glass rod. The mixture was immediately poured in to pre-silanated glass petri-dishes, kept in the oven under vacuum to remove evolved gases and facilitate curing for 4 hours. After cooling the hydrogel discs were removed by immersing the petri-dishes in distilled water for 4-5 hours. The unreacted monomers were removed by washing the hydrogels in excess distilled water for a few days with frequent replenishment of fresh distilled water. Using the same procedure, hydrogels with different HT contents were prepared and the stoichiometry for reactions is given in Table-1.

3.2.3 Preparation of porous PEG-PU hydrogels

Porous PEG-PU xerogels were prepared by cryogenic treatment of chemically crosslinked PEG-PU hydrogels followed by removal of ice crystals by lyophilization. The swollen hydrogels (16mm length x 10mm width x 3mm height) were placed in liquid nitrogen for 15 minutes and then freeze-dried in a lyophilizer (Christ Alpha 1-4, Germany) for 8-10 hours.

3.3 Characterization

3.3.1 Structural Characterization

3.3.1.1 FTIR Spectroscopy

The structural characterization of PEG-PU hydrogels was performed by FTIR and ^{13}C Solid-state NMR spectroscopy. The FTIR spectra of xerogels (dried gel) were recorded using Perkin Elmer spectrum one (USA) in a diffuse reflectance spectroscopy (DRS) mode and the samples were mulled with KBr powder.

3.3.1.2 ^{13}C Solid-state NMR

The ^{13}C Solid-state CP-MAS NMR spectra of samples (xerogel) were obtained using Bruker Avance AQS spectrometer (Bruker, Germany) operating at a carbon frequency of 75 MHz. The samples were spun at 8 kHz using 4mm triple resonance probe. About 4000 scans were accumulated to get good spectra using inter scan delay of 2.5 s.

3.3.2 Swelling Measurements

The swelling behaviour of the PEG-PU hydrogels was studied using gravimetric method. The xerogel samples were immersed in distilled water kept at 37 ^0C using shaking water bath. The swollen samples were removed from the water at the prescribed time, gently pressed between two filter papers to remove any excess water on the surface, and weighed in an electronic analytical balance (FX300, Afcoset, India). Weights of the gels were recorded after reaching equilibrium swelling. The swelling ratio (Q) was determined using an equation,

$$Q = \frac{W_s - W_d}{W_d} \times 100 \qquad (1)$$

Where, W_s and W_d are the mass of swollen and dry samples, respectively.

3.3.3 Micro structural Characterization

3.3.3.1 Wide-angle X-ray diffraction (WAXD)

The wide-angle X-ray diffraction (WAXD) technique was used to detect the microstructure of PEG-PU xerogels with varying degrees of crosslinking. The measurements were made at room temperature on a Rigaku DMAX 2500 diffractometer operated at 40 kV and 100 mA with Cu Kα radiation (wavelength, λ = 1.5418 Å). The samples were scanned between 2θ = 2^0 to 40^0 and the diffraction patterns were collected at RT and 60 ^0C.

3.3.3.2 Small-angle X-ray scattering (SAXS)

Small-angle X-ray scattering (SAXS) measurements were performed on a Bruker Nanostar machine (Germany) equipped with a rotating anode generator (18 kW) operating at a voltage of 45 kV and current of 100 mA. The X-rays were collimated through a three-pinhole system, and data was acquired using a 2D gas filled Hi-Star detector over a q-range of 0.011-0.2 Å-1. The detector was calibrated using a silver behenate sample. PEG-PU samples were sandwiched between Kapton films and were mounted on the Bruker heating stage. Data was corrected for background scattering. The 2D data was reduced to 1D by circularly averaging, using the software provided with the instrument.

3.3.4 Thermal Analysis

The melting behaviour of the PEG-PU xerogels was investigated by Differential Scanning Calorimetry (DSC Q10, TA Instruments, USA) equipped with a mechanical intercooler under a continuous nitrogen purge. The following procedure was used: after annealing each sample at 50 ^{0}C for 24hrs and dried, the samples (5-10 mg) were cooled to -50 ^{0}C with a ramping rate of 2 ^{0}C/ min and then heated up to 70 ^{0}C with a ramping rate of 5 ^{0}C/ min. The dependence of melting enthalpy (heat of fusion) and melting point of PEG-PU xerogel as a function of degree of crosslinking was examined.

3.3.5 Mechanical Properties

Mechanical properties of the PEG-PU hydrogels were measured using dynamic mechanical analyzer (RSAIII, TA Instruments, USA). Uni-axial compression was performed on cylindrical samples (8mm diameter x 3mm height) mounted on parallel plates with a cross-head speed of 1mm/min. The pre-tension load was ~0.03N. Force experienced by the transducer was recorded as a function of strain applied. Dynamic strain sweep was performed on samples at constant frequency of 1 Hz to obtain the linear visco-elastic region. Then, dynamic frequency sweep experiments were carried out from 0.01 to 0.5 Hz, within the linear visco-elastic region of the specimen in the compression mode to obtain the storage and loss moduli of the specimen.

3.3.6 Morphological Analysis

3.3.6.1 Scanning electron microscopy (SEM)

Scanning electron microscopy (SEM) was employed to investigate the morphology of hydrogels, xerogels and porous xerogels using Quanta 200 3D dual beam ESEM (FEI, Finland). The electron source was tungsten (W) filament with thermionic emission at the resolution of 3nm (30kV) in high vacuum. Before SEM imaging, the hydrogel, xerogel and porous xerogels were sputter-coated with a thin layer of gold.

3.3.6.2 Microcomputed Tomography or Micro-CT (μ-CT)

Three-dimensional non-destructive imaging of porous PEG-PU xerogels was performed using a high-resolution X-ray microcomputed tomography (μ-CT), model Versa XRM – 500 (Xradia Inc., USA). Porous PEG-PU xerogel was placed in the sample stage, scanned using X-ray of energy 40kV and 0.7 microns voxel size. To study the permeability in porous hydrogel, flow simulation was performed on the resultant three-dimensional model of porous PEG-PU xerogel using Avizo XLab Hydro (VSG, France) software along the three co-ordinates individually.

Two-dimensional cross-sectional images of porous xerogel were reconstructed from X-ray projections recorded during scanning and later segmented using Avizo Fire 7.0 (VSG, France) software to generate three-dimensional models of porous PEG-PU xerogels. Pore size distribution of the specimen is obtained after applying edge-preserving smoothing filter and watershed algorithm based segmentation of the 2D images using Avizo Fire 7.0 software.

Avizo XLab Hydro is a finite volume Stokes solver for absolute permeability integrated with Avizo Fire software. The methodology of flow simulation experiment is based on the computation of absolute permeability by simulating an experiment, by hermetically closing a given sample on four faces while experimental set-ups are added on two opposite faces to guide the flow along one direction. This solver works directly on the segmented 3D image without requiring any meshing step. Thus, it can be run quickly on different regions of a 3D model.

Initially, the struts in the segmented 3D data set were separated and uniquely identified to generate a 3D mesh for simulation. Later, 3D mesh was optimized and XLab Hydro solver was used to perform post-processed simulation of velocity field to study absolute permeability in x, y and z directions. While simulating along one axis, rest of the axis/boundaries were closed to allow the orientation of velocity field only in one axis at a time. The resulting 3D simulation data sets were coloured by velocity magnitude and flow visualized using stream lines.

3.3.7 In vitro Biological Test

3.3.7.1 Cytotoxicity Test (Direct Contact Method)

For preliminary in-vitro cytotoxicity study, PEG-PU xerogels with 8mm diameter x 2mm height disc (n=3) were sterilized using 70% ethanol. The sterilized xerogels were swollen to equilibrium using sterile deionized water for the removal of excess ethanol. Excess water was removed and 7 ml of DMEM F-12 medium containing 10% FBS was added, kept at 5 % CO_2 in incubator. Empty wells containing medium alone were used as controls. Media was removed after overnight incubation and one aliquot of the media was subjected to sterility analysis using LB broth. The hydrogels were placed in 6 well plates; A549 cells (Adenocarcinomic human alveolar basal epithelial cells) were seeded at approximately 50000 cells/well with 3 ml of media volume/well in all wells including controls. Microscopic images of the well plates were taken at 0, 24, 48 and 72 hours after seeding.

3.3.7.2 MTT assay

MTT assay was performed to assess cell viability with PEG-PU-1.0 hydrogel. MTT solution was prepared freshly by dissolving MTT in serum free Dulbecco's modified eagle medium (DMEM) at a concentration of 5.0 mg/ml. L929 fibroblast and MCF-7 cells were seeded into 48 well plates at a density of 2.5×10^4 cells/well. Cells were incubated at 37 ^{0}C, 5% CO_2, 95% relative humidity. All scaffolds were washed with 70% ethanol, re-washed with DI water and allowed to dry under laminar air flow. They were sterilized with UV light for 30 min prior to seeding the cells. After 72 hrs of incubation cells were washed with warm PBS. Then MTT was added to each well and kept for 4 hrs incubation. The reaction mixture was removed and 200µL of DMSO was added to dissolve the formazan crystals. It was then kept for 10

minutes and the absorbance was taken at 550nm. The cells were washed with PBS along with 4% paraformaldehyde and images were taken after staining them with nucleus stain.

$$\%\ of\ cell\ viability\ = \frac{Avg\ absorbance\ of\ test}{Avg\ absorbance\ of\ control} \times 100 \qquad (2)$$

3.4 Results and discussion

3.4.1 Synthesis of PEG-PU

Previous reports on the synthesis of PEG and H_{12}MDI based hydrogels employ toxic solvents, chain extenders and required multiple steps,[12-13] whereas we report here on the one-pot, solvent-free method for the synthesis of PEG-PU xerogels by the reaction between neat PEG and H_{12}MDI in the presence of HT as a cross-linking agent. Such benign and prudent approach is the most desirable strategy for the synthesis of polymers for biomedical applications. The reaction was catalysed by DBTDL. The reaction pathway is shown in **Scheme 3.1**.

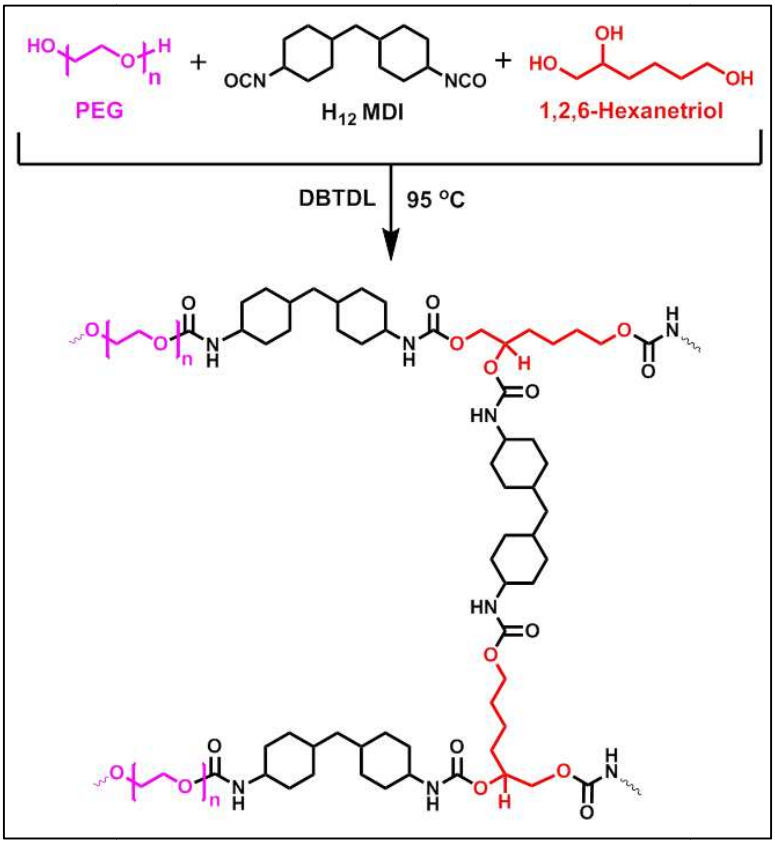

Scheme 3.1: *Reaction scheme for the synthesis of PEG-PU xerogel*

The urethane linkages were formed through the addition reaction between the isocyanate groups of H_{12}MDI and the hydroxyl groups of PEG. The PEG segments contribute as soft segments, whereas the H_{12}MDI part contributes as hard segments. The network structure in the gel is induced by the crosslinking agent, HT. The gels obtained were easy to handle both in the dry and swollen state and found to be mechanically quite strong (the details of the modulus will be discussed in separate section). The as-prepared gels after drying at 37 ^{0}C in an oven for 24hrs (Xerogels) were found to be opaque but became transparent upon hydration with water which indicated the ease of water permeability in the dry gels. The flexibility of the hydrogel strongly depended on the degree of crosslinking. The stoichiometry for the synthesis of PEG-PU Hydrogels with different contents of crosslinking agent is shown in **Table 3.1**. The advantage with this method of synthesis is that, the samples can be prepared into any shape and size.

Table 3.1: *Stoichiometry for the synthesis of PEG-PU Hydrogels*

Sample	**Hexanetriol (mol%)**	**PEG_{4000} (mol x 10^{-3})**	**DBTDL (mol x 10^{-3})**	**H_{12}MDI (mol x 10^{-3})**
PEG-PU-0.25HT	0.25	2.5	0.0237	6.35
PEG-PU-0.5HT	0.5	2.5	0.0237	6.35
PEG-PU-1.0HT	1.0	2.5	0.0237	6.35
PEG-PU-1.5HT	1.5	2.5	0.0237	6.35

3.4.2 Structural Characterization

3.4.2.1 FTIR Spectroscopy

The structural elucidation of PEG-PU gel was performed by FTIR spectroscopy. The stacked plots of FTIR spectra of reactants, PEG-4000, H_{12}MDI and the product, PEG-PU-1.0 HT gel are shown in **Figure 3.1(a)**.

In **Figure 3.1(a)** shows the strong absorption band at 2270 cm^{-1} in H_{12}MDI is ascribed to the C=N (Nitrile) stretch in the isocyanate group (-N=C=O). Whereas, a weak, broad absorption band of hydroxyl end groups (-OH) of PEG-4000 appear at 3400-3500 cm^{-1} due to low density of (-OH) groups. In the case of PEG-PU gel, the

characteristic absorption bands of (–NCO) groups from H_{12}MDI (at 2270 cm^{-1}) and (-OH) groups of PEG-4000 (at 3400cm^{-1}) disappeared indicating the reaction between (–NCO) and (–OH) to form urethane (-NH-COO-) linkages. At the same time, two new peaks appeared in PEG-PU spectrum: one at 3310cm^{-1}, attributed to the N-H stretching in the urethane linkage and the other at 1730cm^{-1}, attributed to the stretching of ester carbonyl groups (>C=O) within the urethane linkages. Further, we also observed strong absorption bands in the range of 2800-3000cm^{-1} which can be ascribed to C-H stretching vibrations. Finally, the absorption band at 1115cm^{-1} in PEG-PU gel is attributed to the characteristic –C-O-C- stretching vibration of the repeating unit -O-CH_2-CH_2- of the PEG-4000. These observations in the FTIR spectroscopy, clearly confirmed the structure of PEG-PU gels.

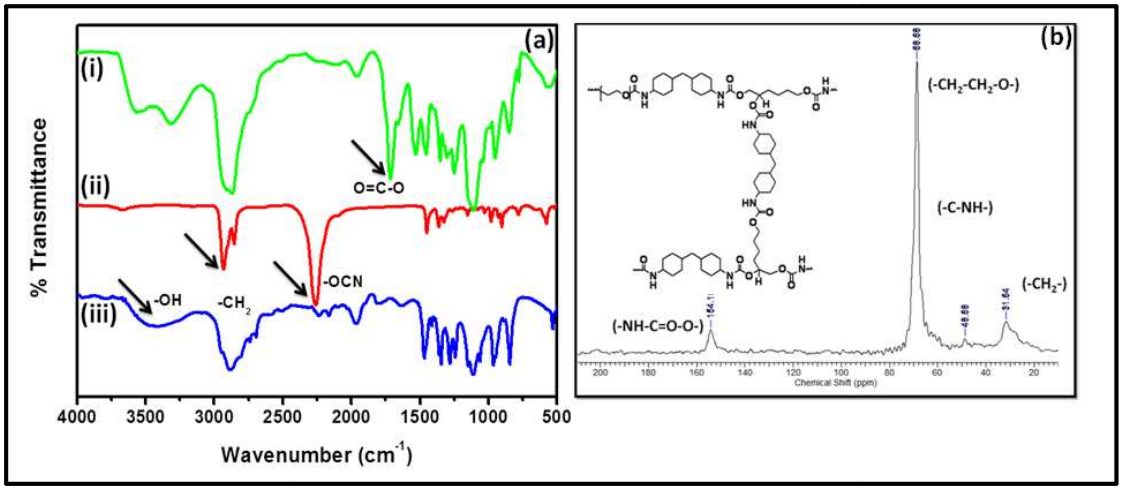

Figure 3.1: *(a) FTIR Spectra of (i) PEG-PU-1.0-HT Xerogel, (ii) H_{12}MDI and (iii) PEG-4000. (b) ^{13}C Solid-state CP-MAS NMR Spectrum of PEG-PU-1.0-HT Xerogel.*

3.4.2.2 ^{13}C Solid-state NMR Spectroscopy

We show in **Figure 3.1(b)**, the Solid-state ^{13}C NMR CP-MAS spectrum of PEG-PU-1.0-HT xerogel. The inset in **Figure 3.1(b)** shows the chemical structure of PEG-PU gel. It can be readily seen from **Figure 3.1(b)** that the methylene groups of PEG attached to oxygen (-CH_2-CH_2-O-) show a strong peak at 68.70 ppm. The (–CH_2) carbon atoms and carbon attached to Nitrogen (–C-NH) appear at 31.6 and 48.6ppm, respectively. The peak due to carbonyl carbon of the urethane linkage (–NH-C=O-O-) is slightly shifted to upfield and appear at 154.1ppm. The observations in the ^{13}C NMR spectrum clearly confirmed the structure of PEG-PU gel.

3.4.3 Swelling Measurements

Swelling in hydrogels is very important in controlled drug delivery and tissue engineering applications. It strongly depends on the degree of crosslinking and the hydrophilicity of the polymer. In the PEG-PU hydrogels that we have synthesized, the degree of crosslinking was controlled by the amount of HT incorporated. Accordingly, we prepared gels by varying the mole ratio of PEG: HT (1: 0.25 - 1.5) and keeping the MW of the PEG constant at 4000g/mol.

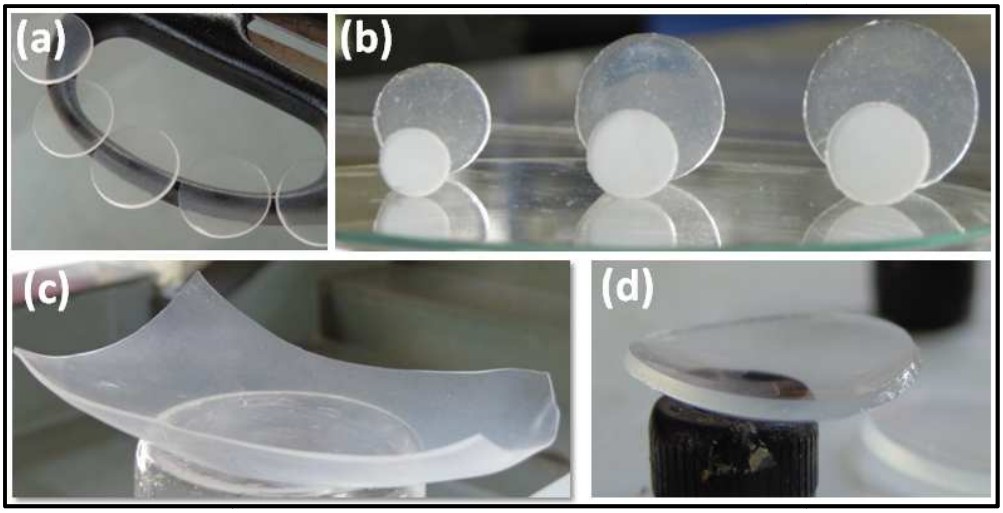

Figure 3.2: *PEG-PU gels (a) Thin swollen disc (b) Dry and water swollen disc (c) Sheet and (d) Thick disc.*

The hydrophilicity of the gel which drives the swelling, comes from PEG segment and can be controlled by varying the MW of PEG. We show in **Figure 3.2 (b),** the dry (Xerogel) and water swollen hydrogels for visual observations. It can be seen that the xerogels are opaque and turn into translucent upon hydration/swelling. The opaque nature of the xerogel can be attributed to the presence of crystallinity in the gel matrix exhibited by the PEG segments. However, this crystallinity is lost upon hydration with water and the hydrogels become translucent/or partially transparent. Upon immersing the xerogel in water, the water molecules diffuse into the polymer to hydrate the polar/hydrophilic groups, leading to the expansion of network and eventually coming to an equilibrium swelling capacity. The equilibrium swelling capacity is determined by a balance between enthalpically favourable water-polymer interaction and the entropic penalty of network chain expansion, as given by Flory-Rehner's theory.[14-16]

We show in **Figure 3.3 (a)**, the equilibrium swelling capacities of PEG-PU hydrogels with four different degrees of crosslinking (4 different contents of HT) measured at room temperature. It can be seen that, the equilibrium swelling ratio decreases with increase in degree of crosslinking and the values reduced from 900% to 300% with HT content increasing from 0.25 to 1.5mol%. The decrease in equilibrium swelling can be attributed to the formation of more compact/interconnectivity structure of network with more degree of crosslinking which prevents the expansion of network.

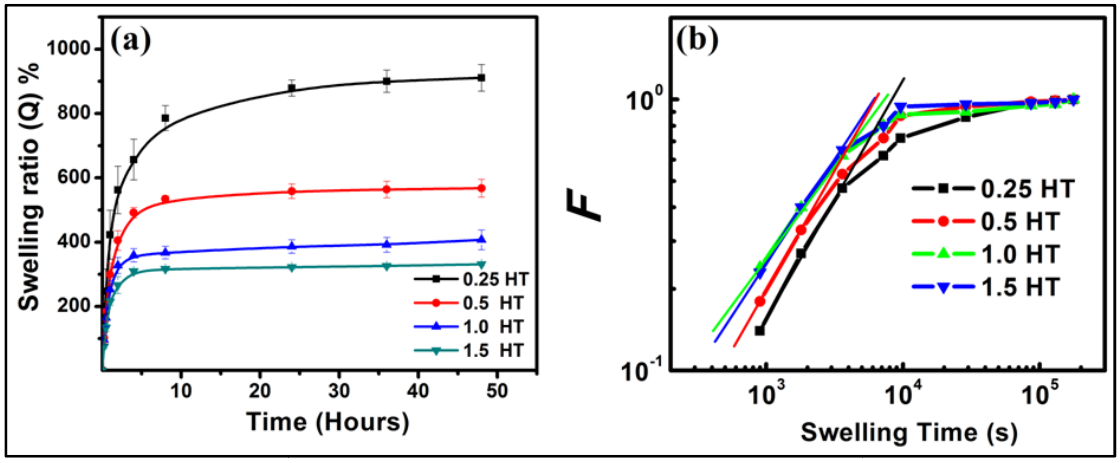

Figure 3.3: *(a) Swelling studies with respect to time for PEG-PU gels with different contents of hexanetriol. (b) Swelling ratio with time at the initial stages of swelling.*

We show in **Figure 3.3 (a)**, the swelling ratio (*Q*), as a function of time'*t*' for PEG-PU gels with 4 different contents of HT. In general, the kinetics of swelling i.e. the time dependence of water uptake in gels can be given as,[17]

$$F(t) = \frac{W_s - W_d}{W_\infty - W_d} = kt^n \qquad (3)$$

Where '*k*' is a swelling rate constant, '*n*' is the swelling exponent, W_d is the weight of dry samples, W_s and W_∞ are the swollen weights at time '*t*' and at equilibrium, respectively. It can be readily seen from **Figure 3.3 (a)** that, the equilibrium swelling reached within 3-4 hours for all the samples indicating reasonably faster diffusion of water molecules in the gel matrix. However, it is important to note here that, the diffusion of water molecules into hydrogel strongly depends on the polymer chain mobility which in turn depends on the glass transition

temperature (T_g) of the polymer.[18] In general, higher the crosslink density, higher is the T_g. If the T_g of the polymer is well below the measurement temperature, then the polymer chains exist in a rubbery state and exhibit a higher mobility. In this case, the water uptake follows Fickian diffusion with swelling exponent, '*n*' close to 0.5. On the other hand, if the T_g of the polymer is higher than the experimental temperature, then the chains are more rigid with a limited mobility in which the polymer chain relaxation rate is lower than water molecule diffusion rate. In such case, the diffusion will be non-Fickian and the value of swelling exponent, '*n*' will be between 0.5 and 1.0.

We show in **Figure 3.3 (b)**, the log-log plots of swelling kinetics for PEG-PU hydrogel with 4 different contents of HT. In the initial stage of swelling, the swelling kinetics profiles increase linearly, following a power law behaviour and then level off upon approaching the equilibrium state of swelling. The swelling exponent, '*n*' could be estimated from the slope of the initial linear region of swelling profile. The values of '*n*' are very close to 0.5 indicating the Fickian diffusion of water molecules into PEG-PU hydrogels.

3.4.4 Micro structural Characterization

3.4.4.1 Wide-Angle X-ray Diffraction (WAXD)

We show in **Figure 3.4 (a)**, the Wide-Angle X-ray Diffraction patterns of PEG-PU xerogels with different contents of HT along with neat PEG-4000. The diffraction patterns of neat PEG-4000 shows two characteristic peaks centered at d-spacing of 4.6 Å ($2\theta=19.2^0$) and 3.8Å ($2\theta=23.4^0$) which can be attributed to the 120 and 132 reflections of PEG monoclinic unit cell,[19-21] respectively.

In order to ascertain the exclusive contribution of PEG segments to the crystalline domain of the gel matrix, we performed WAXD experiments of PEG-PU-1.5HT sample from room temperature to 60 ^{0}C. It can be readily seen from the **Figure 3.4 (b)** that, the diffraction peaks initially observed at *d*-spacing values of 4.6 Å and 3.8 Å at room temperature disappear and give a broad peak at ~4.2 Å, which can be considered as an amorphous halo. This clearly indicates that the crystalline nature of the gel mainly arises from the PEG segments.

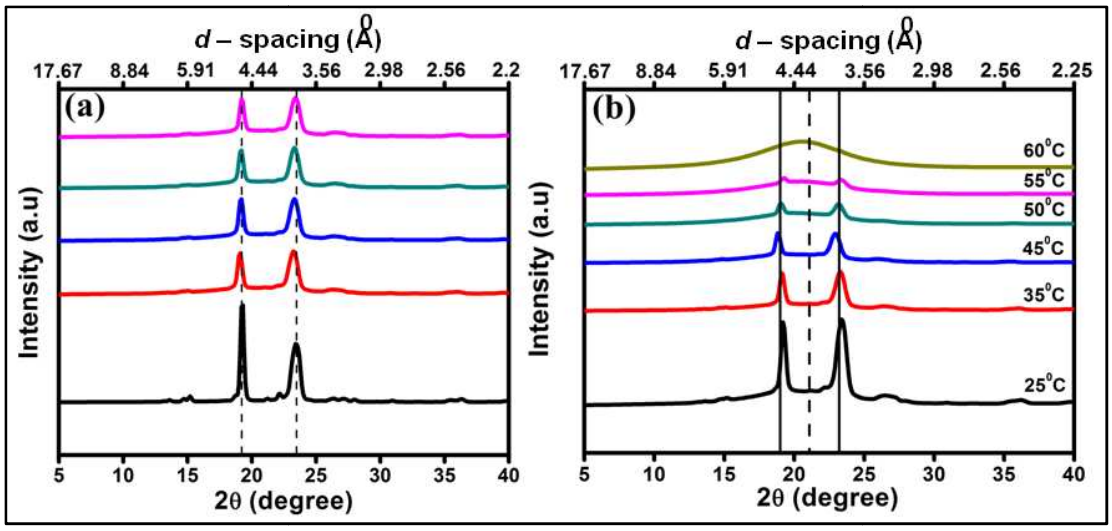

Figure 3.4: ***(a)*** *Wide-Angle X-ray Diffraction patterns of PEG-PU xerogels with different degrees of crosslinking and comparison with neat PEG-4000 at 25 ^{0}C (b) Wide-Angle X-ray Diffraction patterns of PEG-PU-1.5HT xerogels at different temperatures.*

In the case of PEG-PU Xerogels with different contents of HT, the diffraction peaks appear at the same 2θ angles of pure PEG with a similar *d*-spacing value, indicating that only the PEG segments are involved in exhibiting the semi crystalline nature of PEG-PU gels. It is important to note that inspite of the crosslinking of the network, the PEG segments in the gel matrix are able to show the crystalline nature with a reasonable ordering in the structure.

3.4.4.2 Small-Angle X-ray Scattering (SAXS)

To explore further on the microstructure of gels, we performed SAXS experiments on PEG-PU gels at both RT and at 60 ^{0}C. The profiles of scattering intensity as a function of scattering vector are shown in **Figures 3.5 (a-c)**.

Upon heating PEG-PU xerogels closer to the melting of the soft segments (~45 ^{0}C), the scattering peaks in the SAXS spectra shift to the low '*q*' region indicating that the smaller lamellae melt first thereby shifting the average spacing between lamellae to larger values (low '*q*' shift). Finally, the SAXS peak disappears indicating that these peaks in PEG-PU xerogels originate exclusively from the lamellar packings of soft PEG phase.

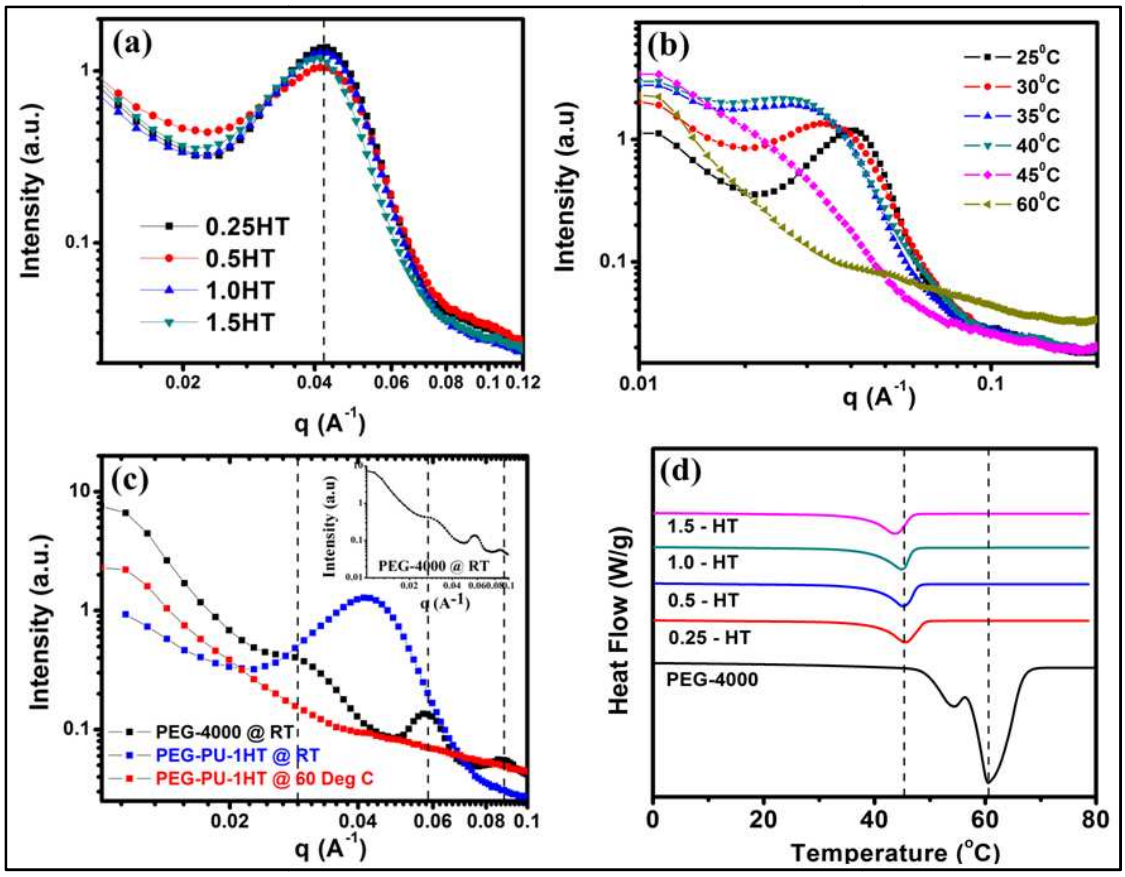

Figure 3.5: *(a) Small-angle X-ray scattering profiles of PEG-PU Xerogels with different degrees of crosslinking at 25 ^{0}C (b) Small-angle X-ray scattering profile of PEG-PU-1.0HT Xerogel at different temperatures (c) overlay of neat PEG-4000, PEG-PU-1.0HT at RT and at 60 ^{0}C and (d) DSC thermograms of neat PEG-4000 and PEG-PU xerogels with different degrees of crosslinking.*

The WAXD peaks also disappear concomitantly in this temperature range, thus further supporting the observation of DSC and SAXS. At the same time, we do not see any separate scattering peaks coming from the hard segments, since the hard segments amount is lower and consists of aliphatic dicyclohexyl diisocyanate (H_{12} MDI).

The scattering vector profiles of PEG-PU gels exhibit a characteristic scattering peak. The relation between scattering vector (q) and scattering angle (θ) is given as,

$$q = \frac{4\pi}{\lambda} sin\ \frac{\theta}{2} \qquad (4)$$

Where 'λ' is the X-ray wavelength (Cu Kα = 1.5418 Å). The average distance'*d*' between domains can be estimated by the peak position using a well established equation as follows:

$$d = \frac{2\pi}{q_{max}} \qquad (5)$$

Where, q_{max} is a scattering vector at maximum intensity of the correlation peak.

In the neat PEG-4000, the multiple scattering peaks upto the third order with relative angular positions of 1:2:3 are discernible. This suggests the crystalline lamellar structure of PEG. From the position of the q_{max} of the first order peak (q_{max} = 0.029Å^{-1}), the *d*-spacing of the crystalline lamellae of PEG was found to be ~23.3nm from the Bragg's equation mentioned above. For the PEG-PU xerogels with different contents of HT, the *d*-spacing value was found to be ~15nm. The lower *d*-spacing values of PEG-PU xerogels is attributed to the intervention of the hard segments in the regular lamellar packing of the segment. It is also important to note that, the scattering peaks in PEG-PU gels can arise due to the crystalline soft segments of PEG or the hard segment domains of isocyanate groups.

However, since the isocyanate content in the PEG-PU xerogels is low and further the isocyanate used is based on aliphatic diisocyanate, we do not expect any major contribution to the crystalline nature of PEG-PU gels. In the SAXS studies, the scattering peaks of PEG-PU gels were shifted to high q region (at 0.042Å) of the neat PEG peak. The shift suggests that, the size of lamellae in the PEG-PU gels are of smaller compared to the lamellar sizes of neat PEG. This observation was further corroborated with DSC measurements on neat PEG and PEG-PU xerogels. From the **Figures 3.5 (d)** the melting endotherm of neat PEG-4000 appeared at ~60 ^{0}C, whereas, the melting endotherms of PEG-PU xerogels appeared in the range of 40-45 ^{0}C. These low melting endotherms indicate the presence of smaller size of PEG lamellae in PEG-PU gels.

3.4.5 Mechanical Properties

The mechanical properties of PEG-PU hydrogels at equilibrium swelling were determined by compression and dynamic oscillatory rheometry at 25 ^{0}C.

We show in the **Figure 3.6 (a)**, the dynamic storage modulus as a function of frequency for PEG-PU xerogels with the crosslinker content of 1.0HT. The dynamic storage modulus (E′), showed slight frequency dependency in 1.0HT Xerogel samples with E′ value closer to 4.2 MPa. We show in **Figure 3.6 (b)**, the visco-elastic behaviour of porous xerogels by performing uni-axial compression studies in which the plots of true stress (true compressive stress is the force per instantaneous cross-sectional area) as a function of strain are given for the xerogel containing 1.0HT. The curves exhibit an initial linear region and slope of which can give the modulus of the gel network. The value of modulus, 5.6MPa obtained is found to be very good compared to other porous hydrogels based on crosslinked PEG-PLLA, which show moduli in the range of 0.02 – 0.160 MPa.[22]

We show in **Figure 3.6 (c)**, the dynamic storage modulus as a function of frequency for PEG-PU hydrogels with different contents of crosslinker, HT. The dynamic storage modulus (E′), showed the frequency independence in all the samples with different contents of HT (0.25 – 1.0HT). However, E′ increased with an increase of degree of crosslinking and reached a value closer to 0.15MPa. This value seems to be on par/slightly better with the many of the hydrogels based on crosslinked poly(ethylene glycol).[23] We show in **Figure 3.6 (e)**, the plots of true stress as a function of strain (**see equations 6 & 7**) for the equilibrium swollen PEG-PU hydrogels containing different amounts of HT. It can be readily seen from the figure that the curves exhibit an initial linear region and the slope of which can give the modulus of the gel network.

The storage modulus (E′) values calculated from the slopes of the initial linear region of curves of PEG-PU hydrogels are plotted against concentration of crosslinker in **Figure 3.6 (d)**. The results indicate that the modulus increases with increase in degree of crosslinking in PEG-PU hydrogels and the values obtained are in the range of 0.002 – 0.23 MPa. It can be seen that even a slight increase in the degree of crosslinking (HT concentration from 0.25 – 1.5%) enhances the modulus (obtained from initial slopes of **Figure 3.6 (e)**) significantly in the PEG-PU hydrogels. These observations clearly indicate that the mechanical strengths of PEG-PU hydrogels can be easily controlled by the degree of crosslinking and the degree of swelling in hydrogels.

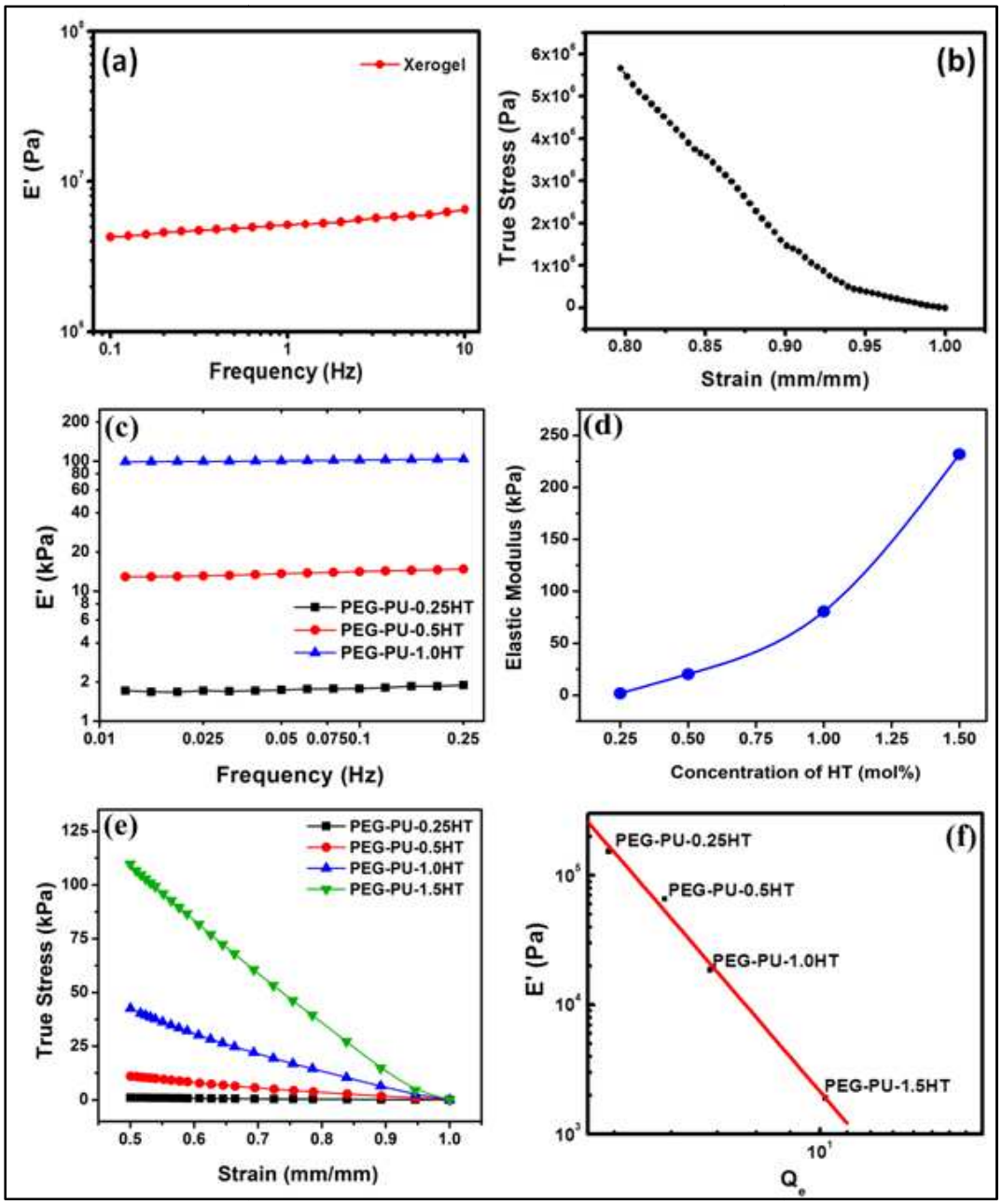

Figure 3.6: *(a) Dynamic oscillatory experiment on PEG-PU-1.0HT xerogel as a function of frequency (b) Uni-axial compression experiment PEG-PU-1.0HT porous xerogel (c) Dynamic oscillatory experiment on PEG-PU hydrogels in swollen state as a function of frequency with different degrees of crosslinking (■) PEG-PU-0.25HT (●)PEG-PU-0.5HT (▲)PEG-PU-1.0HT. (d) Plot of elastic modulus (E') vs crosslinker concentration in mol%. (e) Uni-axial compression experiment of PEG-PU hydrogels in the swollen state with increasing cross linker concentration (■) PEG-PU-0.25HT (●)PEG-PU-0.5HT (▲)PEG-PU-1.0HT (▼) PEG-PU-1.5HT (f) Plot of storage moduli (E') vs equilibrium swelling ratio (Q_e) of PEG-PU hydrogels in water at 25^0C.*

$$\sigma_{true} = normal\ stress \times strain\ (\lambda) \qquad (6)$$

$$Strain\ (\lambda) = \frac{Gel\ thickness\ (h)}{Initial\ thickness\ (h_0)} \qquad (7)$$

It is also important to note that there exists an interesting relationship between the modulus (G') and the equilibrium swelling ratio (Q_e). The classical prediction[24-25] for the relationship between these two parameters is given by eqn (8),

$$G \sim {Q_e}^{-1/3} \qquad (8)$$

This relationship is based on the assumptions that, the network chains follow Gaussian statistics and the network deforms affinely. We show in **Figure 3.6 (f)**, a log-log plot of storage modulus (E′) versus equilibrium swelling ratio (Q_e) of PEG-PU hydrogels with different contents of crosslinker, HT (0.25-1.5 mol %). It can be seen from the figure that, the storage modulus decreases linearly with increasing swelling ratio (Q_e). According to the power law: $G' \sim {Q_e}^{-m}$ with the value of m = 5.2 is quite high compared to the value of 0.33 for the affine networks. This clearly indicates the striking departure from Gaussian behaviour with no affine deformation of the network.

3.4.6 Inducing Porosity into Hydrogels

To accommodate a large number of cells, the scaffold needs to be highly porous with large surface to volume ratio. The porosity, pore size and pore structure of the scaffold are important for nutrient supply of cells. Open interconnected porous network structure enhances the diffusion rate of nutrients. Several pore forming techniques have been reported in the literature which includes porogen leaching,[26-27] saturation and release of CO_2,[28-32] 3-D printing[33-35] and phase separation.[36]

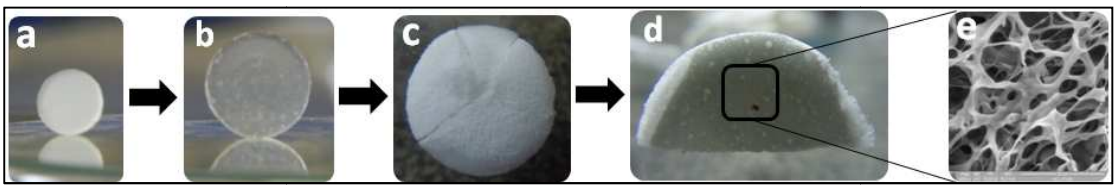

Figure 3.7: *Process of pore formation: (a) PEG-PU-1.0HT Xerogel, (b) PEG-PU-1.0HT Hydrogel, (c) Liquid Nitrogen Quenched PEG-PU-1.0HT Hydrogel (d) Freeze*

dried PEG-PU-1.0HT Porous Xerogel (e) SEM image of PEG-PU-1.0HT Porous Xerogel.

In our work, we have used cryogenic treatment followed by lyophilization method to induce pore structure into PEG-PU hydrogels. The water swollen gels of PEG-PU were subjected to rapid cooling in liquid nitrogen. The frozen water was then removed by sublimation under vacuum leaving behind voids to create porous structure in the hydrogels. We show in **Figure 3.7**, the schematics of the process of pore formation in the PEG-PU hydrogels.

It can be seen from **Figure 3.7** that, the xerogel (a) is opaque and upon swelling in water it becomes transparent (slightly hazy) (b). On liquid nitrogen rapid cooling, the transparent gel becomes opaque again (c) and on lyophilization the gel converts into spongy nature retaining the opaqueness (d). The simple cryogenic treatment method that we have used here is a more faster and template-free approach in comparison with time consuming salt-leaching[37-38] as well as photo-patterning[39] methodology reported for porous hydrogels.

3.4.7 Morphological Analysis

3.4.7.1 Scanning Electron Microscope (SEM)

We show in **Figure 3.8**, the SEM micrographs of lyophilized samples of PEG-PU gels with different contents of HT and compare with the untreated samples of PEG-PU gels.

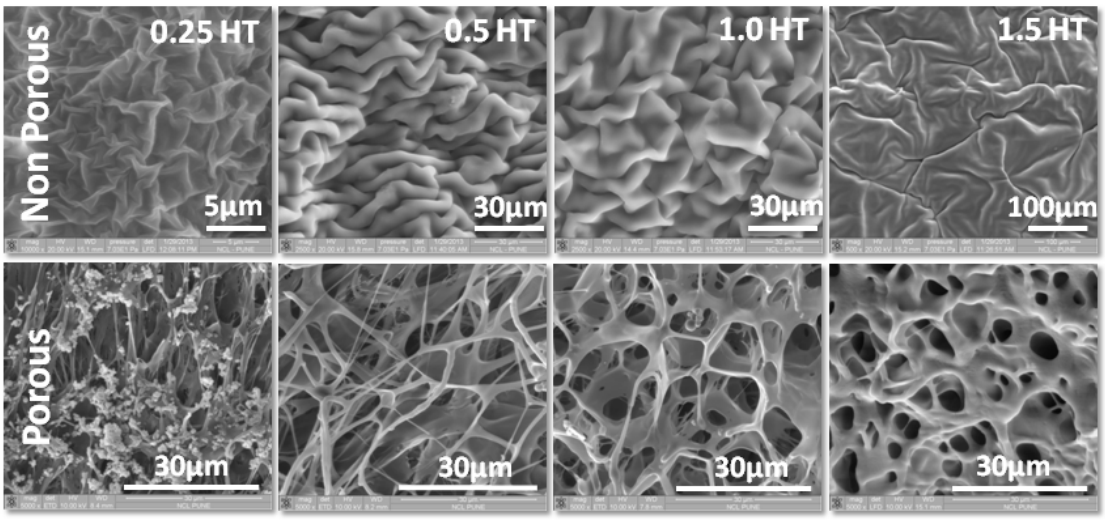

Figure 3.8: *SEM micrographs of the Non-porous and porous PEG-PU gels with different degrees of crosslinking.*

It can be revealed from the figure that, the treated sample exhibits porous structure with the pore sizes in the range of 2-15μm. Pore size ranges required for the adequate growth of different category of cells and/or tissues have been already extensively studied and reported.[40] We found that the pore sizes obtained in our samples are suitable for hosting the endothelial cell transplantation process during the initial stages of tissue regeneration.[41-42]

3.4.7.2 Microcomputed Tomography or Micro-CT (μ-CT)

To investigate further into the microstructure of porous xerogels, a microcomputed tomography [Micro-CT (μ-CT)] technique was used. Micro-CT is a high resolution and non-invasive three-dimensional X-ray imaging technique.[43] The basic principles of the technique are described in Chapter – I.

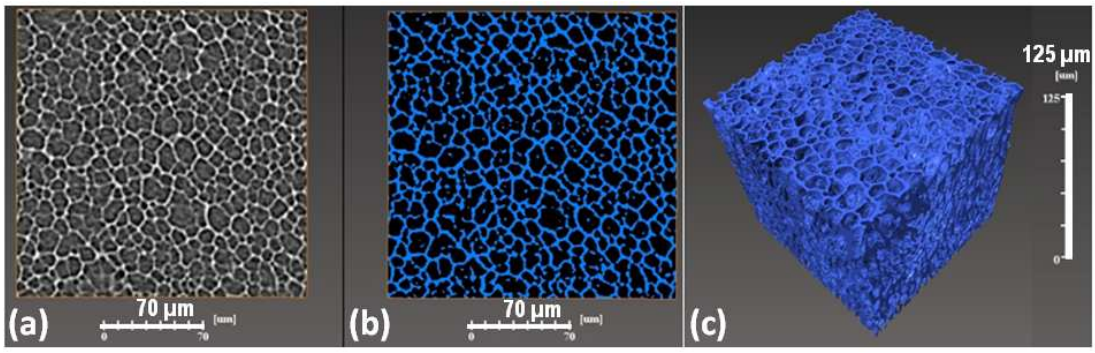

Figure 3.9: *2D-3D μ-CT patterns of the PEG-PU-1.0HT xerogel*

We show in **Figure 3.9 (a)**, the two-dimensional (2D) cross-sectional image of porous PEG-PU- 1.0HT xerogel obtained from μ-CT imaging at 700nm resolution. The cross-sectional image shows interconnected pores with uniform struts of size ranging from 1 to 2 microns. In the 2D image, struts between the pores are clearly visible and show homogenous distribution of pores. Struts of xerogels have adequate contrast even in the absence of contrast agents.

2D images acquired during the imaging were subjected to segmentation **(Figure 3.9 b)** using Avizo Fire 7.0 software (VSG, France) to generate a 3D model **(Figure 3.9 c)** of the porous xerogel. Pore size distribution is evaluated after applying

edge-preserving smoothing filter and watershed algorithm based segmentation of the 2D images. It is important to note that the struts in the 2D images should have sufficient contrast with respect to their background for accurate segmentation.

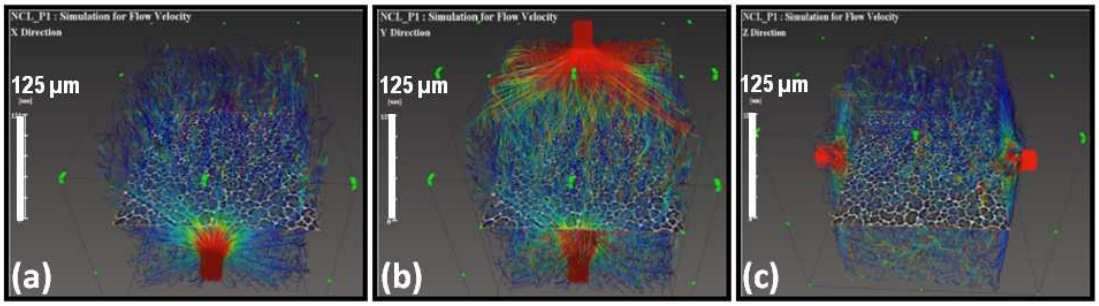

Figure 3.10: *Simulation study of µ-CT patterns of the PEG-PU-1.0HT xerogel.*

The 3D image in **Figure 3.9 c** shows the overall view of the struts as well as pores in three dimensions which can help to qualitatively evaluate their homogeneous distribution. Pore size distribution histogram (**Figure 3.11**), obtained after segmentation of the 2D images shows that the diameter of pores in the porous xerogel ranges from 2 to 16 microns, wherein the pores with 2 microns diameter has higher contribution of up to 40%. This information compliments the data obtained from SEM image of PEG-PU-1.0HT xerogel, which is shown in **Figure 3.8**.

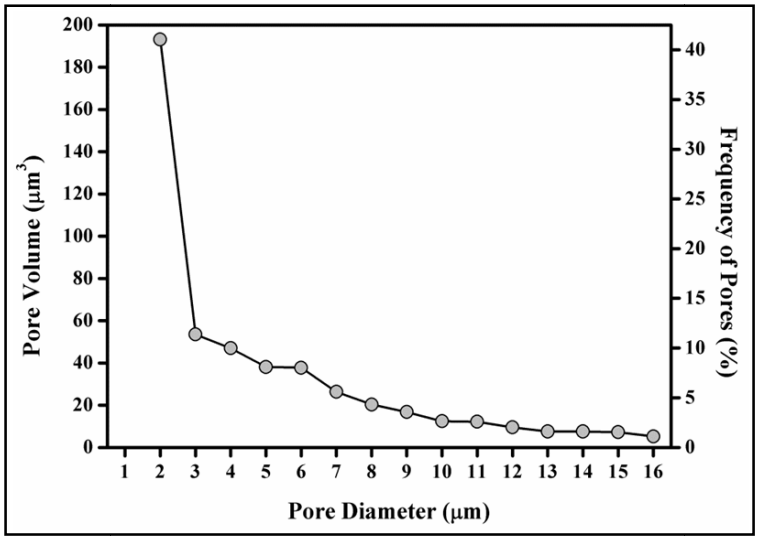

Figure 3.11: *Pore size distribution in porous PEG-PU-1.0HT xerogel.*

Flow simulation performed on the 3D model of PEG-PU-1.0HT xerogel as shown in **Figure 3.10**, is a direct replication of the mass flow taking place in an

implanted scaffold for applications in tissue engineering and regenerative medicine. 3D simulation data sets were coloured by velocity magnitude and flow visualized using stream lines. Red colour end denotes the source of flow into the 3D model of the porous xerogel, which then bifurcates itself into various colours based on the difference in permeability across the specimen. Flow simulation is performed individually on three axes, viz. X, Y and Z, **Figure 3.10 (a-c)** in one direction after arresting rest of the four faces and permeability of the flow is measured using XLab Hydro 7.0 module software (VSG, France).

Among the three co-ordinates, Y axis **Figure 3.10 (b)** shows higher permeability of the order of 8 and 5 times higher than that of X and Z axis respectively (see **Figure 3.10 (a-c))**. This variation in the permeability along Y axis is attributed to the method adopted for pore generation in these xerogels. Forced sublimation taking place during lyophilization of frozen hydrogels follows a uni-axial direction dependent upon the position of the specimen. Hence, the resulting porous xerogel exhibits orientation of the struts along the same direction.

The porous xerogels with tunable micro porosity enable to attain desirable permeability which is very essential for its end use application. Flow simulation provides direct precise permeability analysis based on the exact 3D geometry of the scaffold apart from the diffusion model based analysis which requires additional fluorescent dyes as well as theoretical assumptions.

3.4.8 In vitro Cytotoxicity Test

3.4.8.1 Direct Contact Method

Preliminary studies demonstrate that cells are viable on this substrate. The *in vitro* cytotoxicity of PEG-PU-1.5HT hydrogels was examined using direct contact method. The morphology of cells in direct contact with the surface of PEG-PU-1.5HT hydrogels (**Figure 3.12 e-h**) at different intervals (0, 24, 48 and 72 hours) were similar to that of the cells in the control wells (**Figure 3.12 a-d**) and were viable as indicated by optical micrographs.

Figure 3.12 (a,b) shows that the cells in control wells at 0 and 24 hours shows exponential increase in their population. Similar increase in population of cells was

visible in the PEG-PU-1.5HT gels at 0 and 24 hours (**Figure 3.12 e,f**). **Figure 3.12 g,h** shows continuous cells growth in PEG-PU-1.5HT gels at 48 and 72 hours respectively, which is in terms with the corresponding control wells shown in **Figure 3.12 c,d**. Since the direct contact method shows good cytocompatibility even after 72 hours, further viability analysis were not performed.

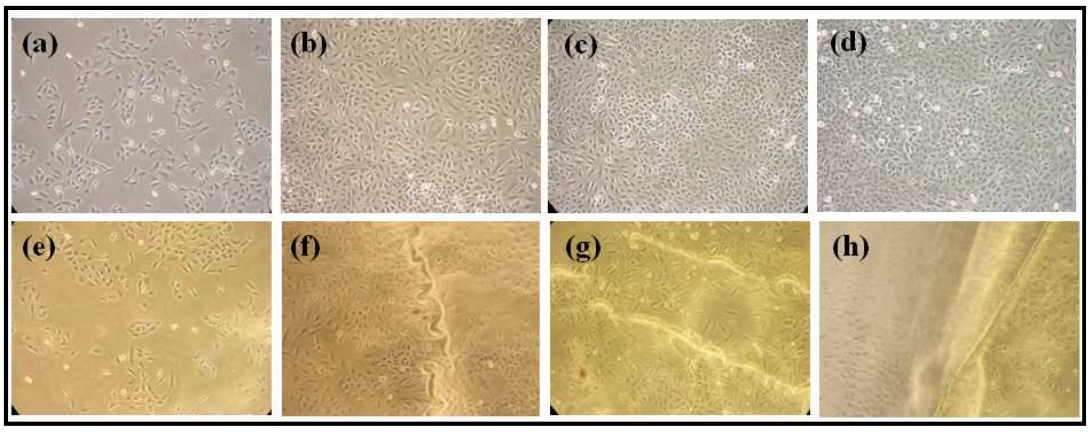

Figure 3.12: *Optical phase contrast images of PEG-PU-1.5HT hydrogels in direct contact with A549 cells for 72 h at 37 ^{0}C. Morphologies of cells in control wells and those in contact with PEG-PU-1.5HT hydrogels are shown in figures (a-d) and (e-h) respectively at 0, 24, 48 and 72 hours.*

3.4.8.2 MTT Assay

Cytotoxicity of PEG-PU-1.0.HT hydrogels was evaluated by MTT assay which is based on the principle of reduction of enzyme succinate dehydrogenase in the presence of dye MTT to purple coloured formazan crystals.

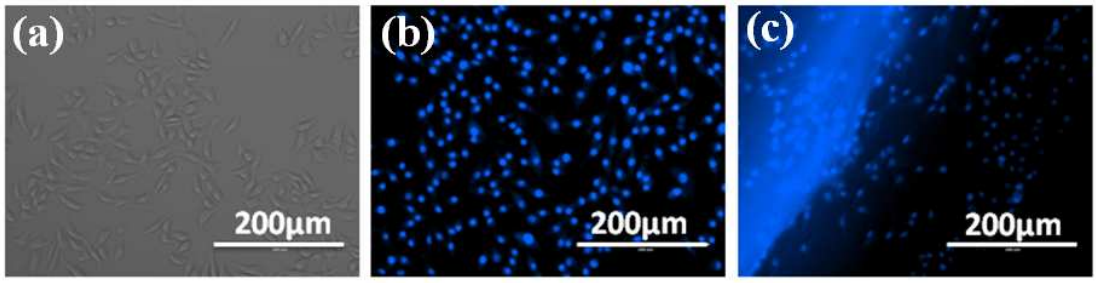

Figure 3.13: *Optical phase contrast images of PEG-PU-1.0 HT hydrogels in MTT Assay with L 929 fibroblast cells for 72 h at 37 °C. (a) Control for L929 Fibroblast cell lines an optical image (b) Control for L929 Fibroblast cell lines an fluorescent image (c) L929 Fibroblast cell after 72hrs treating with the hydrogels.*

Figure 3.13 shows that L-929 fibroblast cells showed almost similar cell viability as compared to the control. Results clearly indicate that PEG-PU-1.0.HT hydrogels are non toxic and exhibit biocompatibility to L-929 fibroblast cells.

3.5 Conclusions

In conclusion, we have synthesized PEG-PU hydrogels using PEG-4000 as soft segment and H_{12}MDI as the hard segment by solvent-free one-pot method. Different degree of crosslinking was effected using different contents of HT in the gel. The chemical structure of the gels was confirmed by FTIR and solid-state ^{13}C NMR spectroscopy. The micro-structural characterization of gels by WAXD and SAXS indicated the presence of crystallinity which was attributed to the ordering of PEG segments in the gel structure. The presence of lamellar structure was shown by the SAXS studies. The DSC studies on PEG-PU gels and the neat PEG-4000 showed comparable decrease in the crystalline melting of (T_m) of PEG-PU gels compared to neat PEG-4000. This can be due to the formation of smaller size of crystalline lamellae of PEGs in the gel structure. The swelling studies on PEG-PU gels at 37 ^{0}C showed Fickian diffusion of water into the hydrogels. The mechanical properties of gels were studied in dry and swollen states using uniaxial compression and dynamic oscillatory rheometry. The results showed an increase in the strength of hydrogels with increase in crosslink density. The porosity in the hydrogel was induced by a method of cryogenic treatment followed by lyophilization. The morphological characterization by SEM, X-ray Micro-CT revealed the porous structure with 2-15μm pore size and the presence of interconnectivity of pores. The cytotoxicity studies of PEG-PU hydrogels showed the continuous growth of cells, which indicated the non-toxic nature of the hydrogels. These hydrogels show a great potential in Tissue Engineering applications.

3.6 References

1. Corneillie, S.; Lan, P. N.; Schacht, E.; Davies, M.; Shard, A.; Green, R.; Denyer, S.; Wassall, M.; Whitfield, H.; Choong, S., Polyethylene glycol-containing polyurethanes for biomedical applications. *Polymer International* **1998,** 46, (3), 251-259.
2. Petrini, P.; Farè, S.; Piva, A.; Tanzi, M. C., Design, synthesis and properties of polyurethane hydrogels for tissue engineering. *Journal of Materials Science: Materials in Medicine* **2003,** 14, (8), 683-686.
3. Patel, A.; Mequanint, K., Novel Physically Crosslinked Polyurethane-block-Poly(vinyl pyrrolidone) Hydrogel Biomaterials. *Macromolecular Bioscience* **2007,** 7, (5), 727-737.
4. Hu, J.; Chen, B.; Guo, F.; Du, J.; Gu, P.; Lin, X.; Yang, W.; Zhang, H.; Lu, M.; Huang, Y.; Xu, G., Injectable silk fibroin/polyurethane composite hydrogel for nucleus pulposus replacement. *Journal of Materials Science: Materials in Medicine* **2012,** 23, (3), 711-722.
5. Gradinaru, L.; Ciobanu, C.; Vlad, S.; Bercea, M.; Popa, M., Synthesis and rheology of thermoreversible polyurethane hydrogels. *Central European Journal of Chemistry* **2012,** 10, (6), 1859-1866.
6. Guan, J.; Fujimoto, K. L.; Sacks, M. S.; Wagner, W. R., Preparation and characterization of highly porous, biodegradable polyurethane scaffolds for soft tissue applications. *Biomaterials* **2005,** 26, (18), 3961-3971.
7. McNeill, M. E.; Graham, N. B., Vaginal pessaries from crystalline/rubbery hydrogels for the delivery of prostaglandin E2. *Journal of Controlled Release* **1984,** 1, (2), 99-117.
8. Graham, N. B.; McNeill, M. E.; Rashid, A., The release of prostaglandin E2 from a novel crystalline-rubbery poly (ethylene oxide) network crosslinked by 3,4-dihydro-2H-pyranyl-2-methyl-(3,4-dihydro-2H-pyran-2-carboxylate). *Journal of Controlled Release* **1985,** 2, 231-244.
9. Badiger, M. V.; McNeill, M. E.; Graham, N. B., Porogens in the preparation of microporous hydrogels based on poly(ethylene oxides). *Biomaterials* **1993,** 14, (14), 1059-1063.

10. Romaškevič, T. B., Saulutė; Pielichowski, Krzysztof; Pielichowski, Jan, Application of polyurethane-based materials for immobilization of enzymes and cells: a review. *Chemija* **2006,** 17, (4), 74.
11. Wu, J.; Ge, Q.; Mather, P. T., PEG−POSS Multiblock Polyurethanes: Synthesis, Characterization, and Hydrogel Formation. *Macromolecules* **2010,** 43, (18), 7637-7649.
12. Wen, T.-C.; Chen, H.-H., Soft segmental effect of methylene bis(p-cyclohexyl isocyanate) based thermoplastic polyurethane impregnated with lithium perchlorate/propylene carbonate on ionic conductivity. *Journal of Applied Polymer Science* **2001,** 80, (7), 935-942.
13. C-H. Yang; W-C. Lin; Liu, F.-J., Waterborne polyurethane single-ion electrolyte from aliphatic diisocyanate and various molecular length of polyethylene glycol. *Polymer Letters* **2007,** 1, (3), 142-149.
14. Flory, P. J.; Rehner, J., Statistical mechanics of cross-linked polymer networks I Rubberlike elasticity. *Journal of Chemical Physics* **1943,** 11, (11), 512-520.
15. Flory, P. J.; Rehner, J., Statistical mechanics of cross-linked polymer networks II Swelling. *Journal of Chemical Physics* **1943,** 11, (11), 521-526.
16. Gusler, G. M.; Cohen, Y., Equilibrium Swelling of Highly Cross-Linked Polymeric Resins. *Industrial & Engineering Chemistry Research* **1994,** 33, (10), 2345-2357.
17. Peppas, N. A., Analysis of Fickian and Non-Fickian Drug Release from Polymers. *Pharmaceutica Acta Helvetiae* **1985,** 60, (4), 110-111.
18. Bajpai, A. K.; Shrivastava, M., Swelling kinetics of a hydrogel of poly(ethylene glycol) and poly(acrylamide-co-styrene). *Journal of Applied Polymer Science* **2002,** 85, (7), 1419-1428.
19. Tadokoro, H.; Chatani, Y.; Yoshihara, T.; Tahara, S.; Murahashi, S., Structural Studies on Polyethers, [-(Ch-2)M-O-]N .2. Molecular Structure of Polyethylene Oxide. *Makromolekulare Chemie* **1964,** 73, 109-127.
20. Takahash, Y.; Sumita, I.; Tadokoro, H., Structural Studies of Polyethers .9. Planar Zigzag Modification of Poly(Ethylene Oxide). *Journal of Polymer Science Part B-Polymer Physics* **1973,** 11, (11), 2113-2122.

21. Takahash, Y.; Tadokoro, H., Structural Studies of Polyethers, (-(Ch2)M-O-)N .10. Crystal-Structure of Poly(Ethylene Oxide). *Macromolecules* **1973,** 6, (5), 672-675.
22. Chiu, Y.-C.; Kocagöz, S.; Larson, J. C.; Brey, E. M., Evaluation of Physical and Mechanical Properties of Porous Poly (Ethylene Glycol)-co-(L-Lactic Acid) Hydrogels during Degradation. *Plos One* **2013,** 8, (4), e60728.
23. Nguyen, Q. T.; Hwang, Y.; Chen, A. C.; Varghese, S.; Sah, R. L., Cartilage-like mechanical properties of poly (ethylene glycol)-diacrylate hydrogels. *Biomaterials* **2012,** 33, (28), 6682-6690.
24. Flory, P. J., *Principles of polymer chemistry*. Cornell University Press: Ithaca, **1953**.
25. Treloar, L. R. G., *The physics of rubber elasticity*. Oxford Univ. Press: Oxford, **2005**.
26. Suh, S. W.; Shin, J. Y.; Kim, J. H.; Kim, J. G.; Beak, C. H.; Kim, D. I.; Kim, S. J.; Jeon, S. S.; Choo, I. W., Effect of different particles on cell proliferation in polymer scaffolds using a solvent-casting and particulate leaching technique. *Asaio Journal* **2002,** 48, (5), 460-464.
27. Zhang, J.; Wu, L.; Jing, D.; Ding, J., A comparative study of porous scaffolds with cubic and spherical macropores. *Polymer* **2005,** 46, (13), 4979-4985.
28. Cansell, F.; Aymonier, C.; Loppinet-Serani, A., Review on materials science and supercritical fluids. *Current Opinion in Solid State & Materials Science* **2003,** 7, (4-5), 331-340.
29. Barry, J. J. A.; Gidda, H. S.; Scotchford, C. A.; Howdle, S. M., Porous methacrylate scaffolds: supercritical fluid fabrication and in vitro chondrocyte responses. *Biomaterials* **2004,** 25, (17), 3559-3568.
30. Quirk, R. A.; France, R. M.; Shakesheff, K. M.; Howdle, S. M., Supercritical fluid technologies and tissue engineering scaffolds. *Current Opinion in Solid State & Materials Science* **2004,** 8, (3-4), 313-321.
31. Barry, J. J. A.; Silva, M. M. C. G.; Popov, V. K.; Shakesheff, K. M.; Howdle, S. M., Supercritical carbon dioxide: putting the fizz into biomaterials. *Philosophical Transactions of the Royal Society a-Mathematical Physical and Engineering Sciences* **2006,** 364, (1838), 249-261.

32. Tai, H.; Popov, V. K.; Shakesheff, K. M.; Howdle, S. M., Putting the fizz into chemistry: applications of supercritical carbon dioxide in tissue engineering, drug delivery and synthesis of novel block copolymers. *Biochemical Society Transactions* **2007,** 35, 516-521.

33. Dhariwala, B.; Hunt, E.; Boland, T., Rapid prototyping of tissue-engineering constructs, using photopolymerizable hydrogels and stereolithography. *Tissue Engineering* **2004,** 10, (9-10), 1316-1322.

34. Hollister, S. J., Porous scaffold design for tissue engineering. *Nature Materials* **2005,** 4, (7), 518-524.

35. Arcaute, K.; Mann, B. K.; Wicker, R. B., Stereolithography of three-dimensional bioactive poly(ethylene glycol) constructs with encapsulated cells. *Annals of Biomedical Engineering* **2006,** 34, (9), 1429-1441.

36. Ricciardi, R.; D'Errico, G.; Auriemma, F.; Ducouret, G.; Tedeschi, A. M.; De Rosa, C.; Laupretre, F.; Lafuma, F., Short time dynamics of solvent molecules and supramolecular organization of poly (vinyl alcohol) hydrogels obtained by freeze/thaw techniques. *Macromolecules* **2005,** 38, (15), 6629-6639.

37. Chang Mo, H.; Shilpa, S.; Mahdokht, M.; Nezamoddin, N. K.; Behnam, Z.; Sang-Hoon, L.; Ali, K., Fabrication of three-dimensional porous cell-laden hydrogel for tissue engineering. *Biofabrication* **2010,** 2, (3), 035003.

38. Park, J. H.; Chung, B. G.; Lee, W. G.; Kim, J.; Brigham, M. D.; Shim, J.; Lee, S.; Hwang, C. M.; Durmus, N. G.; Demirci, U.; Khademhosseini, A., Microporous cell-laden hydrogels for engineered tissue constructs. *Biotechnology and Bioengineering* **2010,** 106, (1), 138-148.

39. Bryant, S. J.; Cuy, J. L.; Hauch, K. D.; Ratner, B. D., Photo-patterning of porous hydrogels for tissue engineering. *Biomaterials* **2007,** 28, (19), 2978-2986.

40. Nasim Annabi, J. W. N., Xia Zhong, Chengdong Ji, Sandeep Koshy, Ali Khademhosseini, Fariba Dehghani, Controlling the Porosity and Microarchitecture of Hydrogels for Tissue Engineering. *Tissue Engineering Part B: Reviews* **2010,** 16, (4), 371-383.

41. Lee, M.; Wu, B. M.; Dunn, J. C. Y., Effect of scaffold architecture and pore size on smooth muscle cell growth. *Journal of Biomedical Materials Research Part A* **2008,** 87A, (4), 1010-1016.

42. Narayan, D.; Venkatraman, S. S., Effect of pore size and interpore distance on endothelial cell growth on polymers. *Journal of Biomedical Materials Research Part A* **2008,** 87A, (3), 710-718.

43. Ho, S. T.; Hutmacher, D. W., A comparison of micro CT with other techniques used in the characterization of scaffolds. *Biomaterials* **2006,** 27, (8), 1362-1376.

Influence of hydrophilic/hydrophobic diols on the properties of polyurethane hydrogels

Chapter – IV

In the fourth chapter, we have synthesized and characterized PU hydrogels using different diols namely, Polycaprolactone diol (PCL), Poly (hexamethylene carbonate) diol (PCD), and Tetraol (FTL) in combination with Polyethylene glycol (PEG). The characterization techniques such as, FTIR, WAXD, SEM, in vitro drug release, in vitro degradation, biological tests etc., used for studying the structural, micro-structural, surface morphology, mechanical behavior, drug release kinetics, degradation profile and cytotoxicity of the hydrogels were briefly explained.

Patent Application No: 3555DEL2015 (Prov. Date: 02/11/2015)

4.1 Introduction

A great variety of building blocks are commercially available that allow the chemical and physical properties of polyurethanes (PUs) to be tailored to their biomedical and pharmaceutical applications.[1-17] In PUs, the hard segment block consists of a diisocyanate and a chain extender, whereas the soft segment is usually a polyol, either hydroxyl- or amine- terminated polyester, polyether, or polycarbonate.[18-29] The flexible soft segment gives the PUs great elasticity, whereas the hard segment contributes strength. Generally speaking, the two segments are incompatible with each other and tend to form a nanoscale phase-separated morphology. It has been recognized that polyester-based polyurethanes are not suitable for long-term implant because of their susceptibility to hydrolytic degradation. Polyether based polyurethanes, while hydrolytically stable, are subject to oxidative degradation.[30-35]

In this chapter, we have synthesized and characterized PU hydrogels using different diols namely, polycaprolactone diol (PCL), poly (hexamethylene carbonate) diol (PCD), and tetraol (FTL) in combination with polyethylene glycol (PEG). The ratio of PEG to other diol was varied in three different samples. The objective was to study the influence of different types of diols on the properties of the obtained hydrogels and their effect on the controlled release of active pharmaceutical ingredients from the hydrogels.

4.2 Experimental

4.2.1 Materials

PEG (MW~4000g/mol) and dibutyltin dilaurate (DBTDL) were obtained from Merck India; 4,4' methylenebis(cyclohexyl isocyanate) (H_{12}MDI), Polycaprolactone diol (MW~2000g/mol), Poly (hexamethylene carbonate) diol (MW~2000g/mol) and Amano Lipase PS, from Burkholderia cepacia was purchased from Sigma Aldrich, USA; 1,2,6 Hexanetriol (HT) was obtained from Fluka USA. Dulbecco's Modified Eagle Medium (DMEM) and Fetal Bovine Serum (FBS) were purchased from Invitrogen USA; Dulbecco's Phosphate buffered saline (DPBS) was obtained from

HiMedia India. Tetraol (gifted sample from Solvay, Italy). All the chemicals were of analytical grade and used as received.

4.2.2 Synthesis of PU Hydrogels

PEG [MW ≈ 4000 g/mol] and PCL [MW ≈ 2000 g/mol] was vacuum-dried at 60 °C and 70^0 C respectively for 6 h in a rotary evaporator to remove any residual moisture and stored in a sealed flask in an oven at 70 °C until use. To the 10 g of molten PEG, 5 g of molten PCL and 0.335 g of HT were added and kept in a rotary evaporator for 2 h to form homogeneous solution. To this solution, 1.5 mL of 4,4′ methylenebis (cyclohexyl isocyanate) and 13.6 μL of DBTDL were added using a syringe under nitrogen atmosphere. The whole mixture was kept in a rotary evaporator for 20−30 min at 70 °C until the mixture becomes more homogeneous and then poured in to presilanated glass Petri-dishes, or appropriate Teflon molds (as per the dimensions required for studies). The Petri dishes/molds were kept in oven at 95 °C for 4 h for gelation. After gelation, the Petri dishes/molds were cooled, and the hydrogel discs were removed by immersing the Petri dishes in distilled water for 4−5 h. The unreacted PEG was removed by washing the hydrogels in excess distilled water for a few days with frequent replenishment of fresh distilled water.

Table 4.1: *Stoichiometry for the synthesis of PU Hydrogels with different polyols*

Sample	Hexanetriol (molx10^3)	PEG_{4000} (molx10^3)	DBTDL (molx10^3)	$H_{12}MDI$ (molx10^3)	PCL_{2000} (molx10^3)	PCD_{2000} (molx10^3)	FTL_{2150} (molx10^3)
PEG-PCL-0.25	2.5	2.5	0.0237	6.66	0.62	-	-
PEG-PCL-0.5	2.5	2.5	0.0237	7.01	1.25	-	-
PEG-PCL-1.0	2.5	2.5	0.0237	8.19	2.5	-	-
PEG-PCD-0.25	2.5	2.5	0.0237	6.66	-	0.62	-
PEG-PCD-0.5	2.5	2.5	0.0237	7.01	-	1.25	-
PEG-PCD-1.0	2.5	2.5	0.0237	8.19	-	2.5	-
PEG-FTL-0.25	2.5	2.5	0.0237	6.66	-	-	0.62
PEG-FTL -0.5	2.5	2.5	0.0237	7.01	-	-	1.25
PEG-FTL -1.0	2.5	2.5	0.0237	8.19	-	-	2.5

By using the same procedure, hydrogels with different PCL contents were prepared with 0.0, 0.25, 0.5, and 1.0, mol % of PCL abbreviated as PU-PEG (without PCL), PU-PCL-0.25, PU-PCL-0.5, and PU-PCL-1.0, respectively. Using the same

procedure, hydrogels with different content of different diols (PCD [MW ≈ 2000 g/mol] and FTL [MW ≈ 2150 g/mol]) were also prepared and the abbreviations and stoichiometry used for all the reactions is given in **Table 4.1.**

4.2.3 Preparation of porous PU hydrogels

Porous PU xerogels were prepared by cryogenic treatment of fully swollen PU-hydrogels followed by removal of ice crystals by lyophilization. The fully swollen hydrogels (20 mm diameter × 10 mm height) were placed in liquid nitrogen for 15 min and then freeze-dried in a lyophilizer (Christ Alpha 1−4, Germany) for 10−12 h.

4.3 Characterization

4.3.1 Structural Characterization

4.3.1.1 FTIR

The structural characterization of PU-PCL, PU-PCD and PU-FTL hydrogels was performed by FTIR. Experimental details are given in Chapter 3 (Section-3.3.1.1).

4.3.2 Swelling Measurements

The swelling behaviour of the above hydrogels was studied using gravimetric method. Experimental details are given in Chapter 3 (Section-3.3.2).

4.3.3 Micro structural Characterization

4.3.3.1 Wide-angle X-ray diffraction (WAXD)

Wide-angle X-ray diffraction (WAXD) technique was used to detect the microstructure of PU-PCL, PU-PCD, PU-FTL xerogels. Experimental details are given in Chapter 3 (Section-3.3.3.1).

4.3.4 Mechanical Properties

Tensile tests were carried out with Instron Universal Testing Machine (UTM-33R) with a load cell of 10 kN, at room temperature with an elongation rate of 10 mm/sec. The hydrogel samples for tensile testing were having dimension of 35mm

length x 10mm width x1mm thickness. Compressive tests were carried out in the same machine with a load cell of 10 kN, at room temperature with a compression speed of 10 mm/sec. The swollen hydrogel samples for compression testing were having length to diameter ratio of 1:1.

4.3.5 Morphological Analysis

4.3.5.1 Scanning electron microscopy (SEM)

Scanning electron microscopy (SEM) was used to investigate the morphology of the hydrogels, xerogels and porous xerogels using Quanta 200 3D dual beam ESEM (FEI, Finland). Experimental details are given in Chapter 3 (Section-3.3.6.1).

4.3.6 In vitro Degradation study

The mass loss (ML) study was conducted by immersing 20 mg xerogel (n = 3) into 5 mL of PBS (pH = 7.4) and incubating at 37 °C. At various time intervals, the hydrogel was washed with deionized water and weighed. Similarly, mass loss study was also conducted with Amano lipase PS enzyme in combination with PBS (7.4). The mass loss was monitored as a percentage of peak weight as shown in eqn (1).

$$\%\, degradation = \frac{M_S}{M_{max}} \times 100 \qquad (1)$$

Where, M_S is hydrogel sample were collected at regular intervals and their mass after swelling and M_{max} equilibrium swollen hydrogel.

4.3.7 In vitro Release Study

Previously weighed dry hydrogel samples were loaded with doxorubicin by immersing them in PBS 7.4 solution of a drug until equilibrium was reached. The loaded hydrogels were then dried at room temperature for 5 days and weighed to obtain the concentration of drug in the hydrogels. To study the drug delivery kinetics, the loaded hydrogels were immersed in 5 ml PBS solution (pH 7.4) at 37^0 C, which was kept in shaking water bath and maintained till the complete release. To follow the kinetics of release, aliquots (1 ml) were withdrawn at specific intervals of time and replenished with an equal amount of fresh pH solution so as to maintain the constant volume. These aliquots were analyzed by UV spectrophotometer (UV-1601 PC,

Shimadzu Scientific Instrument) at wavelength 480 nm and the drug concentration was determined using calibration curve.

4.3.8 In vitro Biological Test

4.3.8.1 MTT assay

MTT assay was performed to assess cell viability with all PU hydrogels. Experimental details are given in Chapter 3 (Section-3.3.7.2).

4.4 Results and discussion

4.4.1 Synthesis of PU hydrogels

PU xerogels were synthesized by the reaction between neat PEG, PCL, PCD, FTL and H_{12}MDI in the presence of HT as a cross-linking agent. The reaction was catalysed by DBTDL and the reaction pathway is shown in **Scheme 4.1**.

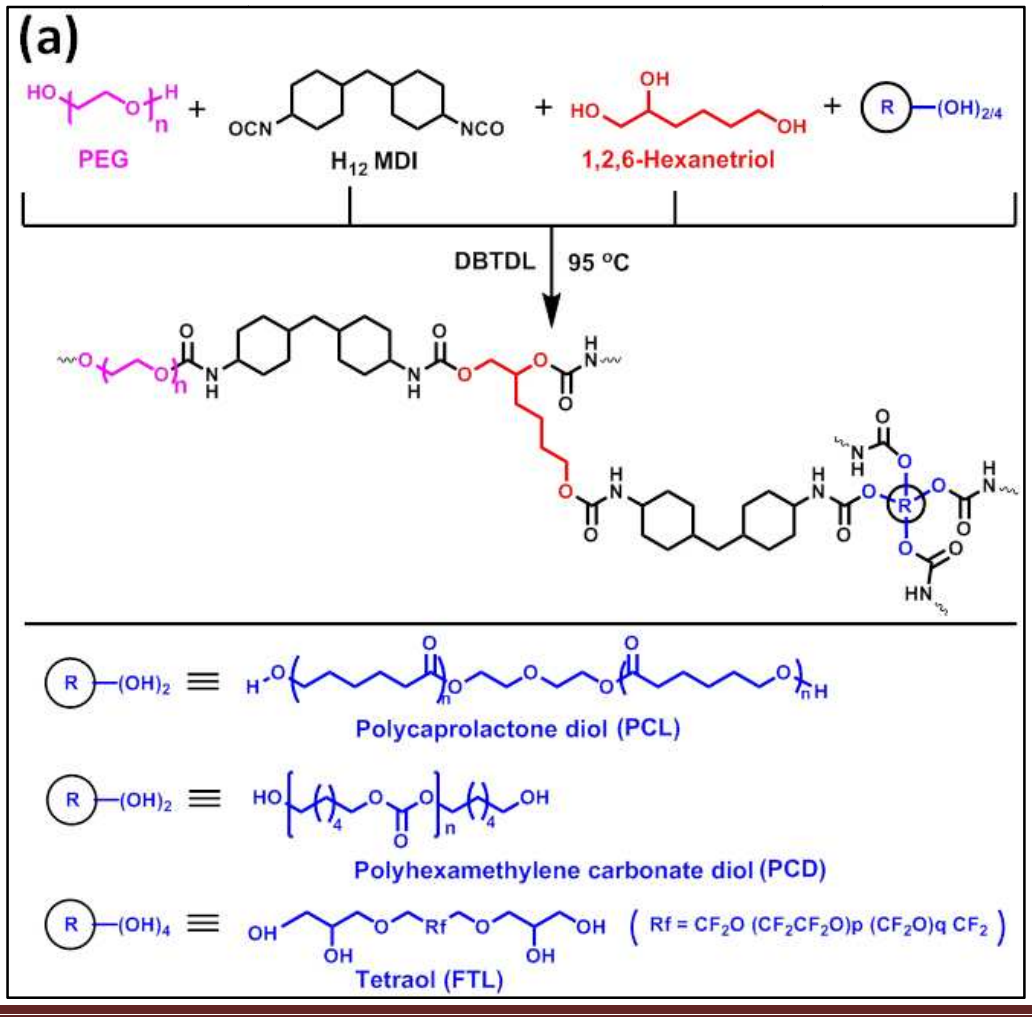

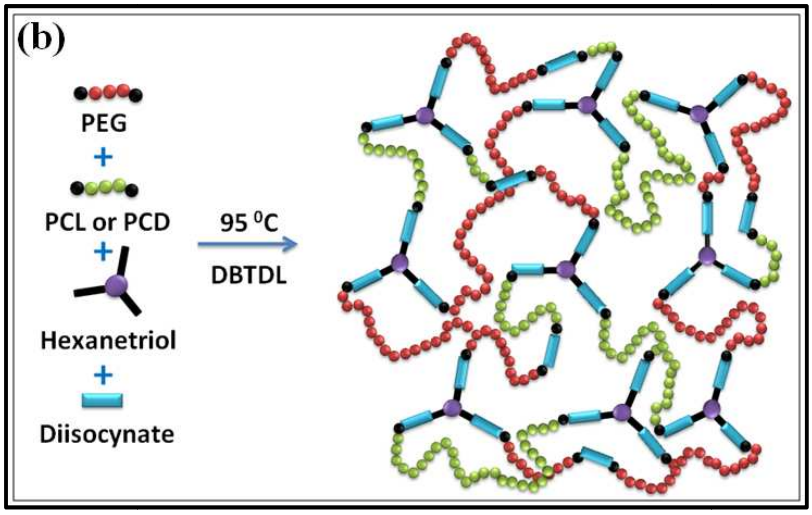

Scheme 4.1: *Reaction scheme for the synthesis of PU xerogel (a) schematic representation and (b) graphical representations.*

The urethane linkages were formed through the addition reaction between the isocyanate groups of H_{12}MDI and the hydroxyl groups of PEG, PCL, PCD and FTL. The PEG, PCL, PCD and FTL segments contribute as soft segments, whereas the H_{12}MDI part contributes as hard segments. The network structure in the gel is induced by the crosslinking agent, HT. The PU gels obtained were easy to handle both in the dry and swollen state and found to be mechanically quite strong (the details of the modulus will be discussed in separate section). The as-prepared gels after drying at 37 ^{0}C in oven for 24hrs (Xerogels) were found to be opaque but became transparent upon hydration which indicated the ease of water permeability in the dry gels. The flexibility of the hydrogel strongly depended on the degree of crosslinking. The advantage with this method of synthesis is that, the samples can be prepared into any shape and size.

4.4.2 Structural Characterization

4.4.2.1 FTIR Spectroscopy

The structural elucidation of PU hydrogels was performed by FTIR spectroscopy. The stacked plots of FTIR spectra of reactants, PEG-4000, PCL-2000, PCD-2000, FTL-2150, H_{12}MDI and the product, PU gels are shown in **Figure 4.1 (a, b and c)**. These observations in the FTIR spectroscopy, clearly confirm the structure of PU gels.

In **Figure 4.1 (a, b and c),** the strong absorption band at 2270 cm^{-1} in $H_{12}MDI$ is ascribed to the C≡N (Nitrile) stretch in the isocyanate group (-N=C=O). Whereas, a weak, broad absorption band of hydroxyl end groups (-OH) of PEG-4000 appear at 3400-3500 cm^{-1} due to low density of (-OH) groups. In the case of PU gels, the characteristic absorption bands of (–NCO) groups from $H_{12}MDI$ (at 2270 cm^{-1}) and (-OH) groups of PEG-4000 (at 3400cm^{-1}) disappeared indicating the reaction between (–NCO) and (–OH) to form urethane (-NH-COO-) linkages. At the same time, two new peaks appeared in PU spectrums: one at 3310cm^{-1}, attributed to the N-H stretching in the urethane linkage and the other at 1730cm^{-1}, attributed to the stretching of ester carbonyl groups (>C=O) within the urethane linkages. Further, we also observed strong absorption bands in the range of 2800-3000cm^{-1} which can be ascribed to C-H stretching vibrations. Finally, the absorption band at 1115cm^{-1} in PU gels is attributed to the characteristic –C-O-C- stretching vibration of the repeating unit -O-CH_2-CH_2- of the PEG-4000.

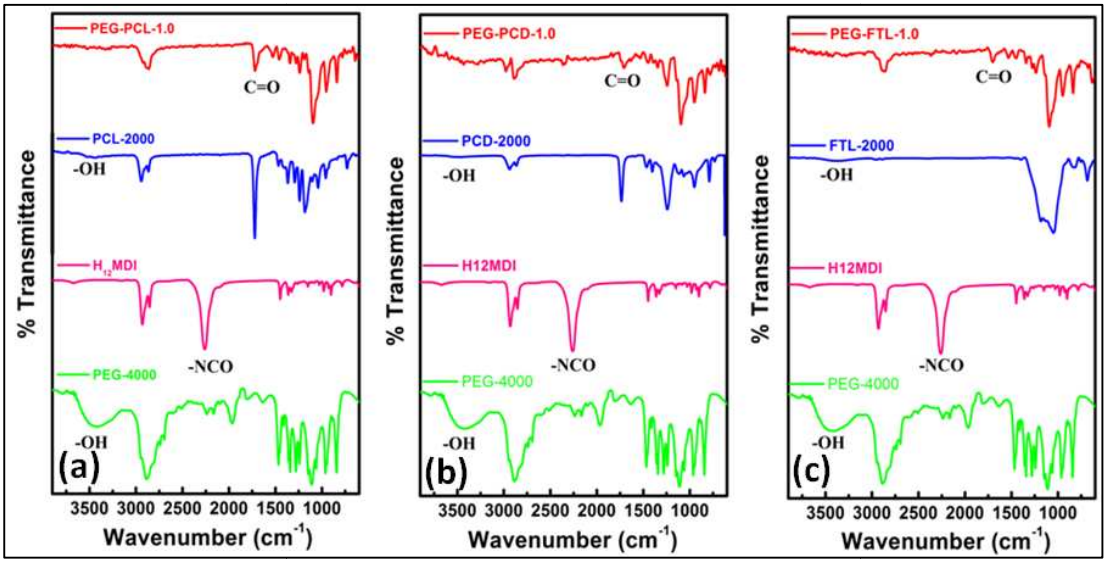

Figure 4.1: *FTIR Spectra of (a) PU-PCL Xerogel, (b) PU-PCD Xerogel, and (c) PU-FTL Xerogel.*

4.4.3 Swelling Measurements

Swelling in hydrogels strongly depends on the degree of crosslinking and the hydrophilicity of the polymer. In the PU hydrogels that we have synthesized, the degree of crosslinking was controlled by the amount of HT incorporated and the

hydrophobicity of diols. Accordingly, we prepared gels with different contents of diols.

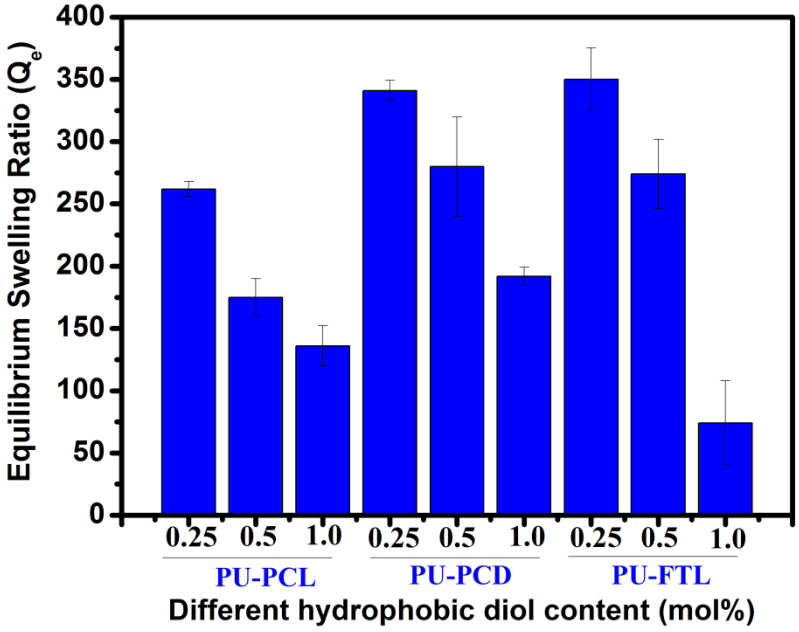

Figure 4.2: *Equilibrium swelling ratio of PU gels with different hydrophobic diols.*

We show in **Figure 4.2**, the equilibrium swelling capacities of PU hydrogels with three different hydrophobic diols incorporated in 3 different levels. It can be seen that, the equilibrium swelling ratio decreases with increase in different hydrophobic diols content and the values reduced from 400% to 75%. The decrease in equilibrium swelling can be attributed to the increase in the overall hydrophobicity of the gels. It shows that hydrophobic character of the gels is clearly manifested in the swelling of gels.

The hydrophilicity of the gel which drives the swelling comes from PEG segment and can be controlled by varying the MW of PEG. Higher the MW of PEG, higher will be the swelling ratio. We show in **Figure 4.3,** the dry (Xerogel) and water swollen PU hydrogels for visual observations. It can be seen that the xerogels are opaque and turn into translucent upon hydration/swelling. The opaque nature of the xerogel can be attributed to the presence of crystallinity in the gel matrix exhibited by the PEG, PCL and PCD segments. However, this crystallinity is lost upon hydration with water and the hydrogels become translucent/or partially transparent.

Figure 4.3: *PU- PCL, PU- PCD and PU- FTL gels*

4.4.4 Micro structural Characterization

4.4.4.1 Wide-Angle X-ray Diffraction (WAXD)

The versatility of polymeric materials, widely used in various forms, arises from the complex structural organization in these materials. X-ray diffraction has been successfully used to study various aspects of these structures in semi-crystalline polymers. It could be hypothesized that a hydrophobic segment might adversely affect the stability of the materials. However, these hydrogels may behave like semi-crystalline polymers utilizing both crystalline regions and amorphous regions. Crystallinity is known to have a positive effect on the mechanical properties and solubility of polymers. It is assumed that the hydrophilic segments could provide the water absorption, fluid flow, and lubricious properties needed while the hydrophobic segments (crystalline regions) provide the strength, tear, and shear resistance. The polymer properties may be varied based on the ratio of hydrophobic to hydrophilic composition. Further, because the polymers must overcome the heat and entropy

factors associated with the crystalline regions during dissolution, the polymers are expected to have excellent dissolution resistance in the body.

We show in **Figure 4.4**, the Wide-Angle X-ray Diffraction patterns of PU xerogels containing PCL, PCD and FTL along with neat PEG-4000. In **Figure 4.4 (a)** the diffraction patterns of neat PEG-4000 shows two characteristic peaks centered at *d*-spacing of 4.6 Å ($2\theta=19.2^0$) and 3.8Å ($2\theta=23.4^0$) which can be attributed to the 120 and 132 reflections of PEG monoclinic unit cell,[36-38] respectively. The diffraction patterns of neat PCL-2000 shows two characteristic peaks centered at *d*-spacing of 4.1 Å ($2\theta=21.4^0$) and 3.8 Å ($2\theta=23.7^0$) which can be attributed to the 110 and 200 reflections of PCL monoclinic unit cell, respectively. In **Figure 4.4 (b)** the diffraction patterns of neat PCD-2000 shows two characteristic peaks centered at *d*-spacing of 4.4 Å ($2\theta=20.18^0$) and 3.8Å ($2\theta=23.48^0$) which can be attributed to the 110 and 200 reflections of PCD monoclinic unit cell, respectively. As shown in **Figure 4.4 (b)**, two sharp reflection peaks have appeared on the broad hump of amorphous region.

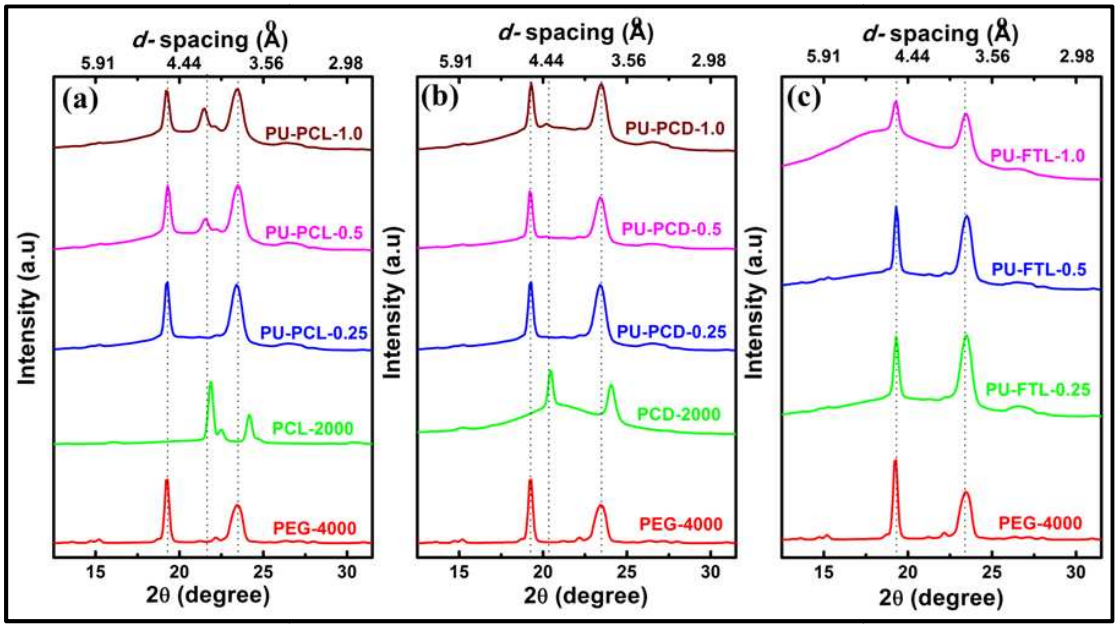

Figure 4.4: *Wide-Angle X-ray Diffraction patterns of the PU xerogels with different hydrophobic diols and comparison with neat PEG-4000, PCL-2000 and PCD-2000 at 25 ^{0}C WAXD patterns of (a) PU-PCL xerogels with different PCL content (b) PU-PCD xerogels with different PCD content and (c) PU-FTL xerogels with different FTL content.*

In the case of PU xerogel with different contents of PCL, the diffraction peaks appear at the same 2θ angles of pure PEG with a similar *d*-spacing value, indicating that only the PEG segments are involved in exhibiting the semi crystalline nature of PU-PCL-0.25 xerogel. As the PCL content increases, the intensity of peak at 4.1Å increases indicating the higher amount of PCL in the PU-PCL gels. Similar observations were made in the WAXD studies of PU-PCD and PU-FTL xerogels where in, the diffraction peaks appears at the same 2θ angles of pure PEG with a similar *d*-spacing value. However, at the higher amount of hydrophobic diols (PCD, FTL), the crystallinity of the gels decreases and the amorphous nature of the gels ensue. It is important to note that inspite of the crosslinking of the network, the PEG, PCL and PCD segments in the PU gel matrix are still able to show the crystalline nature with a reasonable ordering in the structure.

4.4.5 Mechanical Properties

The mechanical properties of PU-PCL, PU-PCD and PU-FTL hydrogels were determined in compression and extension modes using Instron Universal Testing machine (UTM-33R) with a load cell of 10kN. A typical tensile stress-strain and compressive stress-strain curves are shown in **Figure 4.5** (a) and (b). The tensile strength and compressive strength, percentage elongation and percentage compression at break are determined for all the samples. The results are summarized in **Table 4.2.**

Table 4.2: *Mechanical properties of the hydrogels.*

	PU-PEG	**PU-PCL**			**PU-PCD**			**PU-FTL**		
	1.0	**0.25**	**0.5**	**1.0**	**0.25**	**0.5**	**1.0**	**0.25**	**0.5**	**1.0**
Q_e	405	260	175	140	340	280	190	350	275	75
Tensile Strength (MPa)	0.22	0.41	1.02	1.48	0.46	0.94	1.05	0.28	1.04	2.82
Elongation (%)	72	240	35	196	92	68	222	50	43	13
Compressive Strength (MPa)	0.92	2.88	3.37	29.3	1.65	5.44	23.6	1.92	4.6	14.5
Compression (%)	59	66	51	89	43	72	86	51	69	83

It can be readily seen from the **Table 4.2** that, replacing some part of PEG diol with PCL, PCD and FTL diols has improved the mechanical properties of the hydrogels. Compared to the tensile strength of neat PU-PEG hydrogels (0.22 MPa), the tensile strength of PU-PCL, PU-PCD and PU-FTL hydrogels increased from 0.41 MPa to 1.48 MPa; 0.46 MPa to 1.05 MPa and 0.28 MPa to 2.82 MPa, with increase in diol content from 0.25 to 1.0 respectively. Similarly, the compressive strength also increased from 2.88 MPa to 29.3 MPa; 1.65 MPa to 23.6 MPa and 1.92 MPa to 14.5 MPa respectively for PU-PCL, PU-PCD and PU-FTL hydrogels. The percentage of elongation has increased significantly from 70% to ~200% in the case of PU-PCL and PU-PCD hydrogels but decreased considerably in the case of PU-FTL hydrogels. The decrease in % elongation for PU-FTL hydrogels can be attributed to the fact that, fluoro based polyol can induce extra crosslinking in the structure and make the hydrogel harder resulting into decrease in % elongation and compressive strength. Further, the hydrophobic characteristic of the hydrogel increase due to the presence of fluoro groups in the hydrogels which also can play a role in decreasing the % elongation.

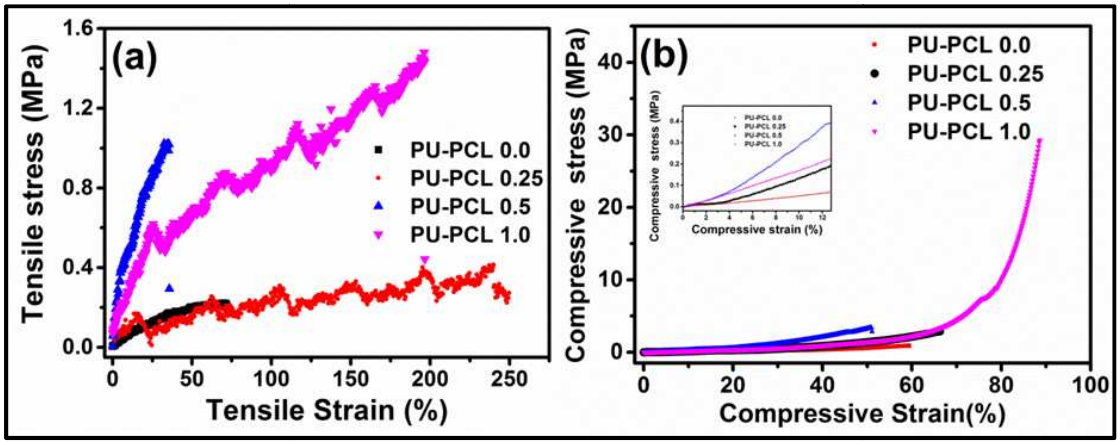

Figure 4.5: *A typical tensile stress-strain (a) and compressive stress-strain curves (b) for PU-PCL hydrogels.*

From the **Table 4.2,** it is discernible that the overall tensile and compressive strength have increased significantly for all the gels compared to the PU-PEG hydrogels. This could be due to the fact that the equilibrium swelling ratios of the PU-PCL, PU-PCD and PU-FTL hydrogels have decreased as compared to the PU-PEG hydrogels. Further, there is also a significant decrease in the swelling ratios as the

PCL, PCD, FTL content increases. However, it is important to note that, even at this swelling ratio the values of tensile and compressive strengths are good for the application in tissue engineering. All the hydrogels could be compressed up to 70-80% without breaking. This is indeed an important parameters required for hydrogels when they are used as implants and scaffolds under deformation/load.

4.4.6 Inducing Porosity into Hydrogels

In our work, we have used cryogenic treatment followed by lyophilization method to induce pore structure into PU hydrogels. The water swollen gels of PU were subjected to rapid cooling in liquid nitrogen. The frozen water was then removed by sublimation under vacuum leaving behind voids to create porous structure in the hydrogels. Porosity, pore size and pore structure required for the cell growth is explained in Chapter -3 (Section-3.4.7).

4.4.7 Morphological Analysis

4.4.7.1 Scanning Electron Microscope (SEM)

We show in **Figure 4.6**, the SEM micrographs of lyophilized samples of PU gels with different contents of hydrophobic diols. It can be revealed from the figure that, the samples exhibit porous structure with the pore sizes in the range of 2-20μm. Pore size ranges required for the adequate growth of different category of cells and/or tissues have been already extensively studied and reported. We found that the pore sizes obtained in our samples are suitable for hosting the endothelial cell transplantation process during the initial stages of tissue regeneration.

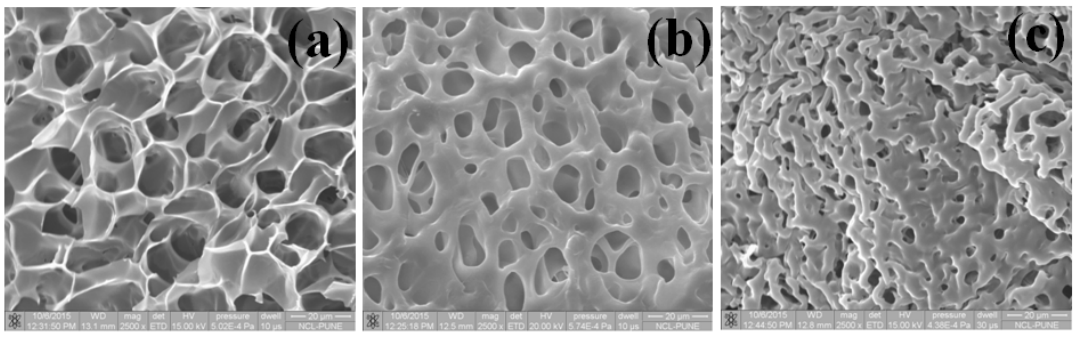

Figure 4.6: *SEM micrographs of the porous xerogels. (a) PU-PCL-1.0 (b) PU-PCD-1.0 and (c) PU-FTL-1.0.*

4.4.8 In vitro degradation

Understanding degradation mechanisms is critical in designing hydrogels for drug delivery applications since the rates of matrix swelling and degradation govern the diffusion of encapsulated or tethered drug molecules. With appropriate design of polymer synthesis and network structure, degradable hydrogel matrices can be engineered with proper degradation profiles for achieving desirable drug release regimes. Enzymatically degradable hydrogels are becoming more important in controlled release applications. In view of this, we have studied the degradation of our hydrogels using enzyme in PBS solution.

Enzyme concentration determines whether gel degradation occurs via surface-erosion (rate of enzyme/ substrate reaction greater than rate of enzyme transport) or bulk-degradation (rate of enzyme transport greater than rate of enzyme/substrate reaction). Therefore, the accuracy of predicting gel degradation largely depends on understanding the cellular physiology and cell–material interactions.

It was found that PEG-based polyurethanes degrade at a faster rate compared with PCL-based polyurethanes due to their hydrophilicity and that this effect is more pronounced when using high molecular weight PEG. Materials containing a higher ratio of PEG exhibit higher water absorbance, higher degradation rate in vitro, and lower mechanical strength in the hydrated state. It was also found that more amorphous PU (i.e. exhibiting more phase mixing and therefore more urethane linkages H-bonded with the soft segment), such as those prepared with HMDI, degrade faster as they absorb more water.

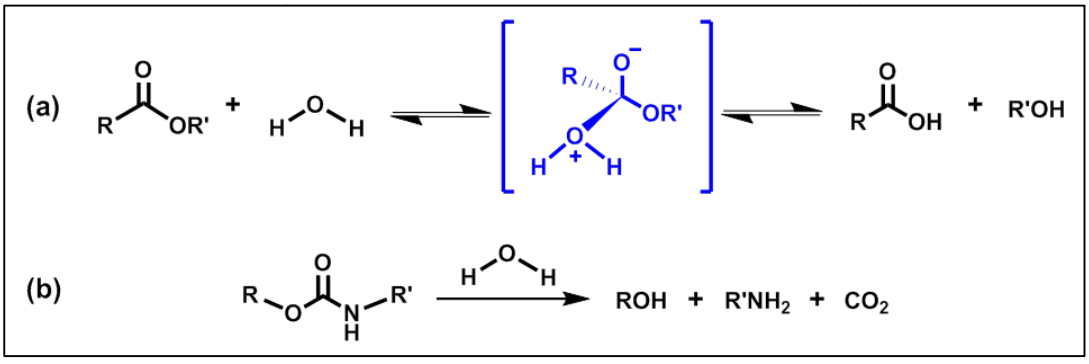

Figure 4.7: *Hydrolytic degradation mechanism of polyester (a) and Polyurethane(b).*

Aliphatic polycarbonates and their copolymers are biodegradable. Aliphatic polycarbonates may have advantages over aliphatic polyesters such as polylactide and lactide-glycolide copolymer, because of their relatively low rate of hydrolysis in aqueous media and their more amorphous nature. Poly (hexamethylene carbonate) has been shown to be successfully biodegraded by environmental microbes.

The hydrogels that we have synthesized comprises of PEG, PCL, FTL and H_{12}MDI and the degradation is considered to be due to hydrolysis of the ester groups, urethane groups and the carbonate groups. Attack of water molecules to the ester groups, urethane groups and carbonate group results in degradation of polymers. The degradation can happen through bulk erosion via chain scission leading to the weight loss in the hydrogel. The mechanism of hydrolytic degradation in Polyester Urethane and Polyurethane is shown in **Figure 4.7.** Further, it is observed that ester linkages hydrolyse faster than urethane linkages. The swelling of hydrogels also plays an important role in the hydrogel degradation. Higher the swelling, higher is the rate of degradation. We show in **Figure 4.8**, % degradation versus time (in days) and the % degradation was measured by the weight loss method in PBS and in the presence of enzyme, Amino lipase PS. The PBS solution and PBS + enzyme solution was replaced every 48hrs during the period of degradation study.

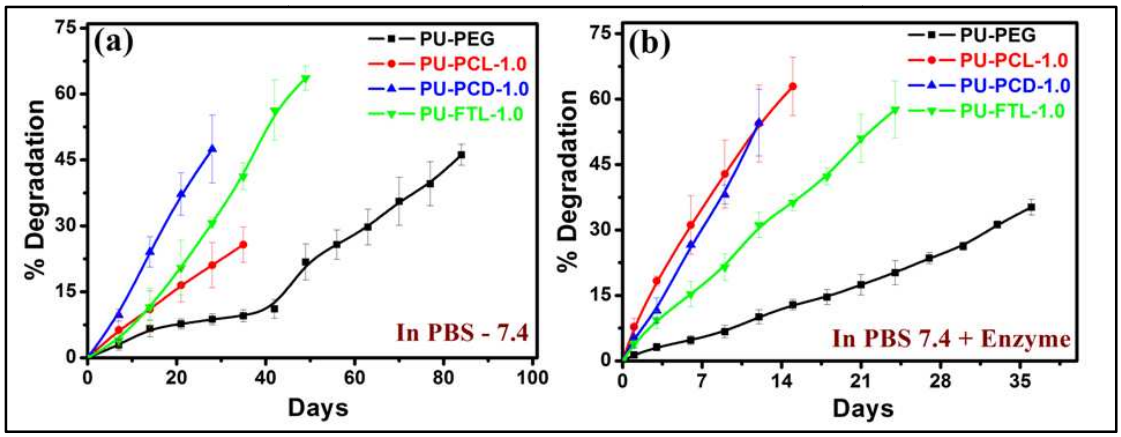

Figure 4.8: *Percentage Degradation of PU hydrogels (a) with PBS 7.4 and (b) with PBS + enzyme.*

In PBS 7.4 the PU-PEG hydrogels were found to be stable up to 80 days with the degradation of 46%. Similarly, the PU-PCL, PU-PCD and PU-FTL hydrogels in

PBS 7.4 showed the stability only up to 35, 28 and 49 days (**Figure 4.8 (a))**. Further, it can be seen from the **Figure 4.8 (b)** that, the presence of enzyme catalyses the degradation significantly and the stability of the hydrogels reduces considerably. Particularly, the PU-PCL and PU-PCD hydrogels degrade much faster due to the attack of enzyme on ester and carbonate linkages.

Table 4.3: *Percentage Degradation of PU hydrogels with time (in days).*

	PU-PEG	PCL-1.0	PCD-1.0	FTL-1.0
PBS	46%	26%	48%	64%
Days	84	35	28	49
PBS + Enzyme	35%	63%	55%	58%
Days	36	15	12	24

4.4.9 In vitro drug release

In order to study the influence of hydrophobic diols and its content on the release of an anticancer drug, doxorubicin hydrochloride (Dox.HCl) from PU-PEG, PU-PCL, PU-PCD and PU-FTL hydrogels, we have performed Dox.HCl release experiments in PBS (pH = 7.4) at 37^0 C. We show in **Figure 4.9 (a, b and c)** the cumulative release profile of Dox.HCl from all the hydrogels over a period of 7 days. In all the samples, a small burst release was observed in the first 4 hours, followed by a relatively constant release of Dox.HCl in the remaining period. It can be seen that as the hydrophobic diol content increases, the release of Dox.HCl is reduced.

The release of Dox.HCl is mainly controlled by the degree of swelling of the hydrogels. With increase in the hydrophobic diol content, the equilibrium swelling ratio of hydrogels decreased and subsequently, the release of Dox is reduced. There is a decrease from 90% to 60% and 80% to 25% in Dox.HCl release as the hydrophobic diol content increases in PU-PCL, PU-PCD and PU-FTL hydrogels. We also show in **Figure 4.9 (d),** a comparative study of Dox.HCl release from the above hydrogels containing the same ratio of PEG and hydrophobic diol (PU-PCL-1.0, PU-PCD-1.0, and PU-FTL-1.0)**.** It can be readily seen that as the hydrophobicity of the diol increase, the equilibrium swelling ratio of hydrogels decrease and consequently, the release of Dox.HCl also decreases. In the case of PU-PEG with the swelling ratio of

~400, nearly 100% release of Dox.HCl is observed. Whereas, for PU-PCL-1.0, PU-PCD-1.0 and PU-FTL-1.0 with swelling ratios of 130, 190, 75 the Dox.HCl release was only 80%, 60% and 25% respectively.

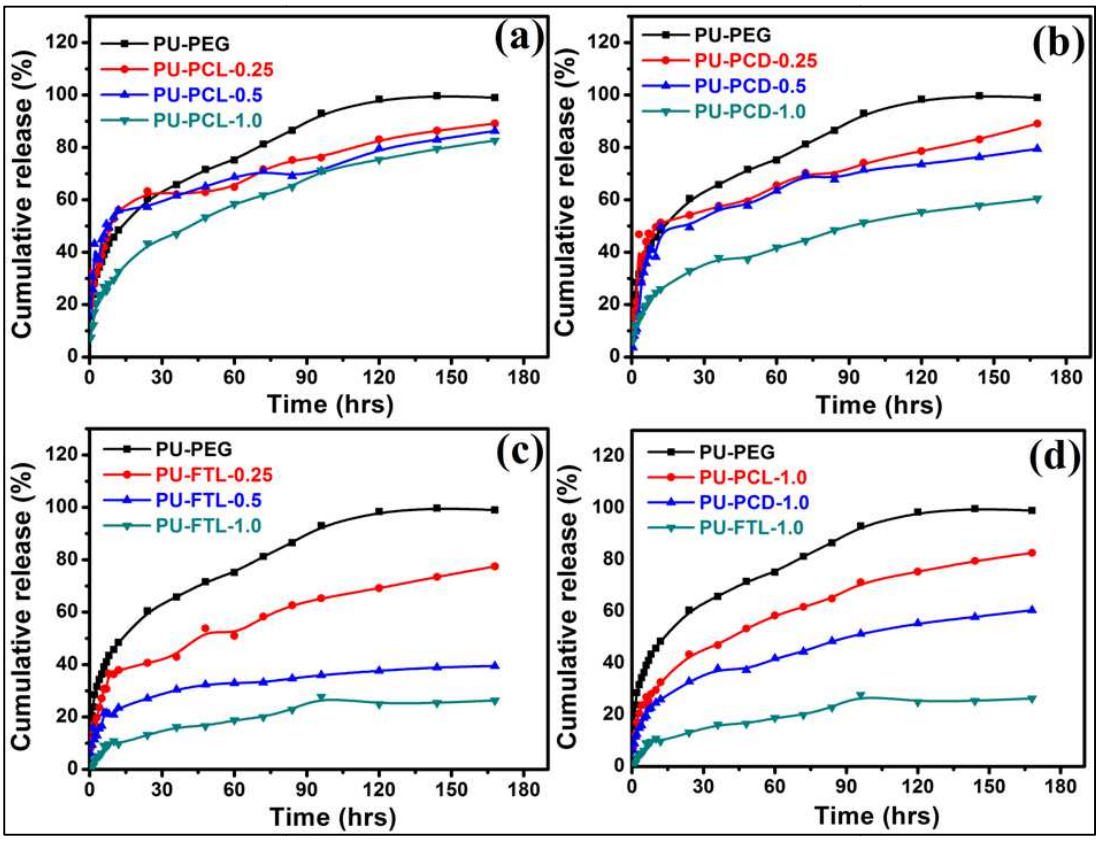

Figure 4.9: *Cumulative release (%) profile of doxorubicin from doxorubicin incorporated PU hydrogels over 7 days. (a) PU-PCL hydrogels, (b) PU-PCD hydrogels (c) PU-FTL hydrogels and (d) Combination of hydrogels.*

However, it is interesting to note here that although PU-PCD hydrogels has higher equilibrium swelling ratio, the release of Dox.HCl is lower (only ~60%) as compared to PU-PCL hydrogel which gives nearly ~80% release of Dox.HCl. This could be attributed to the fact that the positively charged Dox.HCl can electrostatically bind with the negative ions of the carbonate diol and form a complex.[39] As a result, there could be a decrease in the reduction of Dox.HCl release from PU-PCD-1.0 hydrogel. All the above observations clearly indicate that by controlling the hydrophobic diol content and by adjusting the hydrophobic/hydrophilic balance in the hydrogels one can tune the release of Dox.HCl at the desired rate.

4.4.10 In vitro Biological Test

4.4.10.1 MTT Assay

Cytotoxicity of PU hydrogels (PU-PCL-1.0, PU-PCD-1.0 and PU-FTL-1.0) was evaluated by MTT assay which is based on the principle of reduction of enzyme succinate dehydrogenase in the presence of dye MTT to purple coloured formazan crystals. **Figure 4.10** shows that L-929 fibroblast cells exhibited almost similar cell viability as compared to the control. Results clearly indicate that all the PU hydrogels are non toxic and biocompatible to L-929 fibroblast cells.

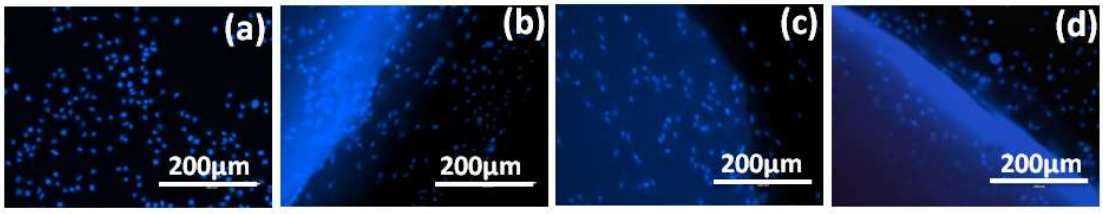

Figure 4.10: *Optical phase contrast images of PU-PCL, PU-PCD and PU-FTL hydrogels in MTT Assay with L 929 fibroblast cells for 72 h at 37°C. Fluorescent image of (a) Control for L929 Fibroblast cell lines (b) PU-PCL with L929 Fibroblast cell lines after 72hrs treating with the hydrogels (c) PU-PCL with L929 Fibroblast cell lines after 72hrs treating with the hydrogels and (d) PU-FTL with L929 Fibroblast cell lines after 72hrs treating with the hydrogels.*

4.5 Conclusions

In the present work, we have synthesized PU hydrogels by incorporating different type of diols in combination with PEG diol by solvent-free one-pot method. The chemical structure of the gels was characterized by FTIR spectroscopy. The micro structural characterization of gels by WAXD indicated the presence of crystallinity, which was attributed to the ordering of PEG, PCL, PCD segments in the gel structure. The equilibrium swelling ratios of the hydrogel decreased with increase in the hydrophobic diol content. Consequently, the tensile and compressive strength of the hydrogels increased. All the hydrogels exhibited good mechanical strength at moderate swelling of the hydrogels. The porosity in the hydrogel was induced by a method of cryogenic treatment followed by lyophilization. The morphological

characterization by SEM revealed the porous structure with 2−20μm pore size and indicated the interconnectivity of pores. The cytotoxicity studies of PU hydrogels showed the continuous growth of cells, which indicated the nontoxic nature of the hydrogels. The in vitro drug release was studied using an anticancer drug doxorubicin hydrochloride. These hydrogels show potential applications in controlled drug delivery and tissue engineering.

4.6 References

1. Stokes, K.; Cobian, K., Polyether polyurethanes for implantable pacemaker leads. *Biomaterials* **1982**, 3, (4), 225-231.
2. Sá da Costa, V.; Merrill, E. W.; Salzman, E. W.; Brier-Russel, D.; Kirchner, L.; Waugh, D. F.; Trudell, G.; Stopper, S.; Vitale, V., Polyurethanes as Biomaterials — Assessment of Blood Compatibility. In *Polymers in Medicine: Biomedical and Pharmacological Applications*, Chiellini, E.; Giusti, P., Eds. Springer US: Boston, MA, **1983**; pp 231-245.
3. Martz, H.; Beaudoin, G.; Paynter, R.; King, M.; Marceau, D.; Guidoin, R., Physicochemical characterization of a hydrophilic microporous polyurethane vascular graft. *Journal of Biomedical Materials Research* **1987**, 21, (3), 399-412.
4. Kimura, Y.; Kumagai, T.; Yamane, H.; Kitao, T.; Sasatani, H.; Kim, S. I., A novel drug delivery system using large intestine-degradable polyurethanes. *Reactive Polymers* **1991**, 15, 251-252.
5. Lai, Y.-C.; Baccei, L. J., Novel polyurethane hydrogels for biomedical applications. *Journal of Applied Polymer Science* **1991**, 42, (12), 3173-3179.
6. Yu, J.; Sundaram, S.; Weng, D.; Courtney, J. M.; Moran, C. R.; Graham, N. B., Blood interactions with novel polyurethaneurea hydrogels. *Biomaterials* **1991**, 12, (2), 119-120.
7. Guidoin, R.; Sigot, M.; King, M.; Sigot-Luizard, M.-F., Biocompatibility of the Vascugraft ®: evaluation of a novel polyester methane vascular substitute by an organotypic culture technique. *Biomaterials* **1992**, 13, (5), 281-288.
8. Liu, S. Q.; Kodama, M., Porous polyurethane vascular prostheses with variable compliances. *Journal of Biomedical Materials Research* **1992**, 26, (11), 1489-1502.
9. Haschke, E.; Sendijarevic, V.; Wong, S.; Frisch, K. C.; Hill, G., Clear Nonionic Polyurethane Hydrogels for Biomedical Applications. *Journal of Elastomers and Plastics* **1994**, 26, (1), 41-57.
10. Ho, S. P.; Britton, D. H. O., Arg—Gly—Asp peptides in polyurethanes: Design, synthesis, and characterization. *Advanced Materials* **1994**, 6, (2), 130-132.

11. Eberhart, A.; Zhang, Z.; Guidoin, R.; Laroche, G.; Guay, L.; De La Faye, D.; Batt, M.; King, M. W., A new generation of polyurethane vascular prostheses: Rara Avis or Ignis Fatuus? *Journal of Biomedical Materials Research* **1999**, 48, (4), 546-558.
12. Zdrahala, R. J.; Zdrahala, I. J., Biomedical Applications of Polyurethanes: A Review of Past Promises, Present Realities, and a Vibrant Future. *Journal of Biomaterials Applications* **1999**, 14, (1), 67-90.
13. Burke, A.; Hasirci, N., Polyurethanes in Biomedical Applications. In *Biomaterials: From Molecules to Engineered Tissue*, Hasirci, N.; Hasirci, V., Eds. Springer US: Boston, MA, **2004**; pp 83-101.
14. Chattopadhyay, D. K.; Raju, K. V. S. N., Structural engineering of polyurethane coatings for high performance applications. *Progress in Polymer Science* **2007**, 32, (3), 352-418.
15. Guelcher, S. A., Biodegradable Polyurethanes: Synthesis and Applications in Regenerative Medicine. *Tissue Engineering Part B: Reviews* **2008**, 14, (1), 3-17.
16. Engels, H.-W.; Pirkl, H.-G.; Albers, R.; Albach, R. W.; Krause, J.; Hoffmann, A.; Casselmann, H.; Dormish, J., Polyurethanes: Versatile Materials and Sustainable Problem Solvers for Today's Challenges. *Angewandte Chemie International Edition* **2013**, 52, (36), 9422-9441.
17. Romaškevič, T. B., Saulutė; Pielichowski, Krzysztof; Pielichowski, Jan, Application of polyurethane-based materials for immobilization of enzymes and cells: a review. *Chemija* **2006**, 17, (4), 74.
18. Corneillie, S.; Lan, P. N.; Schacht, E.; Davies, M.; Shard, A.; Green, R.; Denyer, S.; Wassall, M.; Whitfield, H.; Choong, S., Polyethylene glycol-containing polyurethanes for biomedical applications. *Polymer International* **1998**, 46, (3), 251-259.
19. Petrini, P.; Tanzi, M. C.; Moran, C. R.; Graham, N. B., Linear poly(ethylene oxide)-based polyurethane hydrogels: polyurethane-ureas and polyurethane-amides. *Journal of Materials Science: Materials in Medicine* **1999**, 10, (10-11), 635-639.
20. Iwasaki, Y.; Aiba, Y.; Morimoto, N.; Nakabayashi, N.; Ishihara, K., Semi-interpenetrating polymer networks composed of biocompatible phospholipid

polymer and segmented polyurethane. *Journal of Biomedical Materials Research* **2000**, 52, (4), 701-708.

21. Soeda, Y.; Toshima, K.; Matsumura, S., Synthesis and Chemical Recycling of Novel Poly(ester-urethane)s Using an Enzyme. *Macromolecular Bioscience* **2005**, 5, (4), 277-288.
22. Yeganeh, H.; Jamshidi, H.; Jamshidi, S., Synthesis and properties of novel biodegradable poly(ε-caprolactone)/ poly(ethylene glycol)-based polyurethane elastomers. *Polymer International* **2007**, 56, (1), 41-49.
23. Zhang, C.; Zhang, N.; Wen, X., Synthesis and characterization of biocompatible, degradable, light-curable, polyurethane-based elastic hydrogels. *Journal of Biomedical Materials Research Part A* **2007**, 82A, (3), 637-650.
24. Han, J.; Chen, B.; Ye, L.; Zhang, A.-y.; Zhang, J.; Feng, Z.-g., Synthesis and characterization of biodegradable polyurethane based on poly(ε-caprolactone) and L-lysine ethyl ester diisocyanate. *Frontiers of Materials Science in China* **2009**, 3, (1), 25-32.
25. Wu, J.; Ge, Q.; Mather, P. T., PEG−POSS Multiblock Polyurethanes: Synthesis, Characterization, and Hydrogel Formation. *Macromolecules* **2010**, 43, (18), 7637-7649.
26. Sun, X.; Gao, H.; Wu, G.; Wang, Y.; Fan, Y.; Ma, J., Biodegradable and temperature-responsive polyurethanes for adriamycin delivery. *International Journal of Pharmaceutics* **2011**, 412, (1–2), 52-58.
27. Divakaran, A. V.; Torris At, A.; Lele, A. K.; Badiger, M. V., Porous poly(ethylene glycol)–polyurethane hydrogels as potential biomaterials. *Polymer International* **2015**, 64, (3), 397-404.
28. Divakaran, A. V.; Azad, L. B.; Surwase, S. S.; Torris A. T, A.; Badiger, M. V., Mechanically Tunable Curcumin Incorporated Polyurethane Hydrogels as Potential Biomaterials. *Chemistry of Materials* **2016**, 28, (7), 2120-2130.
29. Polo Fonseca, L.; Bergamo Trinca, R.; Isabel Felisberti, M., Thermo-responsive polyurethane hydrogels based on poly(ethylene glycol) and poly(caprolactone): Physico-chemical and mechanical properties. *Journal of Applied Polymer Science* **2016**, 133, (25).

30. Lamba, N. M. K.; Woodhouse, K. A.; Cooper, S. L., *Polyurethanes in Biomedical Applications*. Taylor & Francis: **1997**.
31. Hollinger, J. O., *An Introduction to Biomaterials*. Taylor & Francis: **2005**.
32. Ratner, B. D.; Hoffman, A. S.; Schoen, F. J.; Lemons, J. E., *Biomaterials Science: An Introduction to Materials in Medicine*. Elsevier Science: **2012**.
33. Szycher, M., *Szycher's Handbook of Polyurethanes, Second Edition*. Taylor & Francis: **2012**.
34. Wright, D. C., *Failure of Polymer Products Due to Chemical Attack*. Rapra Technology Limited: **2001**.
35. Poole-Warren, L.; Martens, P.; Green, R., *Biosynthetic Polymers for Medical Applications*. Elsevier Science: **2015**.
36. Tadokoro, H.; Chatani, Y.; Yoshihara, T.; Tahara, S.; Murahashi, S., Structural Studies on Polyethers, [-(Ch-2)M-O-]N .2. Molecular Structure of Polyethylene Oxide. *Makromolekulare Chemie* **1964**, 73, 109-127.
37. Takahash, Y.; Sumita, I.; Tadokoro, H., Structural Studies of Polyethers .9. Planar Zigzag Modification of Poly(Ethylene Oxide). *Journal of Polymer Science Part B-Polymer Physics* **1973**, 11, (11), 2113-2122.
38. Takahash, Y.; Tadokoro, H., Structural Studies of Polyethers, (-(Ch2)M-O-)N .10. Crystal-Structure of Poly(Ethylene Oxide). *Macromolecules* **1973**, 6, (5), 672-675.
39. Hossain, S.; Yamamoto, H.; Chowdhury, E. H.; Wu, X.; Hirose, H.; Haque, A.; Doki, Y.; Mori, M.; Akaike, T., Fabrication and intracellular delivery of doxorubicin/carbonate apatite nanocomposites: effect on growth retardation of established colon tumor. *Plos One* **2013**, 8, (4), e60428.

Introduction

Chapter – I

In the first chapter, a detailed literature survey was done on hydrogels in terms of their classification, synthesis, properties, advantages and disadvantages and applications for drug delivery and tissue engineering. Literature survey on the state-of-the-art of polyurethane (PU) hydrogels is given. The characterization techniques such as WAXD, SAXS, UTM, μ-CT, biological tests etc., used for studying the micro-structural, surface morphology, mechanical behaviour and cytotoxicity of the hydrogels were briefly explained.

Scope and Objectives

Chapter – II

In the second chapter, we have discussed the scope and objectives of thesis work.

Design, synthesis and characterization of polyethylene glycol – polyurethane hydrogels

Chapter – III

In the third chapter, we report the synthesis of porous poly (ethylene glycol)–polyurethane (PEG-PU) hydrogels using PEG-4000 as a soft segment and 4,4′ methylenebis (cyclohexyl isocyanate) as a hard segment. The degree of swelling in the hydrogels could be controlled by varying the amount of crosslinking agent, namely 1,2,6-hexanetriol. The characterization techniques such as Solid-state ^{13}C NMR, FTIR, WAXD, SAXS, SEM, DMA, μ-CT, biological tests etc., used for studying the structural, micro-structural, surface morphology, mechanical behaviour and cytotoxicity of the hydrogels were briefly explained.

Polymer International. 2015; 64: 397-404

Influence of hydrophilic/hydrophobic diols on the properties of polyurethane hydrogels

Chapter – IV

In the fourth chapter, we have synthesized and characterized PU hydrogels using different diols namely, Polycaprolactone diol (PCL), Poly (hexamethylene carbonate) diol (PCD), and Tetraol (FTL) in combination with Polyethylene glycol (PEG). The characterization techniques such as, FTIR, WAXD, SEM, in vitro drug release, in vitro degradation, biological tests etc., used for studying the structural, micro-structural, surface morphology, mechanical behavior, drug release kinetics, degradation profile and cytotoxicity of the hydrogels were briefly explained.

Patent Application No: 3555DEL2015 (Prov. Date: 02/11/2015)

Curcumin in polyurethane hydrogels

Chapter – V

In the fifth chapter, we report the one-pot synthesis and characterization of curcumin incorporated polyethylene glycol − poly urethane (PU-CUR) hydrogels using PEG-4000, 4,4′-methylenebis (cyclohexyl isocyanate), curcumin in the presence of a cross-linker, 1,2,6-hexanetriol (HT). Besides the physical entrapment, curcumin also provides a partial crosslinking in the 3-D structure of the hydrogel. The characterization techniques such as, FTIR, UV-Vis, HR-MS, WAXD, SAXS, UTM, Confocal microscopy, SEM, μ-CT, biological tests etc., used for studying the structural, micro-structural, surface morphology, mechanical behavior and cytotoxicity of the hydrogels were briefly explained.

Chemistry of Materials. 2016, 28, 2120-2130.

Patent Application No: 3555DEL2015 (Prov. Date: 02/11/2015)

Summary and Conclusions

Chapter – VI

In the sixth chapter, we have discussed the summary and conclusions of thesis work.

5.1. Introduction

As mentioned in the previous chapters, a solvent-free, one-pot synthesis of PEG-PU hydrogels was achieved. The obtained hydrogels exhibited reasonably good tensile and compressive strengths. Additionally, different types of diols were also used in combination with PEG diol to synthesize PU hydrogels. These hydrogels showed significant improvement in the mechanical properties.

In order to focus our work on the hydrogels for bio-medical applications, we were interested in designing and synthesizing hydrogels with biological properties such as, antibacterial,[1-3] anticancerous[4-7] and antifungal.[8-10] To achieve this goal, we identified a biomolecules namely, curcumin[11-20] which can be easily integrated into the hydrogel matrix both chemically and physically.

Accordingly, in this study, we have incorporated curcumin in the preparation of PU hydrogels. The hydrogels were prepared using PEG-4000, 4,4'-methylenebis (cyclohexyl isocyanate) (H_{12}MDI), Curcumin in the presence of a cross linker namely, 1,2,6-hexanetriol (HT). Curcumin is a 1,7-bis-(3-methoxy-4-hydroxy phenyl)-1,6-heptadiene-3,5-diene having phenolic structures connected by two α,β-unsaturated carbonyl groups.[21] It is well established that, curcumin exhibits both anti-microbial and anticancerous properties.[22-30] The obtained hydrogels showed good antibacterial properties. Besides 1,2,6-hexanetriol (HT) cross linking, curcumin with reactive -OH groups also took part in partial cross linking as well as entrapment during the reaction indicating the presence of both physical and chemical linking in the hydrogel structure. The quantitative estimation of curcumin in the PU-CUR hydrogels was made by extraction of hydrogels in ethanol:water mixture (65:35), where the physically entrapped curcumin is expected to diffuse out of the gel matrix.

The structural characterization of hydrogels was performed by FTIR and Solid-state NMR spectroscopy. Interestingly, the obtained hydrogels showed enhanced mechanical properties in terms modulus, % elongation and recovery. The micro structure of the hydrogels was investigated using wide-angle X-ray diffraction (WAXD) and small-angle X-ray scattering (SAXS). The cryogenic treatment with lyophilization was used to generate porosity in the hydrogel matrix. The preliminary antibacterial property and cytocompatibility studies showed the ability of cells to

proliferate in the hydrogel. This is one of the most desirable properties of hydrogels for biomaterials application.

5.2. Experimental

5.2.1 Materials

Polyethylene glycol (MW~4000g/mol), Dibutyltin dilaurate (DBTDL) and Tetrahydrofuran (THF) were obtained from Merck India; 4,4'-methylenebis (cyclohexyl diisocyanate) (H_{12}MDI) was purchased from Sigma Aldrich, USA; 1,2,6 Hexanetriol (HT) was obtained from Fluka USA. Curcumin was a gift sample from Arjuna Natural Extracts, India. Dulbecco's Modified Eagle Medium (DMEM) and Fetal Bovine Serum (FBS) were purchased from Invitrogen USA; Dulbecco's Phosphate buffered saline (DPBS) was obtained from HiMedia India. Escherichia coli (NCIM 2685) were obtained from National Collection of Industrial Microorganisms (NCIM), India. All the chemicals were of analytical grade and used as received.

5.2.2 Synthesis of Curcumin incorporated Polyurethane (PU-CUR) Hydrogels

PEG [MW~4000g/mol] was vacuum-dried at 60 ^{0}C for 6 hours in a rotary evaporator to remove any residual moisture and stored molten in a sealed flask in an oven at 70 ^{0}C until use. To the 10 g of molten PEG, 0.06 g of Curcumin and 0.335 g HT were added and kept in a rotary evaporator for 2 hours to form homogeneous solution. To this solution, 1.5 mL of 4,4′-methylenebis (cyclohexyl diisocyanate) and 13.6 μL of dibutyltin dilaurate (DBTDL) were added using a syringe under nitrogen atmosphere. The whole mixture was kept in a rotary evaporator for 20-30 min at 70 ^{0}C till the mixture become more homogeneous and then poured in to pre-silanated glass petri-dishes, or appropriate teflon molds (as per the dimension required for studies). The petri-dishes/moulds were kept in oven at 95 ^{0}C for 4 hours for gelation. After gelation, the petri-dishes/moulds were cooled and the hydrogel discs were removed by immersing the petri-dishes in distilled water for 4-5 hours. The unreacted monomers were removed by washing the hydrogels in excess distilled water for a few days with frequent replenishment of fresh distilled water. By using the same procedure, hydrogels with different curcumin contents were prepared with 0, 0.5, 1.0, and 1.5 wt % of curcumin abbreviated as PU-CUR-0.0 (without curcumin), PU-CUR-0.5, PU-CUR-1.0, and PU-CUR-1.5, and the stoichiometry used for the reactions is

given in **Table 5.1**. The reaction between PEG, H_{12}MDI, HT, and curcumin is shown in **Scheme 5.1**.

Table 5.1: *Stoichiometry for the synthesis of PU-CUR Hydrogels*

Sample	Curcumin (mol x 10^{-3})	Hexanetriol (mol x 10^{-3})	PEG_{4000} (mol x 10^{-3})	DBTDL (mol x 10^{-3})	H_{12}MDI (mol x 10^{-3})
PU-CUR-0.0	0	2.5	2.5	0.0237	6.35
PU-CUR-0.5	0.162	2.5	2.5	0.0237	6.35
PU-CUR-1.0	0.325	2.5	2.5	0.0237	6.35
PU-CUR-1.5	0.488	2.5	2.5	0.0237	6.35

5.2.3 Synthesis of Curcumin with Phenyl Isocyanate (CUR-PI).

To establish the chemical reaction between curcumin and the H_{12}MDI to form the cross linking in the network structure, a model reaction of curcumin with phenyl isocyanate was carried out **(Scheme 5.2)**.

Table 5.2: *Stoichiometry for the synthesis of CUR-PI compound*

Reagents	Mw (g/mol)	Eq	mmol	Density (g/cc)	Amount taken
Curcumin	368.38	1	0.998	-	0.368g
Phenyl Isocyanate	119.12	1	0.001	1.078	0.12ml
Phenyl Isocyanate	119.12	2	0.002	1.078	0.25ml
Phenyl Isocyanate	119.12	3	0.003	1.078	0.37ml

In a typical reaction procedure, to a solution of curcumin (0.368 g, 1mmol) in dried THF (5 mL), phenyl Isocyanate (0.12 mL, 1 mmol) was added followed by the addition of Dibutyltin dilaurate (DBTDL) (1 mg) as a catalyst. After 12 hours, the reaction mixture was diluted with dried THF (5 mL). The THF was evaporated to obtain the crude product, redissolved in THF and crystallized. Using the same procedure, curcumin was reacted with phenyl Isocyanate with different mole ratio as shown in **Table 5.2**.

5.2.4. Preparation of porous PU-CUR hydrogels

Porous PU-CUR xerogels were prepared by cryogenic treatment of fully swollen PU-CUR hydrogels followed by removal of ice crystals by lyophilization. The fully swollen hydrogels (20 mm diameter x 10 mm height) were placed in liquid nitrogen for 15 min and then freeze-dried in a lyophilizer (Christ Alpha 1-4, Germany) for 10-12 h.

5.3. Characterization

5.3.1 Structural Characterization

5.3.1.1 FT-IR

The structural characterization of PU-CUR hydrogels was performed by FTIR. Experimental details are given in Chapter 3 (Section-3.3.1.1).

5.3.1.2 UV–Vis Spectrophotometer

UV–Vis Spectrophotometer (JASCO V-570) with DRS mode was used to obtain spectra.

5.3.1.3 Fluorescence Spectrophotometer

Steady-state fluorescence studies were performed using Horiba Jobin Yvon Fluorolog 3 spectrophotometer having a 450 W xenon lamp. The emission and excitation slit width was maintained at 1 nm throughout the experiments, and the data was obtained in “S1/R1” mode (to account for the variations in lamp intensity).

5.3.2 Swelling Measurements

The swelling behaviour of the PU-CUR hydrogels was studied using gravimetric method. Experimental details are given in Chapter 3 (Section-3.3.2).

5.3.3 Micro structural Characterization

5.3.3.1. Wide-angle X-ray diffraction (WAXD)

Wide-angle X-ray diffraction (WAXD) technique was used to detect the crystalline morphology of PU-CUR xerogels. Experimental details are given in Chapter 3 (Section-3.3.3.1).

5.3.3.2. Small-angle X-ray scattering (SAXS)

Small-angle X-ray scattering (SAXS) technique was used to detect the microstructure of PU-CUR xerogels. Experimental details are given in Chapter 3 (Section-3.3.3.2).

5.3.4 Mechanical Properties

5.3.4.1. Tensile tests

Tensile tests were carried out with Instron Universal Testing Machine (UTM-33R) with a load cell of 10 kN, at room temperature with an elongation rate of 10 mm/sec. The test specimens for tensile testing were having dimension of 35mm length x 10mm width x 1mm thickness.

5.3.4.2. Compressive tests

Compressive tests were carried out on the same machine with a load cell of 10 kN, at 25 ^{0}C with a compression speed of 10 mm/sec. The swollen hydrogel samples for compression testing were having Length to Diameter ratio of 1:1.

5.3.4.3. Cyclic compression test

The force-gap experiments were carried out with TA instruments ARES-G2, a strain controlled rheometer under ambient conditions. The cylindrical hydrogel samples which are swollen in DI water were having length to diameter ratio of 1:1.

5.3.5 Morphological Analysis

5.3.5.1. Scanning Electron Microscopy (SEM)

Scanning electron microscopy (SEM) was employed to investigate the morphology of the PU-CUR hydrogels and porous xerogels. Experimental details are given in Chapter 3 (Section-3.3.6.1).

5.3.5.2. Microcomputed tomography (μ-CT) or Micro-CT

Three-dimensional nondestructive imaging of PU-CUR xerogels was performed using a high-resolution X-ray microcomputed tomography (μ-CT), model μ-CT 40 (Scanco Medical AG, Switzerland). PU-CUR xerogels were scanned using

X-ray of energy 45 kV and 12 μm voxel resolution. Two-dimensional cross-sectional images of xerogels were thresholded to suppress background noise, and the region of interest was marked to discriminate between polymers as well as pores in the xerogels. The 2D images were compiled, and 3D images of xerogels were generated using the software provided by the manufacturer. Micro-architectural parameters of the xerogels such as porosity, pore size, and wall thickness distribution, etc., were evaluated by applying a distance transformation methodology with the aid of a software supplied by the manufacturer.

5.3.6 In vitro Biological Test

5.3.6.1 Cytotoxicity Test (Direct Contact Method)

For in vitro cytotoxicity study, PU-CUR xerogels with 8mm diameter disc (n=3) were ethanol sterilized. The sterilized xerogels were swollen to equilibrium using sterile deionized water for the removal of excess ethanol. Experimental details are given in Chapter 3 (Section-3.3.7.1).

5.3.6.2 MTT Assay

MTT assay was performed to assess cell viability with all PU hydrogels. Experimental details are given in Chapter 3 (Section-3.3.7.2).

5.3.6.3 Quantification of Cytostatic Dosage

Cytostatic dosage of the curcumin was quantitatively assessed by MTT which measures the metabolic reduction of yellow coloured 3-(4,5-dimethylthiazol-2yl)-2,5,diphenyl tetrazolium bromide to a purple coloured formazan by viable cells. L-929 cell lines cultured and seeded 10000 cell/well to 96 well multiwall plate containing different concentration of curcumin. Incubated at 37±2 ^{0}C in air with 5% CO_2 till a sub confluent monolayer is formed. Culture mediam is removed and added to aliquot of extract at definite dilution to labelled wells along with aliquots of blank reagent. Liquid extracts of positive as well as negative control material and reagent control were added onto additional triplicate wells. Incubated at 37±2 ^{0}C in air with 5% $C0_2$ for a minimum of 24hrs. Cytotoxicity was qualitatively evaluated using phase contrast microscope for general morphology, vacuolization, detachment of cells and cell lysis. Sub confluent monolayers of cells were trypsinize. With a multi channel

pipette added 100μL of the cell suspension to each well of the 10 central column of multi well plate containing 0.5 – 1 x 10^3 cells / well. Growth medium is added and incubated till attaining sub confluency. Medium is removed and the plate is fed with 200 μL of fresh medium and 50 μL of MTT. Wells were incubated from 4 hrs to overnight in humidified atmosphere. Medium and MTT were removed from the wells and the MTT formazan crystals were dissolved by adding 200 μL of DMSO / Propanol. Absorbance at 570nm was recorded immediately, since the product is unstable.

5.3.6.4 Antibacterial study

Bacterial stains were obtained from National Collection of Industrial Microorganisms (NCIM), India. *Staphylococcus aureus (S.aureus)* (NCIM 2079) were used to test the antibacterial potential of the gels by using the Kirby–Bauer disc diffusion method.[31]

5.4. Results and Discussion

5.4.1 Synthesis of Curcumin incorporated PEG-PU Hydrogels (PU-CUR)

In the present work, curcumin is incorporated during the synthesis of PU-CUR xerogels. The idea of using curcumin in the hydrogel was to obtain hydrogels with excellent antimicrobial, antifungal, antiinflammatory properties. Curcumin, commonly known as diferuloyl methane, is a hydrophobic polyphenol derived from the rhizome (turmeric) of the herb curcuma longa.

Chemically, curcumin is a bis- α,β-unsaturated β-diketones that exhibits keto-enol tautomerism **Figure 5.1**. The enol form has been found to be the stable in the ground state. Because of the keto-enol tautomerism, curcumin can undergo end-capping, chain extension and crosslinking in the polyurethane addition reaction. Further, curcumin is soluble in PEG and can be easily incorporated into PU-CUR xerogels without the requirement of any solvent. The reaction between PEG, H_{12}MDI, HT and curcumin is shown in **Scheme 5.1 and Figure 5.2**. The network structure in the gel is induced by both HT and curcumin cross linking in the reaction.

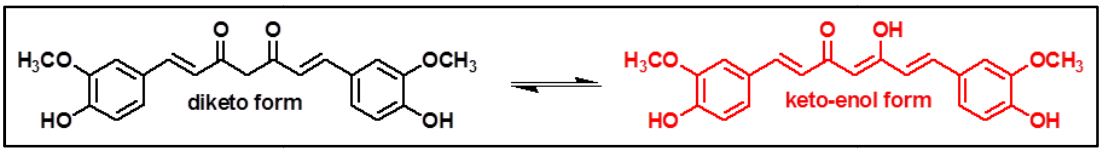

Figure 5.1: *Tautomeric form of curcumin.*

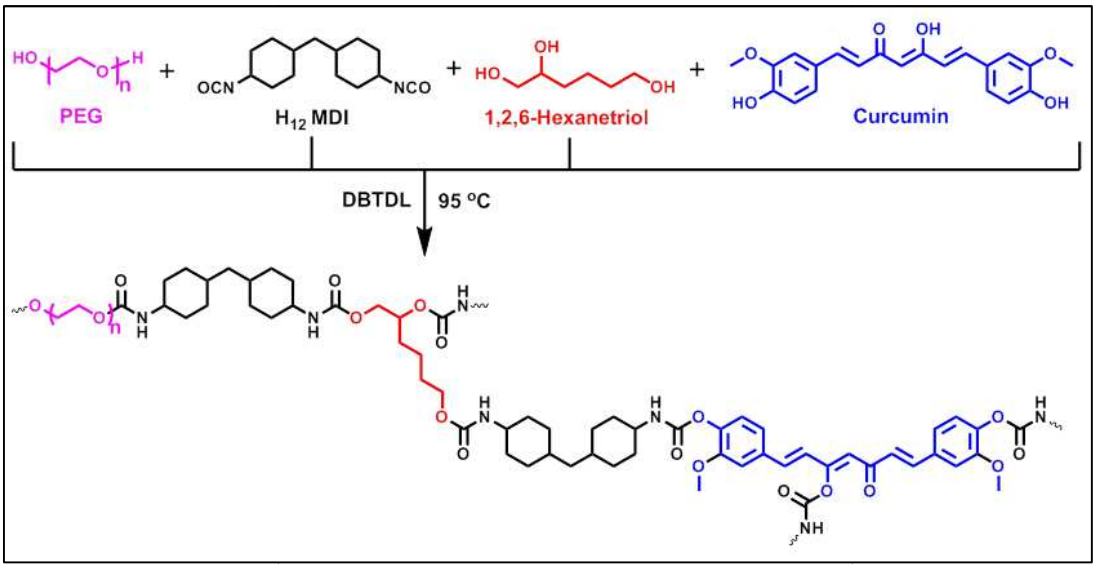

Scheme 5.1: *Reaction scheme for the synthesis of PU-CUR xerogel.*

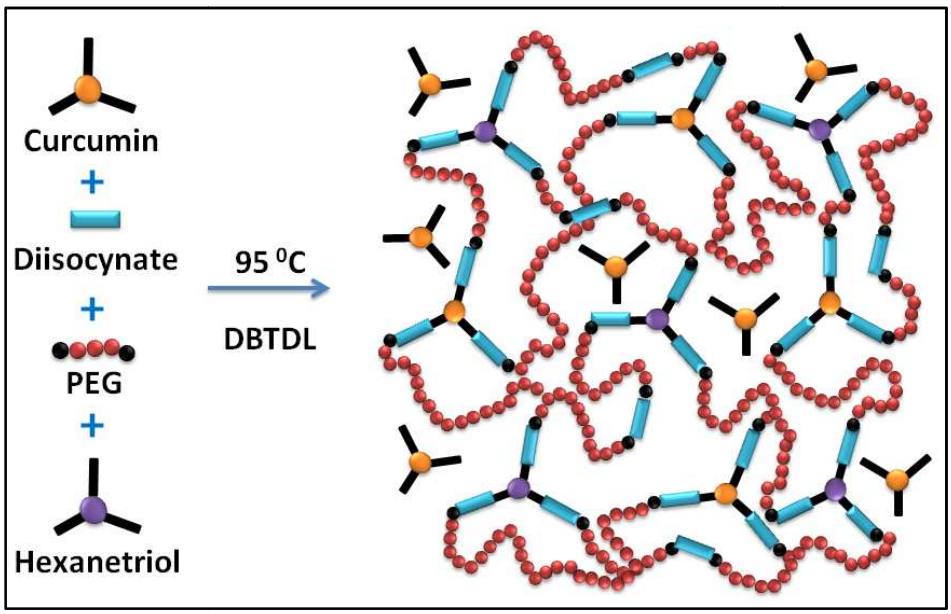

Figure 5.2: *Graphical representation of the PU-CUR hydrogel formation.*

Since the reactivity of the phenolic -OH groups in curcumin is not high as compared to -OH groups in HT towards isocyanate groups, all the curcumin may not

take part in the chemical reaction and hence some amount of the curcumin may be present as physically entrapped curcumin. The curcumin incorporated PU-CUR xerogels obtained were opaque and orange in colour. They exhibited moderate swelling in water and upon swelling they became transparent. Interestingly, depending on the amount of curcumin incorporated, the gel showed variation in the mechanical properties which will be discussed in the later sections.

5.4.2 Synthesis of Curcumin with phenyl Isocyanate (CUR-PI) compound

To confirm reaction between curcumin and diisocyanate a model reaction was performed in which, curcumin was reacted with phenyl isocyanate in different mole ratios. The reaction was carried out in THF at RT and catalysed by DBTDL. The reaction pathway is shown in **Scheme 5.2.**

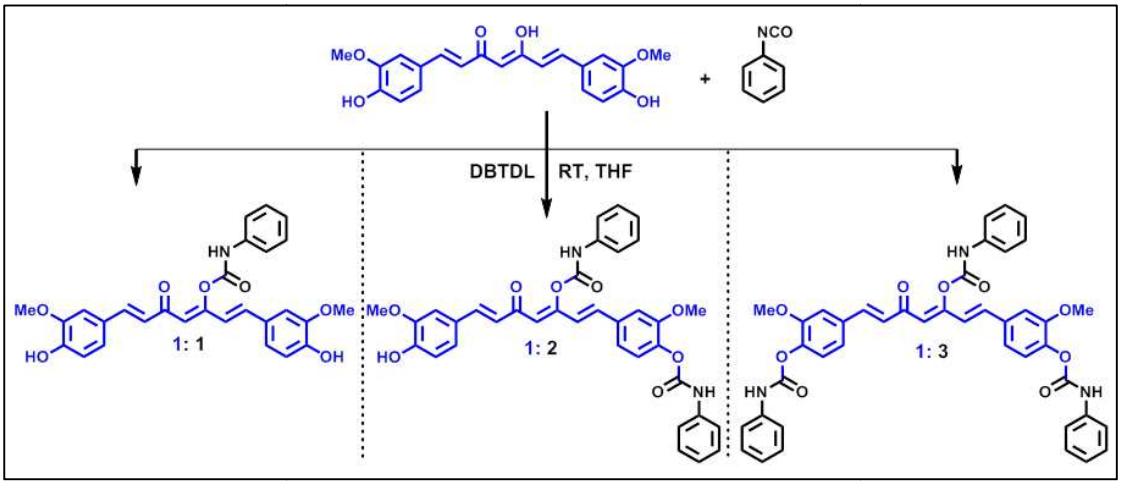

Scheme 5.2: *Reaction scheme for the synthesis of CUR-PI compounds.*

The products were analyzed by FT-IR and high-resolution mass spectrometry (HR-MS).

5.4.3 Preparation of porous PU-CUR hydrogels

Cryogenic treatment followed by lyophilization method was used to induce pore structure into PU-CUR hydrogels. The water swollen gels of PU-CUR were subjected to rapid cooling in liquid nitrogen. The frozen water was then removed by sublimation under vacuum leaving behind voids to create porous structure in the hydrogels. We show in **Figure 5.3**, the schematics of the process of pore formation in the PU-CUR hydrogels.

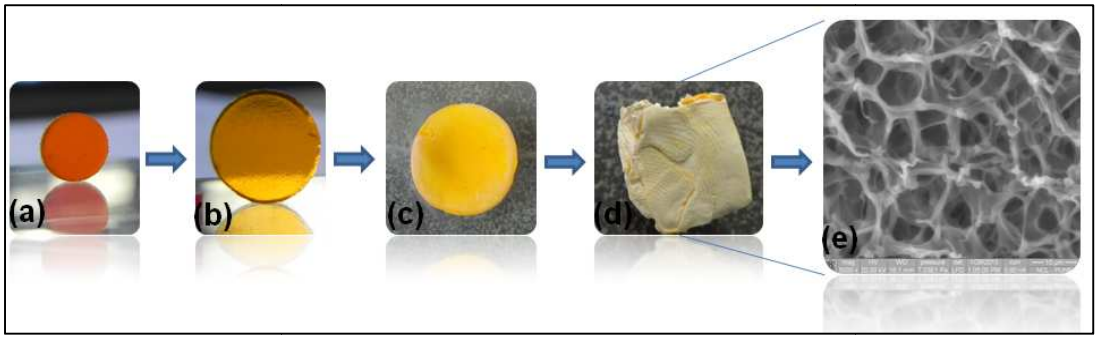

Figure 5.3: *Process of pore formation: (a) PU-CUR-1.0 Xerogel, (b) PU-CUR-1.0 Hydrogel, (c) Liquid Nitrogen Quenched PU-CUR-1.0 Hydrogel (d) Freeze dried PU-CUR-1.0 Porous Xerogel (e) SEM image of PU-CUR-1.0 Porous Xerogel.*

It can be seen from **Figure 5.3** that, the xerogel (a) is opaque and upon swelling in water it becomes transparent (slightly hazy) (b). On liquid nitrogen rapid cooling, the transparent gel becomes opaque again (c) on lyophilization the gel converts into spongy nature retaining the opaqueness (d) and (e) show the SEM images, which display the porosity in the xerogel. The simple cryogenic treatment method that we have used here is a faster and template-free approach in comparison with time consuming salt-leaching as well as photo-patterning methodology reported earlier for porous hydrogels.

5.4.4. Structural Characterization

5.4.4.1 FTIR spectroscopy

The structural elucidation of PU-CUR gel was performed by FTIR spectroscopy. The stacked plots of FTIR spectra of reactants, PEG-4000, H_{12}MDI, Curcumin and the product, PU-CUR-1.0 gel are shown in **Figure 5.4**.

The strong absorption band at 2270 cm^{-1} in H_{12}MDI is ascribed to the C=N (Nitrile) stretch in the isocyanates group (-N=C=O). Whereas, a weak, broad absorption band of hydroxyl end groups (-OH) of PEG-4000 appear at 3400-3500 cm^{-1}. In the case of PU-CUR gel, the characteristic absorption bands of (–NCO) groups from H_{12}MDI (at 2270 cm^{-1}) and (-OH) groups of PEG-4000 (at 3400cm^{-1}) disappeared indicating the reaction between (–NCO) and (–OH) to form urethane (-NH-COO-) linkages.

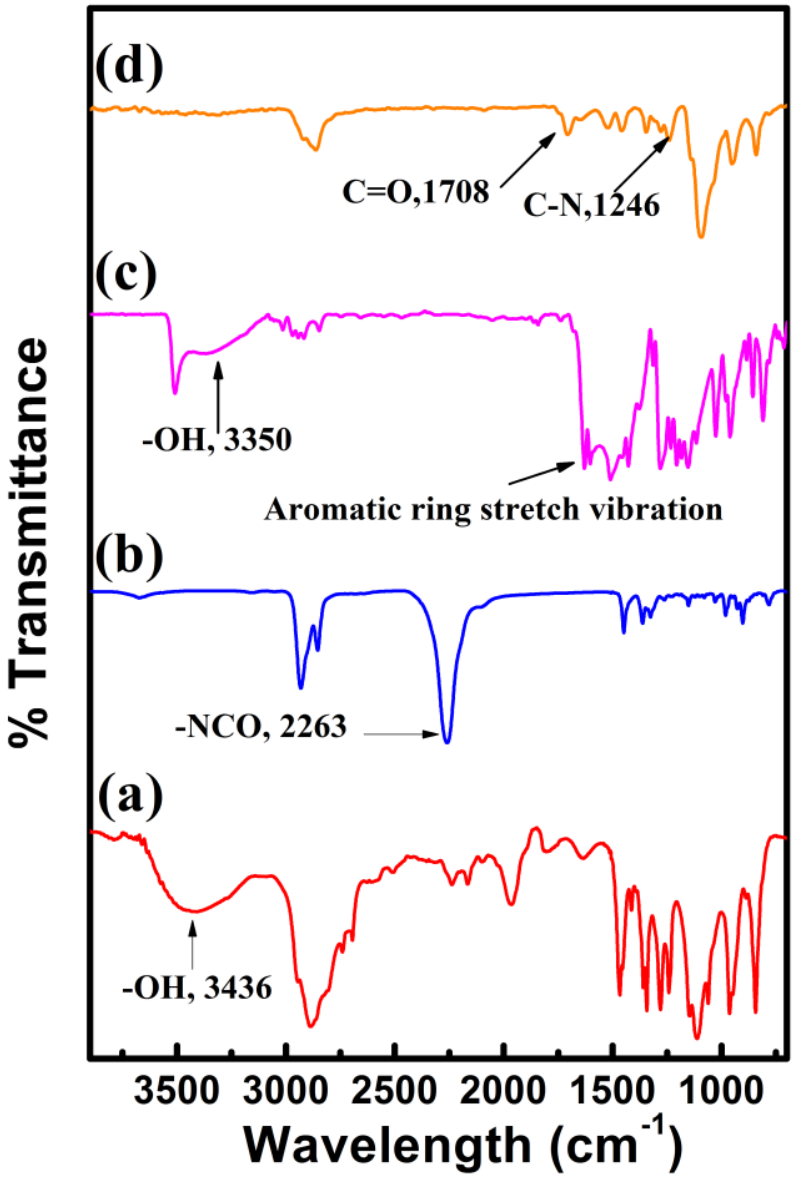

Figure 5.4: *FTIR Spectra of (a) PEG-4000 (b) H_{12}MDI (c) Curcumin and (d) PU-CUR-1.0 Xerogel.*

At the same time, a new peak appeared in PU-CUR spectrum at 1716cm^{-1}, attributed to the stretching of ester carbonyl groups (>C=O) within the urethane linkages. Further, we also observed strong absorption bands in the range of 2800-3000cm^{-1} which can be ascribed to C-H stretching vibrations. Finally, the absorption band at 1115cm^{-1} in PU-CUR gel is attributed to the characteristic –C-O-C- stretching vibration of the repeating unit of -O-CH_2-CH_2- of the PEG-4000. These observations in the FTIR spectra clearly confirm the structure of PU-CUR gels.

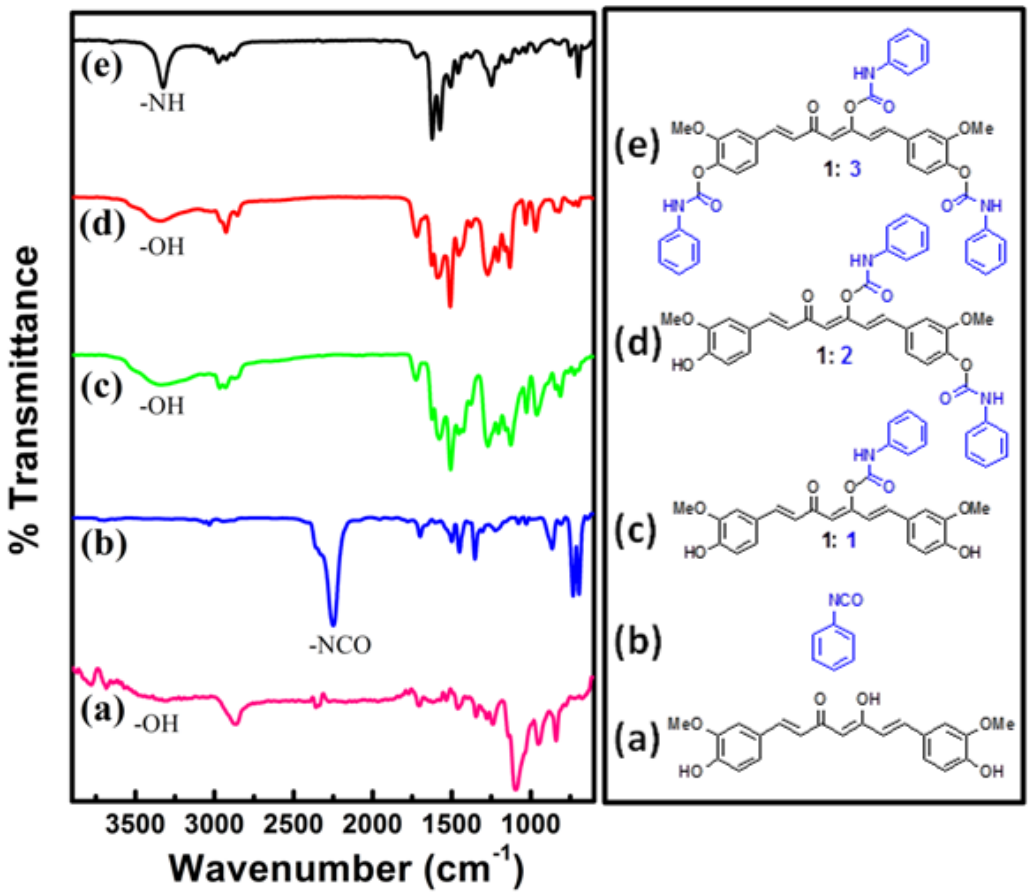

Figure 5.5: *FTIR Spectra of (a) Curcumin (b) phenyl Isocyanate (c) CUR-PI 1:1, (d) CUR-PI 1:2, and (e) CUR-PI 1:3*

Similarly, the structural elucidation of the products from the reaction between Curcumin and Phenyl Isocyanate (CUR-PI) was performed by FTIR spectroscopy. The stacked plots of FTIR spectra of reactants, curcumin, phenyl isocyanate and the product CUR-PI (1:1, 1:2, 1:3 and 1:6) are shown in **Figure 5.5**. These observations in the FTIR spectra clearly confirmed the reaction between curcumin's –OH groups and isocyanate groups in phenyl isocyanate.

5.4.4.2. High Resolution Mass Spectrometry (HR-MS)

The confirmation of the products from the reaction between curcumin and PI at different mole ratios was performed using HR-MS spectroscopy. **Figure 5.6:** HR-MS: m/z calculated for $C_{28}H_{25}NO_7$ for CUR: PI 1:1 = 487.17, **Figure 5.7:** $C_{35}H_{30}N_2O_8$ for CUR: PI 1:2 = 607.21, **Figure 5.8:** $C_{42}H_{35}N_3O_9$ for CUR: PI 1:3 = 725.21.

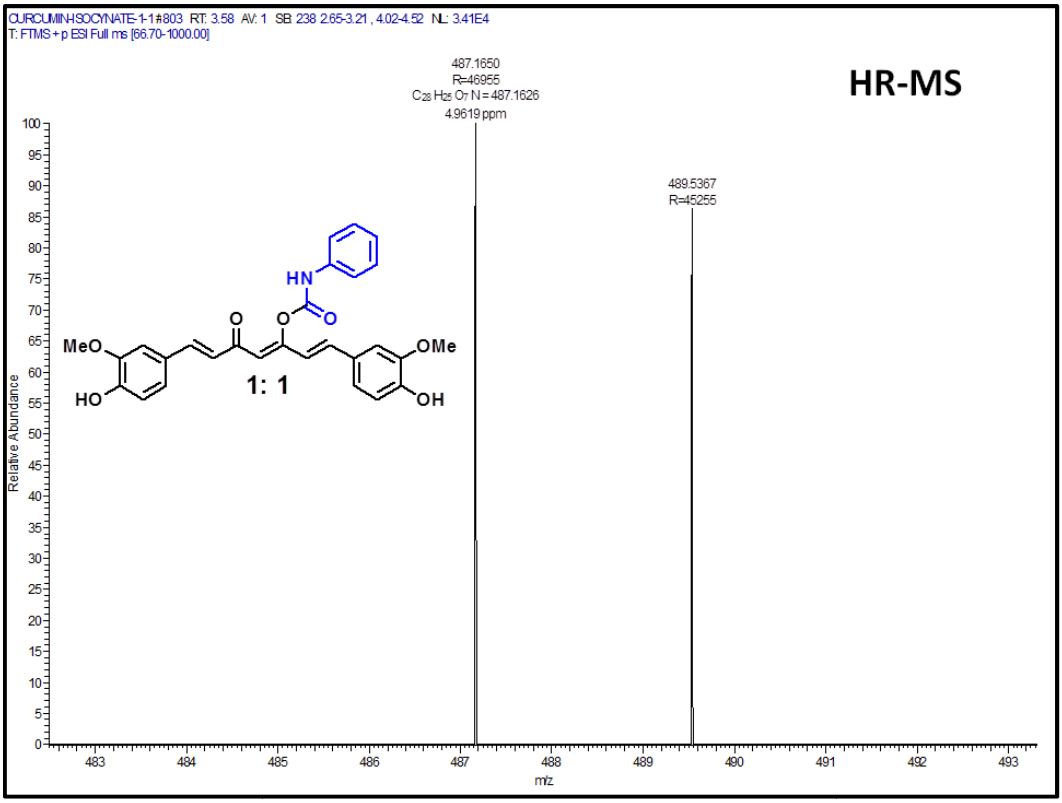

Figure 5.6: *HR-MS of Curcumin – Phenyl Isocyanate 1:1*

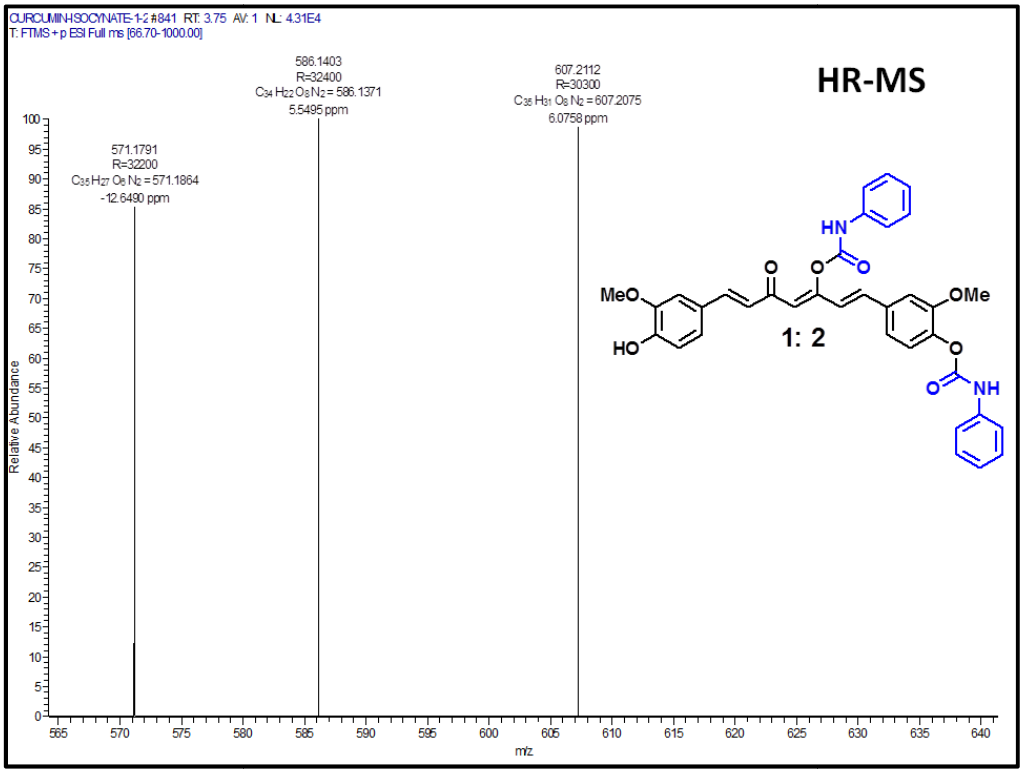

Figure 5.7: *HR-MS of Curcumin – Phenyl Isocyanate 1:2*

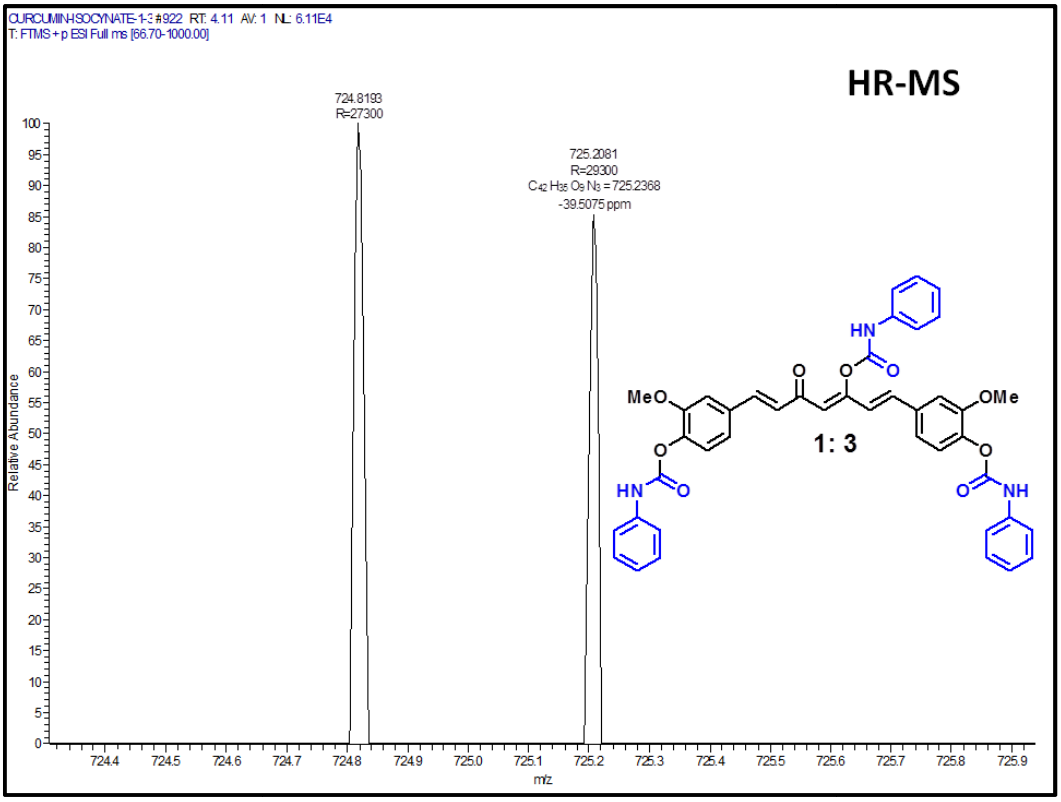

Figure 5.8: *HR-MS of Curcumin – Phenyl Isocyanate 1:3*

5.4.4.3 UV–Vis & Fluorescence Spectrophotometer

The presence of curcumin in the PU-CUR gel was further confirmed by solid state UV-Vis and Fluoresence spectroscopy. **Figure 5.9 (a)** shows the UV-Vis spectra of PU-CUR xerogels with different contents of curcumin.

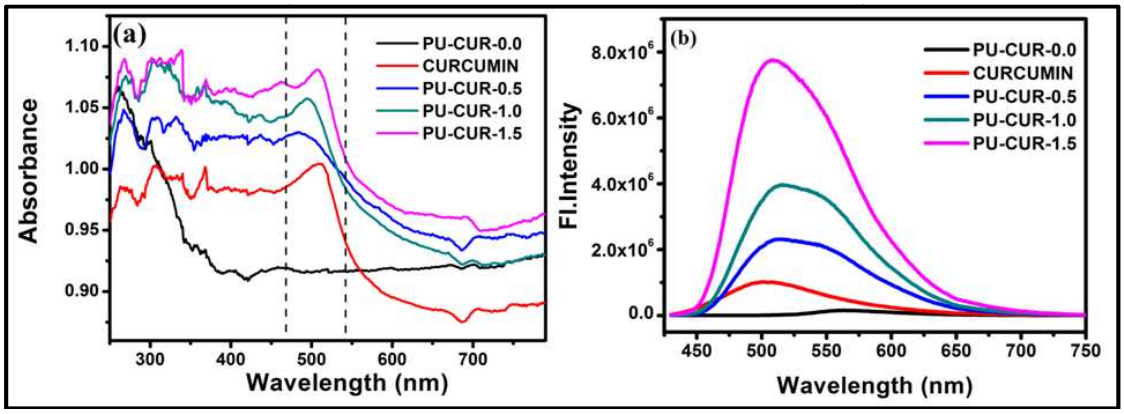

Figure 5.9: *(a) Solid-state UV-Vis spectra of PU-CUR Xerogels and (b) Solid-state Fluorescence spectra of PU-CUR Xerogels*

It can be clearly seen that the gels with curcumin show excitation at 500nm and this peak is absent in the gel without curcumin. Similarly, Fluoresence spectra of xerogel with curcumin **Figure 5.9 (b)** showed emission at 520nm which is not seen in the spectrum of PU-CUR matrix. These observations clearly confirm the presence of curcumin in the xerogels.

5.4.5 Swelling Measurements

Swelling, an important property of the hydrogel strongly depends on the degree of crosslinking and hydrophilicity of the hydrogel. In PU-CUR hydrogels, the contribution to the swelling comes from the hydrophilic part, PEG and controlled by the content of HT and hydrophobic curcumin. It was observed that PU-CUR xerogels were opaque in nature which was attributed to the crystallinity of PEG in the gel matrix. However, the gels became transparent upon swelling due to the loss of this crystallinity **Figure 5.10 (d)**.

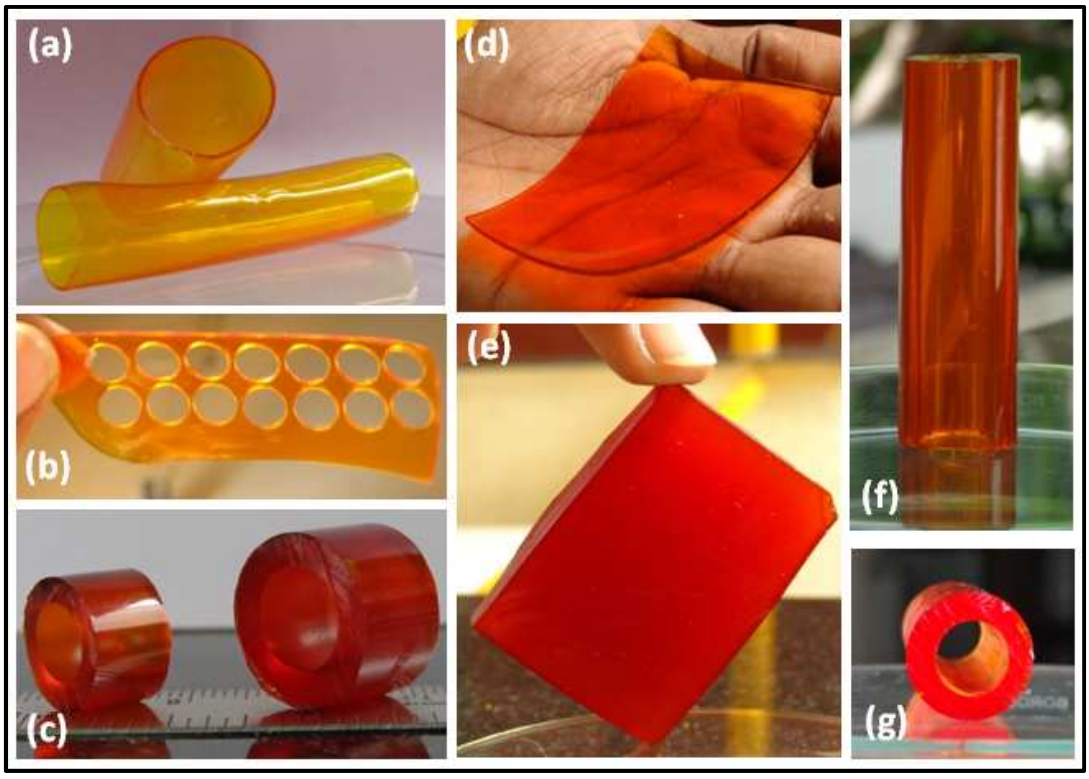

Figure 5.10: *PU-CUR-1.0 gels. (a) Flexible and thin tubes, (b) resistivity to cutting the sample. (c) Dry and water swollen hollow tube, (d) thick film with transparency, (e) block of hydrogel (opaque), (f, g) transparent thick tube and its cross-sectional view.*

We show in **Figure 5.11(a),** the equilibrium swelling capacities of PU-CUR hydrogels with three different contents of curcumin (at constant HT) measured at room temperature. It can be seen that, the equilibrium swelling ratio decreases from 800% to 200% with curcumin content increasing from 0.5 to 1.5wt%. The decrease in equilibrium swelling can be attributed to the formation of more compact/ interconnectivity in the network structure with more degree of crosslinking which prevents the expansion of network.

The degree of crosslinking in the gel matrix is likely due to both HT and partial covalent linking of curcumin into the network structure. Therefore, these gels can be effectively termed as double crosslinked gels.

In general, the kinetics of swelling i.e. the time dependence of water uptake in gels can be given as,

$$F(t) = \frac{W_s - W_d}{W_\infty - W_d} = kt^n \qquad (1)$$

Where 'k' is a swelling rate constant, 'n' is the swelling exponent, W_d is the weight of dry samples, W_s and W_∞ are the swollen weights at time 't' and at equilibrium, respectively. It can be readily seen from **Figure 5.11(a)** that, the equilibrium swelling reached within 10 hours for all the samples indicating reasonably faster diffusion of water molecules in the gel matrix.

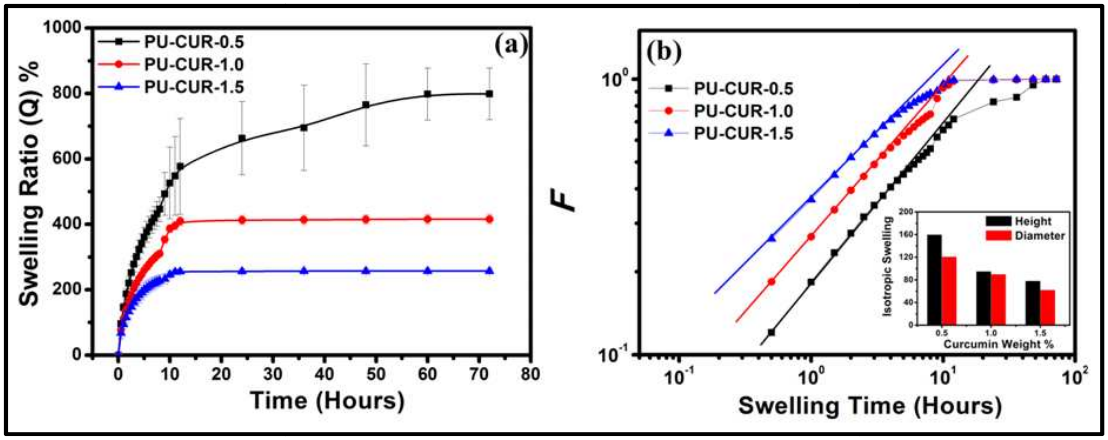

Figure 5.11: *(a) Swelling studies with respect to time for PU-CUR gels with different amount of curcumin. (b) Swelling ratio with time at the initial stages of swelling and inset shows isotropic swelling studies of PU-CUR gels with different amount of curcumin.*

However, it is important to note here that, the diffusion of water molecules into hydrogel strongly depends on the polymer chain mobility which in turn depends on the glass transition temperature (T_g) of the polymer. In general, higher the crosslink density, higher is the T_g. The water uptake follows Fickian diffusion with swelling exponent, '*n*' close to 0.5 when the chains are mobile. On the other hand, if the chains are more rigid with a limited mobility, then the polymer chain relaxation rate is lower than water molecule diffusion rate and the diffusion will be non-Fickian with the value of swelling exponent, '*n*' between 0.5 and 1.0.

We show in **Figure 5.11(b),** the log-log plots of swelling with time for PU-CUR hydrogel with 3 different curcumin contents at constant HT. At the initial stage of swelling, the swelling kinetics profiles increase linearly, following a power law behaviour and then level off upon approaching the equilibrium state of swelling. The swelling exponent, '*n*' could be estimated from the slope of the initial linear region of swelling curve. The values of '*n*' are very close to 0.5 indicating the Fickian diffusion of water molecules into PU-CUR hydrogels. We also observed an isotropic swelling nature in PU-CUR-1.0 gel.

5.4.6. Micro structural Characterization

5.4.6.1 Wide-Angle X-ray Diffraction (WAXD)

We show in **Figure 5.12(a),** the Wide-Angle X-ray Diffraction patterns of PU-CUR0.0 and PU-CUR xerogels with different contents of curcumin. The diffraction patterns of neat PEG-4000 shows two characteristic peaks centered at *d*-spacing of 4.6 Å ($2\theta=19.2^0$) and 3.8Å ($2\theta=23.4^0$) which can be attributed to the 120 and 132 reflections of PEG monoclinic unit cell, respectively.

In the case of PU-CUR Xerogels with different contents of curcumin, the diffraction peaks appear at the same 2θ angles of pure PEG with a similar *d*-spacing value, indicating that only the PEG segments contributed to the semi crystalline nature of PU-CUR gels. We performed WAXD experiments of PU-CUR with different content of curcumin at the same content of HT at room temperature.

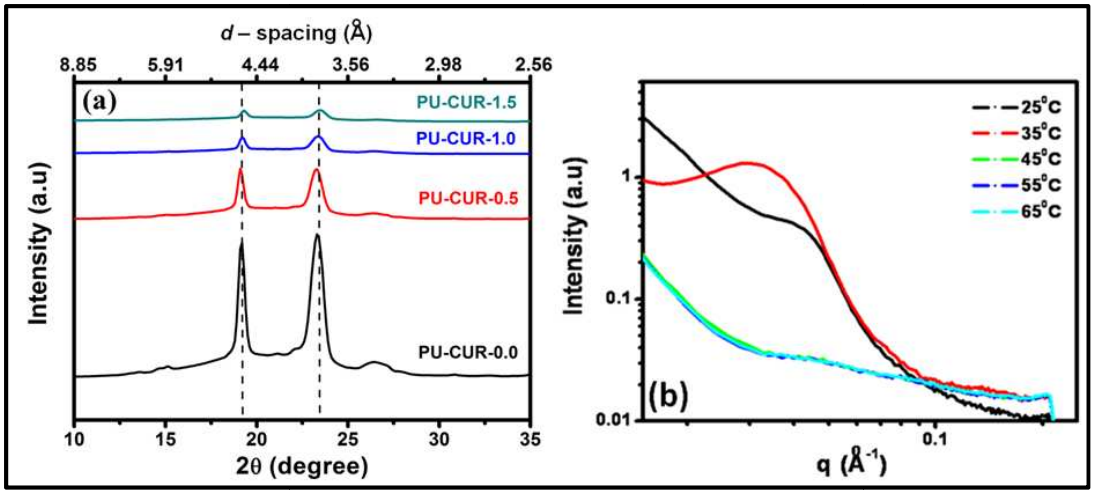

Figure 5.12: *(a) Wide-Angle X-ray Diffraction patterns of PU-CUR-0.0 and PU-CUR xerogels at room temperatures. (b) Small-angle X-ray scattering profile of PU-CUR-1.0 Xerogel at different temperatures.*

It can be readily seen from the **Figure 5.12(a)** that, the diffraction peaks initially observed at *d*-spacing values of 4.6 Å and 3.8 Å at room temperature corresponding to PEG crystalline segment start to show decrease in intensity with increase in curcumin content from PU-CUR-0.5 to PU-CUR-1.5. A substantial decrease in the peak intensity clearly indicates that the curcumin is covalently linked to the polymer backbone.

5.4.6.2 Small-Angle X-ray Scattering (SAXS)

To explore further on the microstructure of gels, we performed SAXS experiments on PU-CUR gels at different temperatures starting from room temperature to 65 ^{0}C. The profiles of scattering intensity as a function of scattering vector are shown in **Figures 5.12(b).** The scattering vector profiles of PU-CUR gels exhibit a characteristic scattering peak. The relation between scattering vector (q) and scattering angle (θ) is given as,

$$q = \frac{4\pi}{\lambda}\sin\frac{\theta}{2} \qquad (2)$$

Where 'λ' is the X-ray wavelength (Cu Kα = 1.5418 Å). The average distance'*d*' between domains can be estimated by the peak position using a well established equation as follows:

$$d = \frac{2\pi}{q_{max}} \qquad (3)$$

Where, q_{max} is a scattering vector at maximum intensity of the correlation peak.

Upon heating PU-CUR xerogels closer to the melting of the soft segments (PEG, ~45 ^{0}C), the scattering peaks in the SAXS spectra shift to the low q region indicating that the smaller lamella melt first thereby shifting the average spacing between lamellae to larger values (low q shift). Finally, the SAXS peak disappears indicating that the peaks in PU-CUR xerogels originate exclusively from the lamellar packing of soft PEG chains. Further, we do not see any separate scattering peaks coming from the hard segments, since their content in the gel matrix is very low.

5.4.7 Mechanical Properties

The mechanical properties of the curcumin incorporated PU-CUR hydrogels were determined using compression, extension and cyclic compression experiments **(see Table 5.3)**. The large deformation experiments are carried out by mechanical testing machine (Instron UTM 33R with a load cell of 10kN) in uniaxial compression or tensile mode. Whereas, the cyclic compression experiments for mechanical hysteresis are carried out using ARES G2 strain controlled rheometer. We show in **Figure 5.14 (a)** the tensile stress-strain curve for hydrogel sample without and with different contents of curcumin.

Table 5.3: *Mechanical properties of PU-CUR hydrogels*

Samples	Tensile		Compression (%)		Compression Strength at break (MPa)	
	Strength (MPa)	Elongation (%)	With entrapped curcumin	Without entrapped curcumin	With entrapped curcumin	Without entrapped curcumin
PU-CUR-0.0	0.22	72	-	-	-	-
PU-CUR-0.5	0.48	46	92	83	1.6	0.7
PU-CUR-1.0	0.64	284	92	78	4.6	2.7
PU-CUR-1.5	0.73	76	75	63	3.7	1.5

Hydrogels with no curcumin (PU-CUR-0.0) showed tensile strength of 0.22 MPa with a percent elongation of 72%. Whereas, hydrogels with curcumin content of PU-CUR-0.5, PU-CUR-1.0 & PU-CUR-1.5 showed tensile strengths of 0.48MPa,

0.64MPa and 0.73MPa with percentage elongation of 46%, 284% and 76% respectively.

We have shown in **Figure 5.14 (b),** the compressive stress-strain curves for equilibrium swollen PU-CUR hydrogels containing curcumin (a) 0.5% (b) 1.0% and (c) 1.5% and compared the results with hydrogels containing no curcumin (0.0%). It can be seen from the figure that, all the curves exhibit an initial linear region, the slope of which can give the modulus of the gel network. The hydrogels with no curcumin (PU-CUR-0.0) breaks at 0.9 MPa with % compression of 58% (λ = 58%). Whereas, hydrogels with PU-CUR-0.5 and PU-CUR-1.0 curcumin showed compressive strength of 1.6 MPa and 4.6 MPa respectively, and could be compressed upto 92% without breaking **Figure 5.13 (a)**.

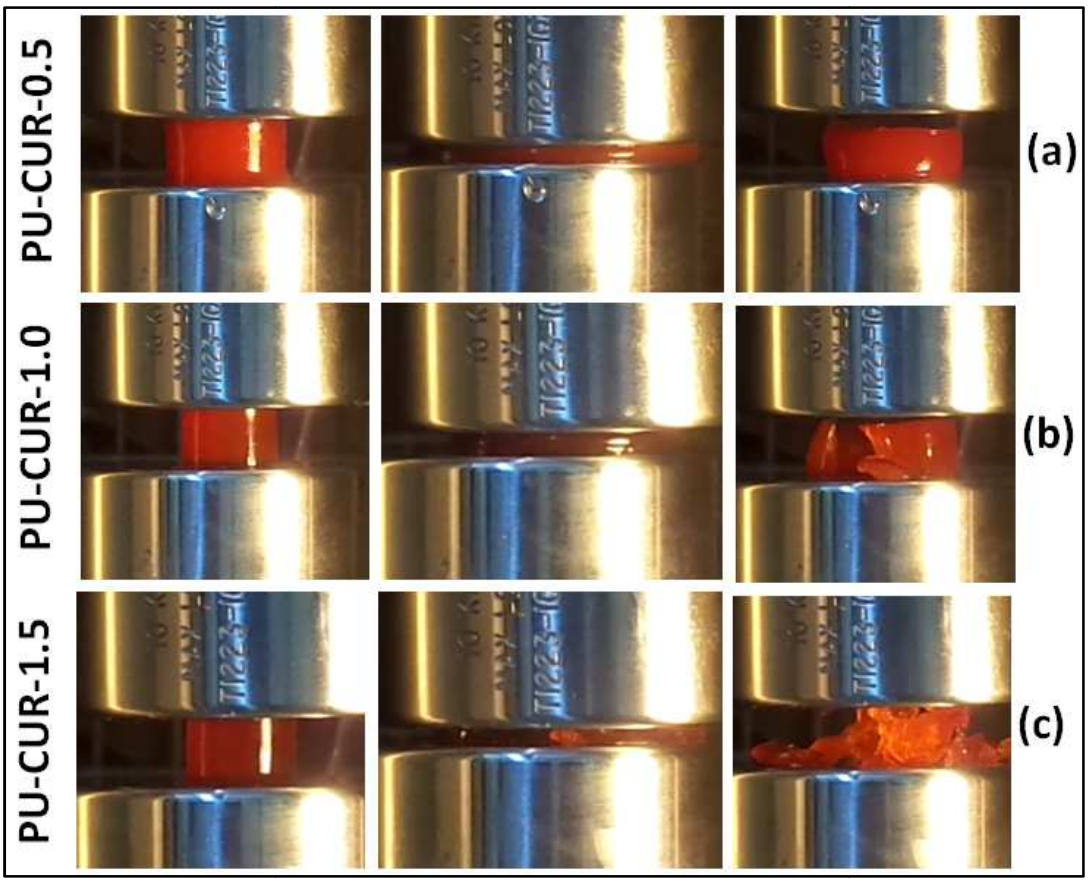

Figure 5.13 *Photographs of compression study demonstrating sustainability of (a) PU-CUR-0.5 at higher compression (90% strain), (b) PU-CUR-1.0 (90% strain), and (c) PU-CUR-1.5 (75% strain), respectively.*

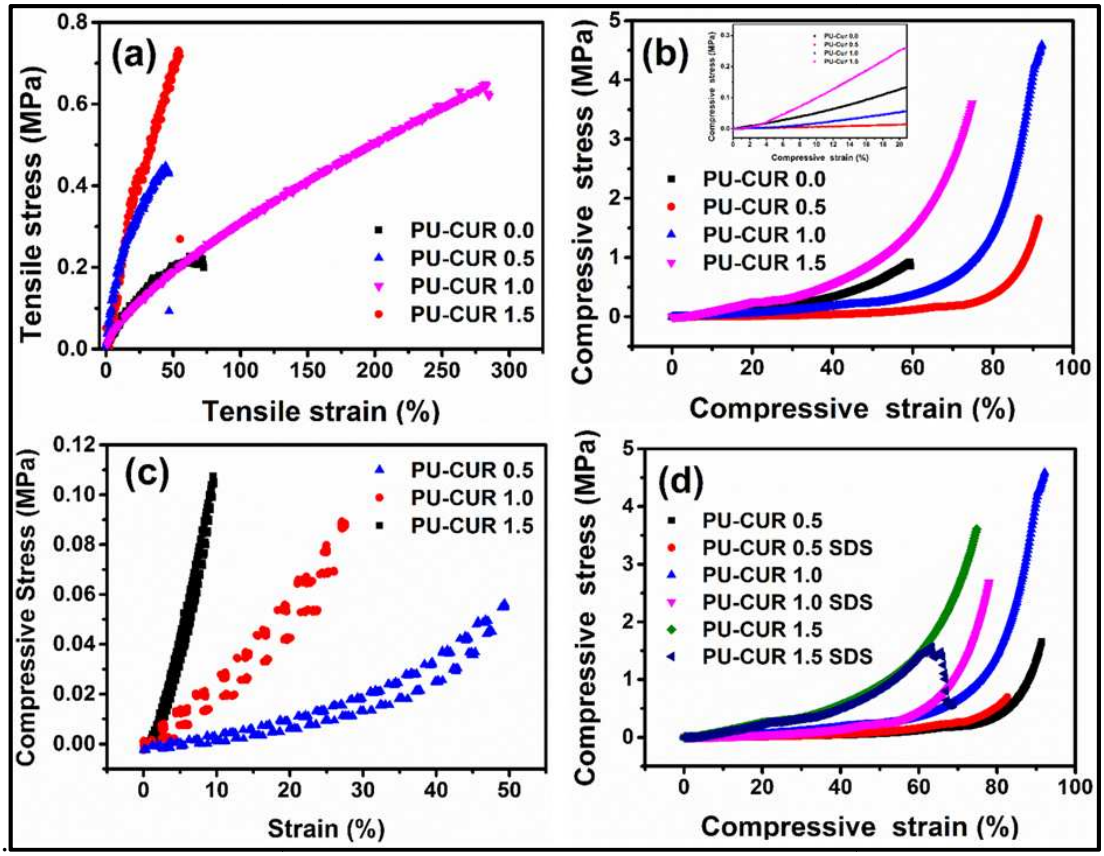

Figure 5.14: *(a) Tensile data for the different amount of curcumin incorporated PU-CUR hydrogels, (b) Uni-axial compression experiment of PU-CUR hydrogels in the swollen state with increasing the amount of curcumin concentration, (c) Cyclic compression study of different amount of curcumin incorporated PU-CUR hydrogels (d) Comparison of mechanical strength of once swell samples vs. samples after SDS Cycle of PU-CUR hydrogels an overlay plot.*

The hydrogels with PU-CUR-1.5 of curcumin however, showed a rupture at compression of 75% with a compressive strength of 3.6 MPa (**Figure 5.13 (c)**). These observations clearly indicate that the curcumin incorporation into PU-CUR hydrogels enhanced the mechanical strength of the hydrogels with high compressibility (~ 90%).

The increase in both compression and tensile strength of curcumin incorporated hydrogels can be attributed to the fact that, curcumin in the hydrogel network is present as partially covalently linked to the network and partially physically entrapped in the network structure. The covalently linked curcumin, along with the HT can provide a dual cross linking nature to the hydrogel network. The

dual cross linking can induce uneven distribution of cross links resulting into the heterogeneity of the network structure. On the other hand, the physically entrapped curcumin can assist in the efficient dissipation of energy. Therefore, both the degree of heterogeneity and energy dissipation play important role in determining the strength of the hydrogels and the presence of both enhances the mechanical strengths of the hydrogels.

To evaluate the energy dissipation in these gels, the cyclic test of loading-unloading were carried out using ARES-G2 strain controlled rheometer, in the compression mode. In **Figure 5.14 (c)** shows the loading-unloading curves of stress vs. strain for hydrogel samples containing different contents of curcumin. A total of 25 cycles were carried out for each sample with loading-unloading speed of 0.25mm/s and at constant compressive strain amplitude. Apparent hysteresis loops are observed on loading-unloading curves, suggesting that hydrogels dissipate energy effectively. Despite the observation of hysteresis loops in the loading-unloading cycle, the recovery in the hydrogel was maintained. Interestingly, it was observed that the curves superimposed for all the 25 cycles in the samples, indicating the breaking and reforming of the network structure in the dynamic mode. This observation also further implies that there is no permanent damage to the network structure in the applied limits of compressive amplitudes.

To understand the influence of physically entrapped curcumin on the mechanical properties of the hydrogels, the entrapped curcumin was extracted out by immersing the hydrogels in ethanol:water mixture (65:35 by vol). The samples PU-CUR-0.5, PU-CUR-1.0 and PU-CUR-1.5, with initial curcumin loading of 15, 30 & 45mg/g were subjected to ethanol:water mixture extraction for almost 10 days. After 10 days the release of curcumin from the hydrogel was almost stopped as seen by the constant value of curcumin release as show in **Figure 5.15 (b)**.

The rationale for selecting ethanol:water mixture of 65:35(vol%) was mainly due to the maximum swelling of gels at this solvent mixtures **Figure 5.15 (a)**. This will also ensure the easy diffusion of entrapped curcumin from the hydrogel due to the loosening of the network structure at the highest swelling ratio. The removal of physically entrapped curcumin was monitored by OD measurement in UV-VIS

spectroscopy. Extraction with ethanol:water mixture resulted in the release of entrapped curcumin in varying extents according to the initial curcumin loading during the synthesis of hydrogels. **Table 5.4** gives an account of chemically linked and physically entrapped curcumin into the hydrogels.

Table 5.4: *Release of Curcumin in EtOH/H_2O (65:35v/v) mixture*

Sample	Curcumin loaded (mg)	Curcumin released (mg)	Curcumin remaining (mg)	Curcumin Remaining (%)
PU-CUR-0.5	15	10.27	4.73	31.5 %
PU-CUR-1.0	30	17.06	12.94	43.1 %
PU-CUR-1.5	45	29.65	15.35	34.1 %

It can be readily seen from the table that about 60-70% curcumin is present in the gels as a physically entrapped. After complete removal of the physically entrapped curcumin, the gels were dried and reswollen in DI water to the equilibrium value. In this process, the gels were subjected to swelling-deswelling-swelling cycle. We propose to term it as swell-deswell-swell (SDS) cycle. The SDS cycle might influence the mechanical properties of the hydrogel to some extent. These aspects however, have not been looked at in this study. The mechanical properties in terms of % compression and compression strength at break were again measured and compared with the data of samples with entrapped curcumin.

From the **Figure 5.14 (d)** it was observed that the % compression decreased from 92% to 83%, 92% to 78% and 75% to 63% for the samples, PU-CUR-0.5, PU-CUR-1.0 and PU-CUR-1.5 respectively. Similarly, the compression strength at break also decreased from 1.6MPa to 0.7MPa, 4.6MPa to 2.7MPa and 3.7MPa to 1.5MPa for PU-CUR-0.5, PU-CUR-1.0 and PU-CUR-1.5 respectively.

These observations clearly indicate that, curcumin incorporated in the PU hydrogels as both crosslinked as well as physically entrapped form exhibit enhanced mechanical properties to the hydrogels. The presence of curcumin in the chemically linked and physically entrapped states induces heterogeneity in the hydrogel structure and easy dissipation of the energy under deformation respectively. These combined effects are desirable for the enhancement of mechanical strengths of hydrogels which can be tuned for application in tissue engineering. Further, curcumin being non-toxic

and antibacterial can give added advantage to these hydrogels in biomedical application.

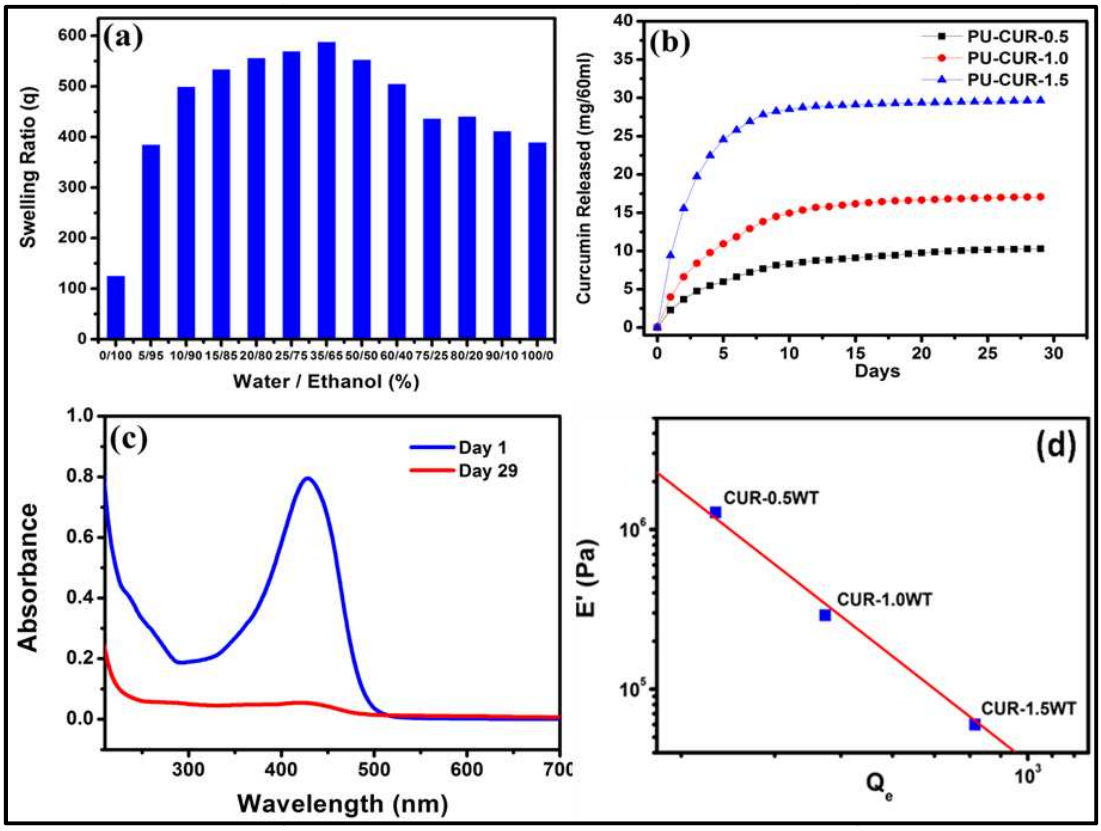

Figure 5.15: ***(a)*** *Swelling studies with respect to Ethanol/water mixture (65:35) for PU-CUR (b) Curcumin release in Ethanol/water mixture (65:35) (c) UV absorbance of curcumin from Day 1 to Day 29 and (d) Plot of storage moduli (E') vs equilibrium swelling ratio (Q_e) of PU-CUR hydrogels in water at 25^{0}C.*

It is also important to note that there exists an interesting relationship between the modulus (G′) and the equilibrium swelling ratio (Q_e). The classical prediction[32-33] for the relationship between these two parameters is given as eqn (4),

$$G \sim Q_e^{-1/3} \qquad (4)$$

It is known that this relationship is based on the assumptions that, the network chains (PEG chains in this case) follow Gaussian statistics and the network deforms affinely. We show in **Figure 5.15 (d)**, a log-log plot of shear modulus (*E′*) versus equilibrium swelling ratio (Q_e) of PU-CUR hydrogels with different contents of curcumin (PU-CUR 0.5 - 1.5). It can be readily seen from the figure that, the storage

modulus decreases linearly with increasing swelling ratio (Q_e). According to the power law: $G' \sim Q_e^{-m}$ with the value of m = 5.2 which is quite high compared to the value of 0.33 for the affine networks. This clearly indicates the striking departure from Gaussian behavior with no affine deformation of the network.

5.4.8. Morphological Analysis

5.4.8.1. Scanning Electron Microscopy (SEM)

We show in **Figure 5.16**, the SEM micrographs of lyophilized samples of PU-CUR gels with different contents of HT and compare with the untreated samples of PU-CUR gels.

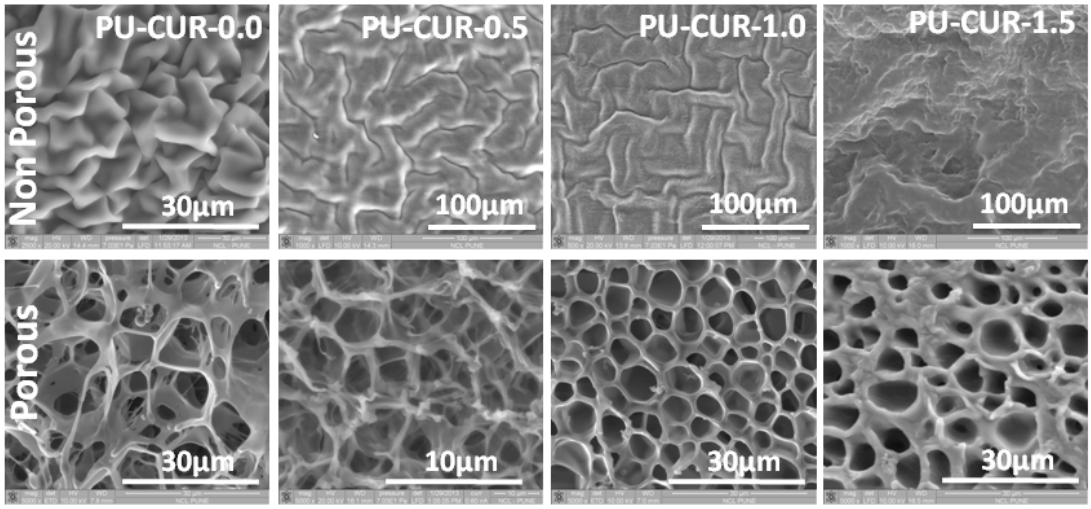

Figure 5.16: *SEM micrographs of the porous PU-CUR xerogels with different curcumin content.*

It can be revealed from the figure that, the treated sample exhibits porous structure with the pore sizes in the range of 2-15µm. Pore size range required for the adequate growth of different category of cells and/or tissues have been already extensively studied and reported. We found that the pore sizes obtained in our samples are suitable for hosting the endothelial cell transplantation process during the initial stages of tissue regeneration.

5.4.8.2. Microcomputed Tomography (µ-CT).

To investigate the micro-architectural parameters of porous xerogels, microcomputed tomography (µ-CT) technique was used. µ-CT is a high resolution

and noninvasive three-dimensional X-ray imaging technique, which has key advantages over other techniques used for the characterization of porous systems. Porous xerogels were imaged using μ-CT, and their micro-architectural characteristics such as porosity, pore size distribution, wall-thickness distribution, were evaluated.

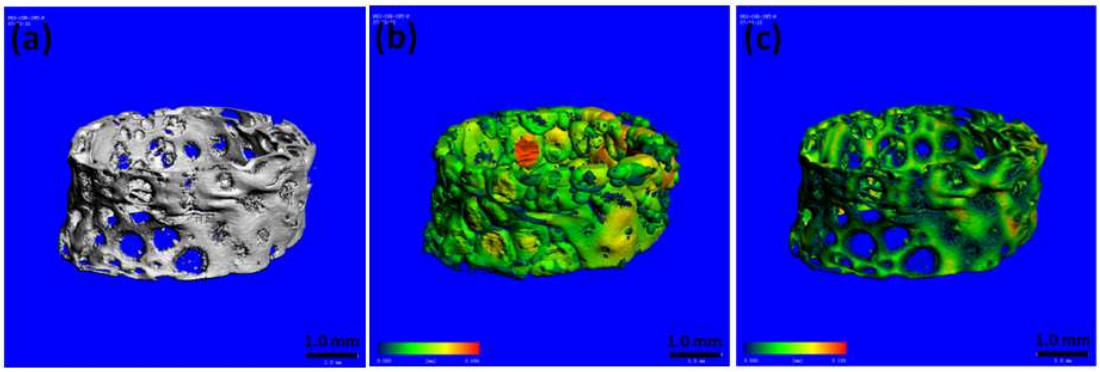

Figure 5.17: *(a) 3D image of the porous PU-CUR-1.0 xerogel obtained from the reconstruction of 2D X-ray projections using μ-CT, (b) pore-size distribution of the xerogel, and (c) wall-thickness distribution of the xerogel. All images are with 1 mm scale bar.*

Figure 5.17 (a), shows the three-dimensional image of porous PUCUR- 1.0 xerogel obtained from μ-CT, which shows homogeneous distribution of pores throughout its volume with an overall porosity of 77%. Pores in the xerogel were imaged by inversion of the 3D image, and their size distribution based on a colour scale is shown in **Figure 5.17 (b)**.

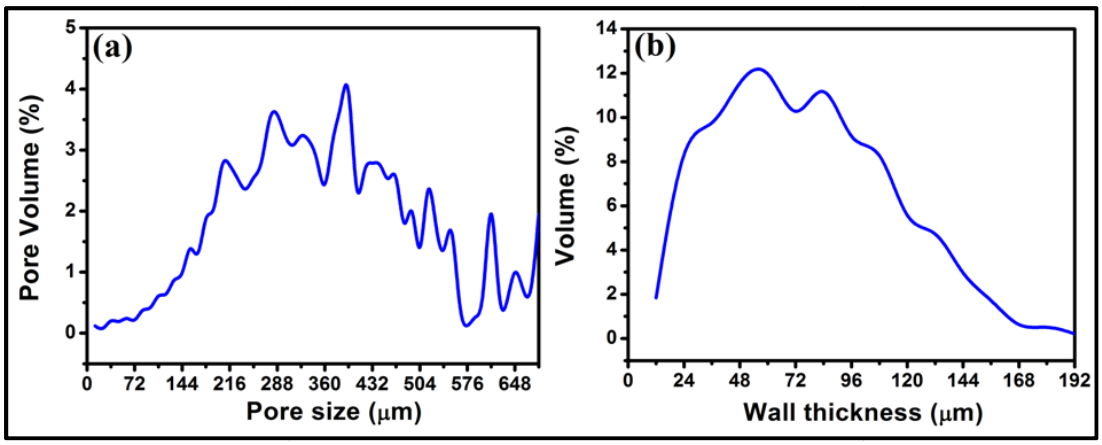

Figure 5.18: *(a) Histogram of the pore-size distribution in PU-CUR-1.0 xerogel and (b) Histogram of the wall-thickness distribution in PU-CUR-1.0 xerogel.*

Histogram of the pore-size distribution illustrated in **Figure 5.18 (a)** shows the distribution of pores with respect to the total pore volume. It is evident that the pores ranging from 200−400 μm contribute to the majority of pore population. **Figure 5.17 (c)**, shows the wall thickness distribution of the xerogel with a colour-coded thickness distribution profile. Histogram of the thickness-distribution shown in **Figure 5.18 (b)** shows a major thickness contribution from 24−108 μm.

5.4.8.3. Confocal Microscopy

Since curcumin has the fluorescence property, its presence in the gel matrix could also be determined by confocal microscopy. The confocal microscopy was performed on a sample which was subjected to 29 days ethanol/water mixture (65:35) extraction for extracting the physically entrapped curcumin in the sample.

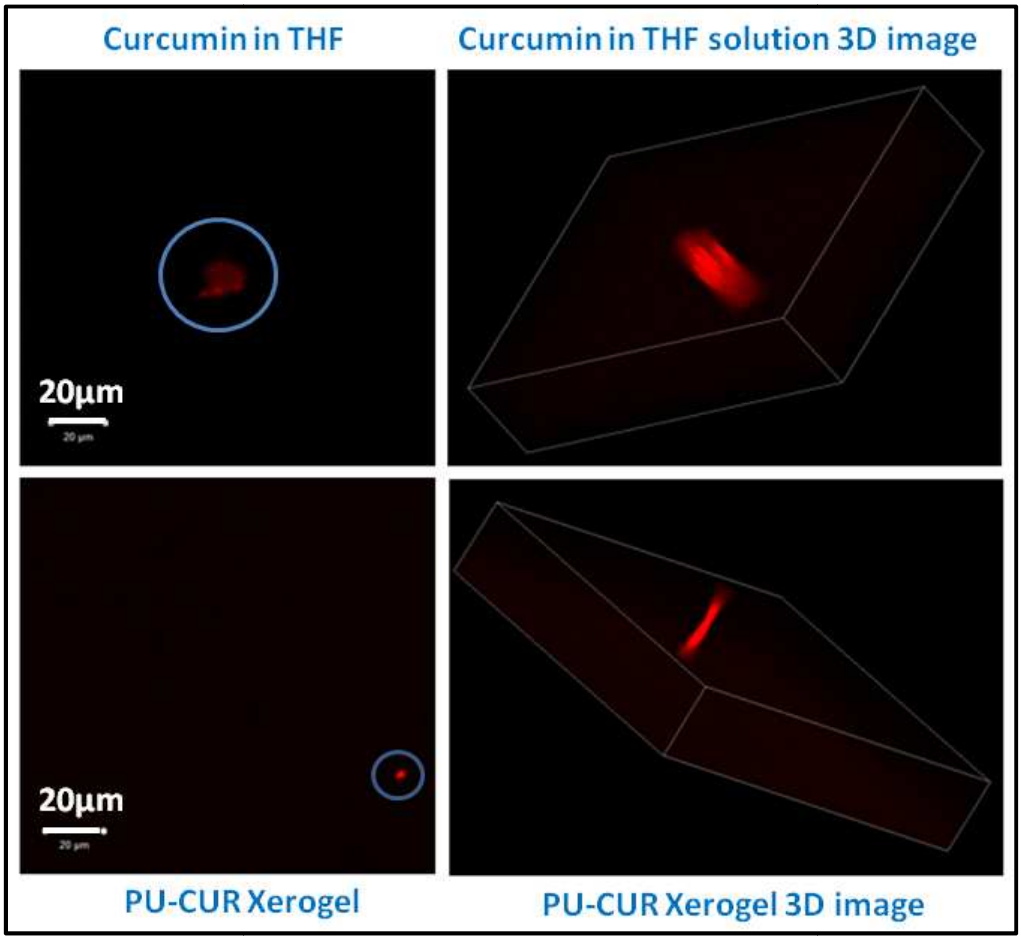

Figure 5.19: *Confocal microscopy image of curcumin in THF and PU-CUR xerogels from both in 2-D and 3-D view.*

Confocal micrographs indicate the presence of curcumin chemically crosslinked with the isocyanate. These results were compared with a solution of curcumin in THF. From **Figure 5.19**, it could be concluded that the curcumin is chemically crosslinked after the removal of all physically entrapped curcumin, moreover, the comparison between the 3D images were also found to be in agreement with the above conclusions.

5.4.9. In vitro Biological Test

5.4.9.1 Cytotoxicity Test (Direct contact method)

A549 (adenocarcinomic human alveolar basal epithelial cells) cell line was used for preliminary studies. Studies demonstrate that cells are viable on this substrate. The *in vitro* cytotoxicity of PU-CUR-1.0 hydrogels was examined using direct contact method.

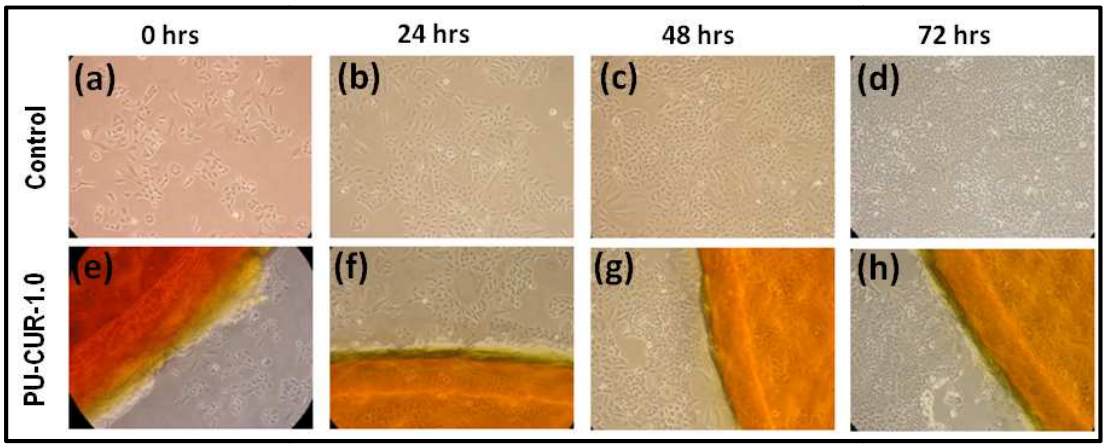

Figure 5.20: *Optical phase contrast images of PU-CUR-1.0 hydrogels in direct contact with A549 cells for 72 h at 37°C. Morphologies of cells in control wells and those in contact with PU-CUR-1.0 hydrogels shown in figures (a-d) and (e-h) respectively at 0, 24, 48 and 72 hours.*

The morphology of cells in direct contact with the surface of PU-CUR-1.0 hydrogels at different intervals (0, 24, 48 and 72 hours) were similar to that of the cells in the control wells and were viable as indicated by optical micrographs. **Figure 5.20(a,b)** shows that the cells in control wells at 0 and 24 hours shows exponential increase in their population. Similar increase in population of cells was visible in the PU-CUR-1.0 gels at 0 and 24 hours **Figure 5.20 (e,f)**. **Figure 5.20 (g,h)** shows

continuous cells growth in PU-CUR-1.0 gels at 48 and 72 hours respectively, which is in terms with the corresponding control wells shown in **Figure 5.20 (c,d)**. Since the direct contact method shows good cytocompatibility even after 72 hours, further viability analysis were not performed.

5.4.9.2. MTT Assay

Cytotoxicity of PU-CUR 1.0 hydrogel was evaluated by MTT assay, which is based on the principle of reduction of enzyme succinate dehydrogenase in the presence of dye MTT to purple coloured formazan crystals. L-929 fibroblast cells showed cell viability for PU-CUR-0.0 and PU-CUR-1.0 (97.1 and 94.6%, respectively, as shown in **Figure 5.21**), but the MCF-7 did not show cell viability for PU-CUR-1.0 (6.4% as shown in **Figure 5.21**). Results clearly indicate that PU-CUR-1.0 hydrogels are selectively nontoxic, which indicates biocompatibility to L-929 fibroblast cells in [**Figure 5.22 (a and b)]** and toxic to MCF-7 cell line as shown in **Figure 5.22 (c and d)**. With these observations, it can be concluded that PU-CUR gels are selectively toxic to human breast cancer cell line (MCF-7 cell line).

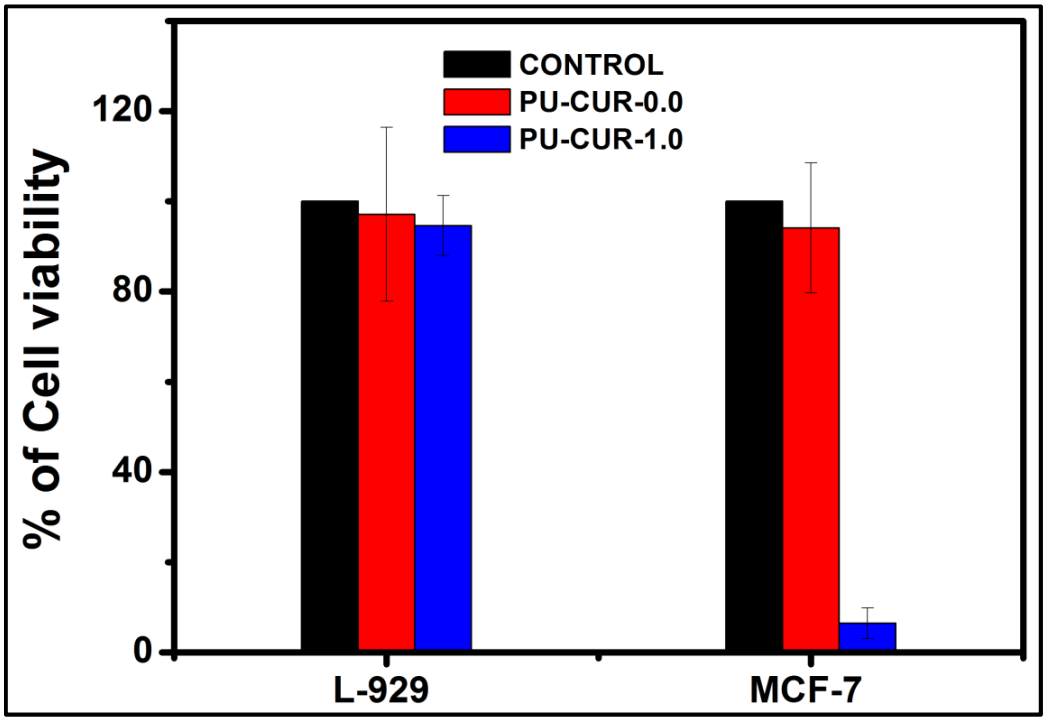

Figure 5.21: *MTT absorbance of PU-CUR-1.0 with L-929 fibroblast and MCF-7 cell lines.*

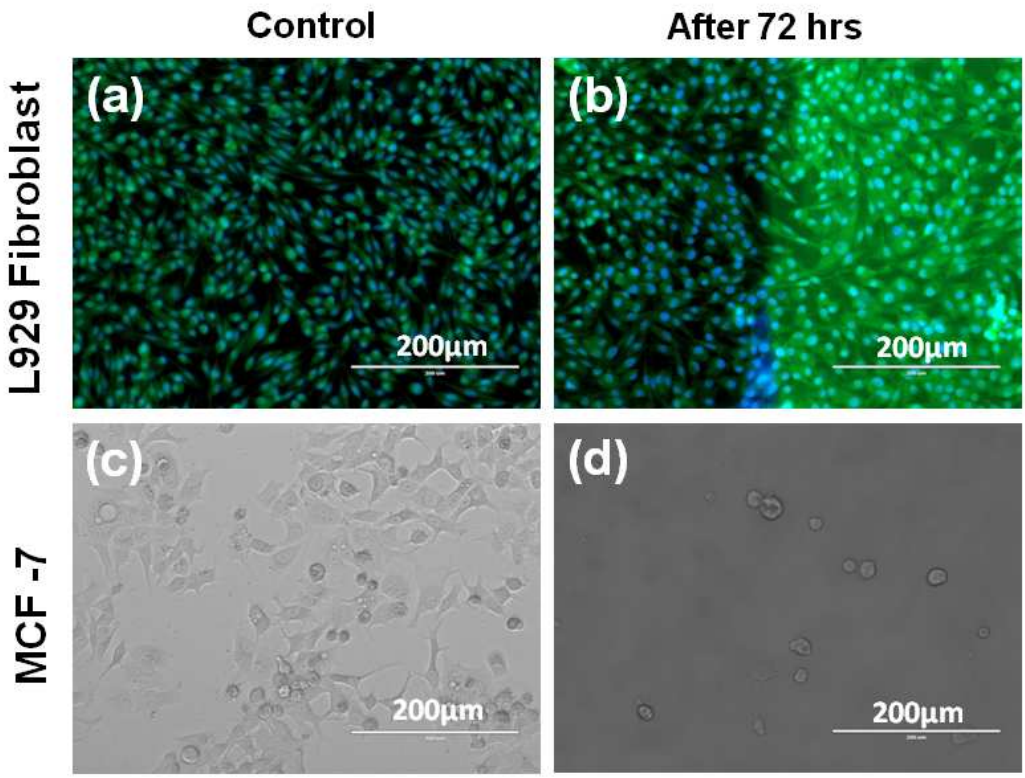

Figure 5.22: *Optical phase contrast images of PU-CUR-1.0 hydrogels in MTT Assay with MCF-7 and L 929 fibroblast cells for 72 h at 37°C. (a) Control for L929 Fibroblast cell lines (b) L929 Fibroblast cell after 72hrs treating with the hydrogels. (c) Control for MCF-7 cell lines (d) MCF-7 cell lines after 72hrs treated with the hydrogels.*

5.4.9.3. Cytostatic concentration of curcumin

An in vitro cytotoxicity test using 'Test on Extract' method was performed on curcumin with concentrations 0.25, 0.5, 1.0, 2.0, and 4.0 µg/mL **(Figure 5.23)**. Extract was prepared by incubating curcumin with DMSO (0.5% in culture medium) for 72 ± 2 h at 37 ± 2 °C. A 99 µL of culture medium was mixed with 1 µL of extract of test samples. A 100µL of test samples, negative control, and positive control in triplicate were placed on subconfluent monolayer of L-929 cells. After incubation of cells with extract of test samples and control at 37 ± 2 °C for 24 h, the cell culture was examined microscopically for cellular response **(Figure 5.24)**.

An in vitro MTT assay was performed with the curcumin samples and showed 100%, 63%, 33%, 17.45%, and 7.5% metabolic activity, respectively. It is known that curcumin is not stable at physiological pH and undergoes chemical degradation

through α−β unsaturated β-diketo moiety. However, this degradation is significantly reduced when curcumin is attached to lipids, liposomes, and polymer structures. Further, it is quite stable when it is used with FBS buffer. In our work, curcumin is chemically attached with the PU matrix as well as physically entrapped in the network structure. Therefore, the chemical degradation is least anticipated.

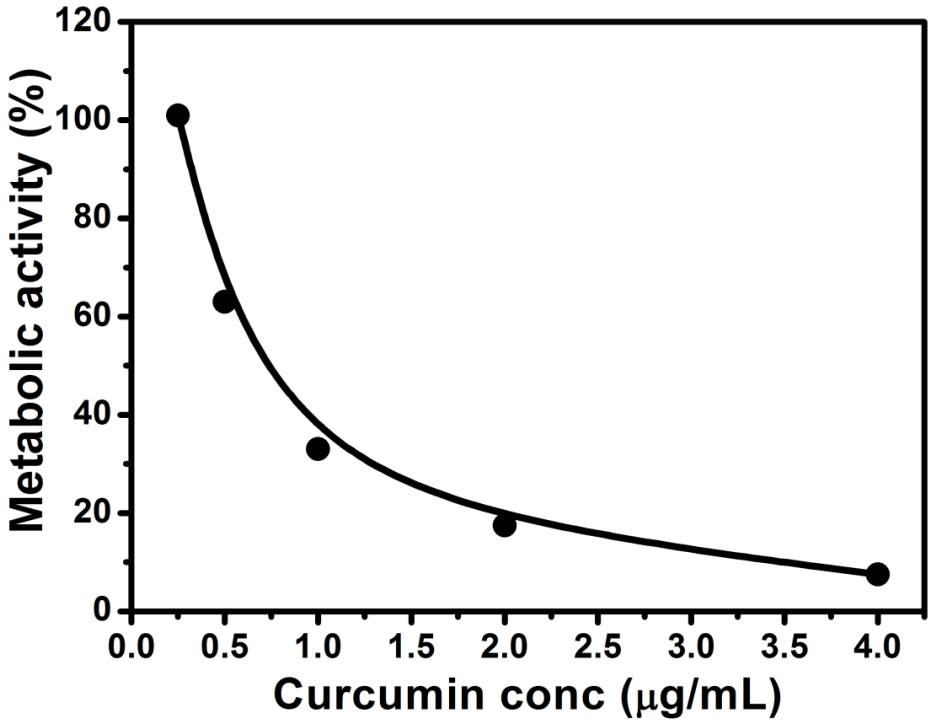

Figure 5.23: *Histogram showing the metabolic activity of various concentrations of curcumin (0.25, 0.5, 1.0, 2.0 and 4.0μg/mL).*

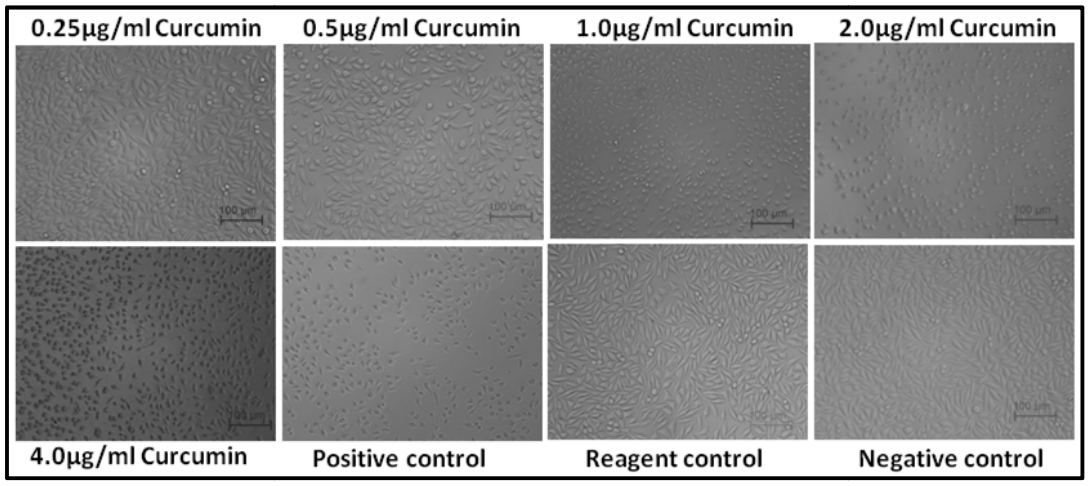

Figure 5.24: *MTT Assay of curcumin with different concentration.*

5.4.9.4. Antibacterial Study

Figure 5.25 shows the results of in vitro antibacterial screening of different hydrogels against *S. aureus*. The screening was performed using the Kirby−Bauer disc diffusion method and the LB Broth method. The bactericidal effects of neat gel and curcumin loaded (0.0%, 0.5%, 1.0%, and 1.5% curcumin content) hydrogels were then comparatively evaluated by observing inhibition zones.

Figure 5.25: *Antibacterial activity of PU-CUR-0.0 and curcumin loaded PU-CUR hydrogels against S.aureus*

As shown in **Figure 5.25**, no inhibition zones were found around the hydrogel, PU-CUR-0.0 (no curcumin), indicating that this hydrogel exhibit no antibacterial property. On the other hand, the curcumin containing hydrogel exhibited an antibacterial effect on Gram-positive *S.aureus*, as seen by a distinguished inhibition zone. However, the zone of inhibition was highest for PU-CUR-0.5, which decreases as the concentration of curcumin increases. This might be because of limited diffusion of curcumin on the agar plate due to a complex network of the hydrogel.

5.5. Conclusions

In the present work, we synthesized curcumin incorporated PU-CUR hydrogels using PEG-4000, H_{12}MDI, Curcumin, HT by solvent-free one-pot method. Different amounts of curcumin were incorporated with constant amount of HT in the

gel. The chemical structure of the gels was confirmed by FTIR, HR-MS, UV-Vis and Fluorescent spectroscopy. The micro-structural characterization of gels by WAXD and SAXS indicated the presence of crystallinity which was attributed to the ordering of PEG segments in the gel structure. The presence of lamellar structure was also indicated by the SAXS studies. This can be due to the formation of smaller size of crystalline lamellae of PEGs in the gel structure. The swelling studies on PU-CUR gels at 37 ^{0}C showed Fickian diffusion of water into the hydrogels. The curcumin was found to be present in the hydrogel in two forms: i) covalently linked to the hydrogel structure and ii) physically entrapped in the gel matrix. The mechanical strengths of the curcumin incorporated PU-CUR gels increased due to the presence of curcumin. This was attributed to the heterogeneity in the hydrogel structure and easy dissipation of the energy under deformation from the entrapped curcumin. These combined effects are desirable for the enhancement of mechanical strengths of hydrogels. The porosity in the hydrogel was induced by a method of cryogenic treatment followed by lyophilization. The morphological characterization by SEM revealed the porous structure with 2-15μm pore size and the presence of interconnectivity of pores. The cytotoxicity studies of PU-CUR hydrogels showed the continuous growth of cells, which indicated the non-toxic nature of the hydrogels. These hydrogels show promising applications in vascular graft and Tissue Engineering applications.

5.6 References

1. Anderson, R.; Groundwater, P.; Todd, A.; Worsley, A., *Antibacterial Agents: Chemistry, Mode of Action, Mechanisms of Resistance and Clinical Applications*. Wiley: **2012**.
2. Hahn, F. E., *Mechanism of Action of Antibacterial Agents*. Springer Berlin Heidelberg: **2012**.
3. Miller, A. A.; Miller, P. F., *Emerging Trends in Antibacterial Discovery: Answering the Call to Arms*. Caister Academic Press: **2011**.
4. Avendano, C.; Menendez, J. C., *Medicinal Chemistry of Anticancer Drugs*. Elsevier Science: **2015**.
5. Pratt, W. B., *The Anticancer Drugs*. Oxford University Press: **1994**.
6. *Bioactive Natural Products (Part E)*. Elsevier Science: **2000**.
7. Thurston, D. E., *Chemistry and Pharmacology of Anticancer Drugs*. CRC Press: **2006**.
8. Jucker, E. M., *Antifungal Agents: Advances and Problems*. Birkhäuser Basel: **2012**.
9. Siegel, M. R.; Sisler, H. D., *Antifungal Compounds: Interactions in biological and ecological systems*. M. Dekker: **1977**.
10. Kavanagh, K., *Fungi: Biology and Applications*. Wiley: **2011**.
11. Aggarwal, B. B.; Surh, Y. J.; Shishodia, S., *The Molecular Targets and Therapeutic Uses of Curcumin in Health and Disease*. Springer US: **2007**.
12. Daniels, S., *Turmeric Curcumin Cures: Miracle Healers From The Kitchen*. Speedy Publishing LLC: **2014**.
13. Sasaki, J.; Kichida, M., *Curcumin: Biosynthesis, Medicinal Uses and Health Benefits*. Nova Science: **2012**.
14. Wattenberg, L.; Lipkin, M.; Boone, C. W.; Kelloff, G. J., *Cancer Chemoprevention*. Taylor & Francis: **1992**.
15. Pouliquen, D. L., *Curcumin: Synthesis, Emerging Role in Pain Management and Health Implications*. Nova Science Pub Incorporated: **2014.**
16. Books, L.; LLC, G. B., *Anti-Inflammatory Agents: Hyssop, Curcumin, Cannabidiol, Allicin, Nr58-3. 14. 3, Broad-Spectrum Chemokine Inhibitor, Anti-Inflammatory*. General Books: **2010**.

17. Romani, A.; Lattanzio, V.; Quideau, S., *Recent Advances in Polyphenol Research*. Wiley: **2014**.
18. Kloesch, B.; Becker, T.; Dietersdorfer, E.; Kiener, H.; Steiner, G., Anti-inflammatory and apoptotic effects of the polyphenol curcumin on human fibroblast-like synoviocytes. *International Immunopharmacology* **2013,** 15, (2), 400-405.
19. Gupta, A.; Vij, G.; Sharma, S.; Tirkey, N.; Rishi, P.; Chopra, K., Curcumin, a polyphenolic antioxidant, attenuates chronic fatigue syndrome in murine water immersion stress model. *Immunobiology* **2009,** 214, (1), 33-39.
20. Fang, Z.; Bhandari, B., Encapsulation of polyphenols–a review. *Trends in Food Science & Technology* **2010,** 21, (10), 510-523.
21. Gupta, S. C.; Prasad, S.; Kim, J. H.; Patchva, S.; Webb, L. J.; Priyadarsini, I. K.; Aggarwal, B. B., Multitargeting by curcumin as revealed by molecular interaction studies. *Natural Product Reports* **2011,** 28, (12), 1937-1955.
22. Lev-Ari, S.; *Anti-cancer Activity of the Natural Cox-2 Inhibitor, Curcumin, Alone and in Combination with Radio-chemotherapy: Translational Study*. Publisher not identified: **2007**.
23. Ma, C.; Fan, R.; Ribas, A., *Cancer Immunotherapy & Immuno-monitoring: Mechanism, Treatment, Diagnosis, and Emerging Tools*. Frontiers E-books: **2014**.
24. Kong, A. N. T., *Inflammation, Oxidative Stress, and Cancer: Dietary Approaches for Cancer Prevention*. CRC Press: **2016**.
25. Agrawal, D. K.; Mishra, P. K., Curcumin and its analogues: potential anticancer agents. *Medicinal research reviews* **2010,** 30, (5), 818-860.
26. Anand, P.; Kunnumakkara, A. B.; Newman, R. A.; Aggarwal, B. B., Bioavailability of curcumin: problems and promises. *Molecular Pharmaceutics* **2007,** 4, (6), 807-818.
27. Aggarwal, B. B.; Surh, Y.-J.; Shishodia, S., *The molecular targets and therapeutic uses of curcumin in health and disease*. Springer Science & Business Media: **2007**; Vol. 595.
28. Bisht, S.; Feldmann, G.; Soni, S.; Ravi, R.; Karikar, C.; Maitra, A.; Maitra, A., Polymeric nanoparticle-encapsulated curcumin ("nanocurcumin"): a novel strategy for human cancer therapy. *J Nanobiotechnology* **2007,** 5, (3), 1-18.

29. Kawamori, T.; Lubet, R.; Steele, V. E.; Kelloff, G. J.; Kaskey, R. B.; Rao, C. V.; Reddy, B. S., Chemopreventive effect of curcumin, a naturally occurring anti-inflammatory agent, during the promotion/progression stages of colon cancer. *Cancer Research* **1999,** 59, (3), 597-601.

30. Negi, P.; Jayaprakasha, G.; Jagan Mohan Rao, L.; Sakariah, K., Antibacterial activity of turmeric oil: a byproduct from curcumin manufacture. *Journal of Agricultural and Food Chemistry* **1999,** 47, (10), 4297-4300.

31. Heggers, J. P.; Robson, M. C., The emergence of silver sulphadiazine-resistant pseudomonas aeruginosa. *Burns* **1978,** 5, (2), 184-187.

32. Flory, P. J., *Principles of polymer chemistry*. Cornell University Press: Ithaca, **1953.**

33. Treloar, L. R. G., *The physics of rubber elasticity*. Oxford Univ. Press: Oxford, **2005**.

Summary and Conclusions

Chapter – VI

In the sixth chapter, we have discussed the summary and conclusions of thesis work.

The objective of the thesis was to design and synthesize novel hydrogels for drug delivery and tissue engineering applications. Although there are wide variety of hydrogels used for the above applications they have severe limitations in terms of poor mechanical strength, less biocompatibility, non-porous nature etc. Therefore, there is a big scientific challenge to design and develop novel hydrogels with improved properties. In this context, Polyurethane based hydrogels have emerged as important class of materials due to their good bio-compatibility, excellent chemical resistance and good mechanical properties. In order to improve the properties of PU hydrogels further and to investigate on their structural attributes in detail we have under taken the work on synthesis and characterization of new polyurethane hydrogels with tunable properties. A solvent free one-pot synthesis method with the combination of different hydrophilic/hydrophobic diols was used to obtain PU hydrogels. Curcumin with the antibacterial, anticancer properties was incorporated in the preparation of PU hydrogel. These aspects of PU hydrogels have not been reported earlier.

In the first chapter, a detailed literature survey was done on hydrogels in terms of their classification, synthesis, properties, advantages and disadvantages and applications for drug delivery and tissue engineering. Literature survey on the state-of-the-art of polyurethane (PU) hydrogels is given. The Characterization techniques such as WAXD, SAXS, UTM, μ-CT, biological tests etc., used for studying the micro-structural, surface morphology, mechanical behaviour and cytotoxicity of the hydrogels were briefly explained.

In the second chapter, we have discussed the scope and objectives of the thesis work which includes the following:

- To design and synthesize Polyurethane based hydrogels by solvent free one-pot method with improved mechanical properties for the applications in drug delivery and tissue engineering.
- To create porous structure in hydrogels which is most desirable feature for the efficient nutrient diffusion for scaffolds in tissue engineering.
- To use combination of hydrophilic/hydrophobic diols to obtain PU hydrogels with tunable properties.

- To characterize hydrogels in terms of their structure/microstructure, swelling, mechanical properties, biological properties etc., using techniques such as FT-IR, NMR, WAXD, SAXS, DMA, UTM, μ-CT, SEM and biological tests like cytotoxicity, MTT assay and antibacterial.
- To obtain bio-compatible and bio-active hydrogels by incorporating biomolecules such as curcumin.
- To demonstrate the potential use of the above hydrogels for drug delivery and tissue engineering applications.

In the third chapter, we have synthesized PEG-PU hydrogels using PEG-4000 as soft segment, H_{12}MDI as the hard segment and HT as a crosslinker by solvent free one-pot method. Hydrogels with different crosslink densities were obtained using different contents of HT. The chemical structure of the gels was confirmed by FT-IR and solid-state ^{13}C NMR spectroscopy. The micro-structural Characterization of gels by WAXD and SAXS indicated the presence of crystallinity which was attributed to the ordering of PEG segments in the gel structure. The presence of lamellar structure was also shown by the SAXS studies. The DSC studies showed a decrease in the crystalline melting of (T_m) of PEG-PU gels as compared to neat PEG-4000. This is attributed to the formation of smaller size of crystalline lamellae of PEGs in the gel structure. The swelling studies on PEG-PU gels at 37 ^{0}C showed Fickian diffusion of water into the hydrogels. The mechanical properties of gels were studied in dry and swollen states using uniaxial compression and dynamic oscillatory rheometry. The results showed an increase in the strength of hydrogels with increase in crosslink density. The porosity in the hydrogel was induced by a method of cryogenic treatment followed by lyophilization. The morphological Characterization by SEM, X-ray Micro-CT revealed the presence of porous structure with the interconnectivity of pores having pore size in the range of 2-15μm. The cytotoxicity studies of PEG-PU hydrogels showed the continuous growth of cells, which indicated the non-toxic nature of the hydrogels. These hydrogels show potential in tissue engineering applications.

In the fourth chapter, we have synthesized PU hydrogels by incorporating different type of diols in combination with PEG diol. The chemical structure of the gels was characterized by FT-IR spectroscopy. The micro structural Characterization

of gels by WAXD indicated the presence of crystallinity, which was attributed to the ordering of PEG, PCL, PCD segments in the gel structure. The equilibrium swelling ratios of the hydrogel decreased with increase in the hydrophobic diol content. Consequently, the tensile and compressive strength of the hydrogels increased. All the hydrogels exhibited good mechanical strength at moderate swelling of the hydrogels. The porosity in the hydrogel was induced by a method of cryogenic treatment followed by lyophilization. The morphological Characterization by SEM revealed the porous structure with 2−20μm pore size and indicated the interconnectivity of pores. The cytotoxicity studies of the obtained hydrogels showed the continuous growth of cells, indicating the nontoxic nature of the hydrogels. The in vitro drug release was studied using an anticancer drug doxorubicin hydrochloride and the release was correlated with the hydrophobicity/swelling of the gels. These hydrogels show potential applications in controlled drug delivery and tissue engineering.

In the fifth chapter, we synthesized curcumin incorporated PU-CUR hydrogels. Different amounts of curcumin were incorporated with constant amount of HT in the gel. The chemical structure of the gels was confirmed by FT-IR, HR-MS, UV-VIS and Fluorescent spectroscopy. The micro-structural Characterization of gels by WAXD and SAXS indicated the presence of crystallinity which was attributed to the ordering of PEG segments in the gel structure. The presence of lamellar structure was indicated by the SAXS studies. The swelling studies on PU-CUR gels at 37 ^{0}C showed Fickian diffusion of water into the hydrogels. The curcumin was found to be present in the hydrogel in two forms: i) covalently linked to the hydrogel structure and ii) physically entrapped in the gel matrix. The mechanical strengths of the curcumin incorporated PU-CUR gels increased due to the presence of curcumin. This was explained on the basis of presence of heterogeneity in the hydrogel structure and easy dissipation of the energy under deformation. These combined effects contributed to the enhancement of mechanical strengths of hydrogels. The porosity in the hydrogel was induced by a method of cryogenic treatment followed by lyophilization. The morphological Characterization by SEM revealed the porous structure having 2-20μm pore size with the interconnectivity of pores. The cytotoxicity studies of PU-CUR hydrogels showed the continuous growth of cells, which indicated the non-toxic nature of the hydrogels. These hydrogels show promising applications in Vascular graft and Tissue Engineering applications.

Finally, we made an attempt to achieve our objectives to develop PU hydrogels for drug delivery and tissue engineering applications. These hydrogels could be prepared in any intricate shape and size by one-pot synthesis method. The hydrophilic/ hydrophobic balance of the hydrogels could be tuned by using different types of diols in the preparation of PU hydrogels for the controlled drug delivery applications. The enhancement in the mechanical properties could be achieved by varying the crosslink density, hydrophobicity of the diols and incorporation of biomolecules such as curcumin. The obtained hydrogels exhibited excellent biological properties with enhanced mechanical strength which is very important for biomedical applications. These hydrogels show great potential in drug delivery, tissue engineering, vascular graft, patches, tissue expanders, various implants in the body etc.

List of Publications

Patent

1. A tunable Polyurethane/Curcumin Hydrogels system for Vascular Graft; Manohar Virupax Badiger and **Anumon Vattaparambil Divakaran**; *Application No: 3555DEL2015 (Prov. Date: 02/11/2015)*

Publications

1. Gold nanoparticle embedded hydrogel matrices as catalysts: Better dispersibility of nanoparticles in the gel matrix upon addition of N-bromosuccinimide leading to increased catalytic efficiency; Vilas Ramtenki, **V. D. Anumon**, Manohar V. Badiger and B. L. V. Prasad; *Colloids and Surfaces A: Physicochemical and Engineering Aspects. 414 (2012) 296– 301.*

2. Synthesis of porous poly(ethyleneglycol) - polyurethane (PEG-PU) hydrogels; **Anumon V. Divakaran,** and Manohar V Badiger; *Cover Page - Microscopy and Analysis. (2014) 3.*

3. Porous poly(ethyleneglycol)-polyurethane hydrogels as potential biomaterials; **Anumon V. Divakaran,** Arun Torris A. T, Ashish K Lele and Manohar V Badiger; *Polymer International. 64 (2015) 397-404.*

4. Mechanically tunable curcumin incorporated polyurethane hydrogels as potential biomaterial **;** **Anumon V. Divakaran**, Lal B. Azad, Sachin S. Surwase and Manohar V Badiger: *Chemistry of Materials. 2016, 28, 2120−2130.*

5. Product distribution in hydrogenation of styrene oxide over Pd/chitosan catalyst; Maya Viswanadhan . Aparna Potdar . **Anumon Divakaran** Manohar Badiger, Chandrashekhar Rode: *Research on Chemical Intermediates. 2016* (doi: 10.1007/s11164-016-2554-3).

6. Influence of hydrophilic/hydrophobic diols on the properties of polyurethane hydrogels; **Anumon V. Divakaran and Manohar V Badiger:** *(Under preparation).*

7. Eugenol in polyurethane hydrogels: An anti-glycational effect; **Anumon V. Divakaran, Priyanka Singh, Ashok P. Giri and Manohar V. Badiger.** *(Under preparation).*

Conferences

1. One pot synthesis of drug conjugated PEG-PU hydrogels for biomedical application; **V.D. Anumon, L.B. Azad and M.V. Badiger;** *International Conference on Polymeric Biomaterials, Bioengineering & Biodiagnostics,* ***NewDelhi, India 2014.***

2. PEG-PU hydrogels for Drug delivery and Tissue engineering application: Synthesis and Characterization; **V. D. Anumon and M.V.Badiger;** *Proc. 9th International Gel Symposium,* ***Epochal Tsukuba, Ibaraki, Japan, Page 259, 2012.***

3. Design and synthesis of PEG-PU Hydrogels for Drug Delivery and Tissue Engineering; **V. D. Anumon and M.V.Badiger**; *National Science Day Celebrations, National Chemical Laboratory,* ***Pune, Maharashtra, India, 2012.***

3. Synthesis and Characterization of Porous PEG-PU Hydrogels for Tissue Engineering Application; **V.D.Anumon and M.V.Badiger;** *Third International multicomponent Polymer Conference (IMPC),* ***Kottayam, Kerala, India, 2012.***

4. Design and synthesis of PEG-PU Hydrogels for Drug Delivery and Tissue Engineering; **V. D. Anumon and M.V.Badiger;** *APA International Congress on Advances in Human Healthcare Systems,* ***New Delhi, India 2012***.

Colloids and Surfaces A: Physicochem. Eng. Aspects 414 (2012) 296–301

Contents lists available at SciVerse ScienceDirect

Colloids and Surfaces A: Physicochemical and Engineering Aspects

journal homepage: www.elsevier.com/locate/colsurfa

Gold nanoparticle embedded hydrogel matrices as catalysts: Better dispersibility of nanoparticles in the gel matrix upon addition of N-bromosuccinimide leading to increased catalytic efficiency

Vilas Ramtenki[a], V.D. Anumon[b], Manohar V. Badiger[b], B.L.V. Prasad[a,*]

[a] Materials Chemistry Division, National Chemical Laboratory, Dr. HomiBhabha Road, Pune 411008, India
[b] Polymer Science and Engineering Division, National Chemical Laboratory, Dr. HomiBhabha Road, Pune 411008, India

HIGHLIGHTS

- Gold NPs were immobilized on polyethylene glycol-polyurethane (PEGPU) hydrogels.
- Such immobilized NPs can be used as catalysts.
- This is a generic method and can be extended to other metals as well.
- Gold NP catalyzed 4-nitroaniline reduction with $NaBH_4$ was used as the test reaction.
- These catalysts are re-usable with appreciable turnover numbers and frequencies.

GRAPHICAL ABSTRACT

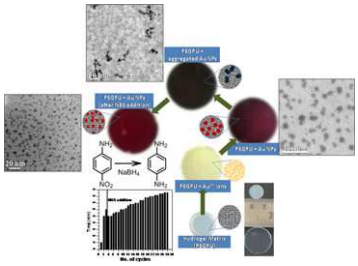

ARTICLE INFO

Article history:
Received 18 April 2012
Received in revised form 2 August 2012
Accepted 15 August 2012
Available online xxx

Keywords:
Nanoparticles
Hydrogels
Immobilization
Catalysis
Turn over numbers

ABSTRACT

A simple and convenient method for generating and immobilizing gold NPs into polyethylene glycol-polyurethane (PEGPU) matrices is presented. The gold NP immobilized PEGPU (Au NP-PEGPU) hydrogel matrices are easy to handle and can be used as catalysts. The efficiency, reusability and durability of the Au NP-PEGPU catalyst matrices were investigated using the reduction of 4-nitroaniline (4NA) to *p*-phenylenediamine (*p-PDA*) by sodium borohydride in the presence of the catalyst as a test reaction. The Au NPs in the PEGPU matrix got aggregated after 3 cycles of catalysis but dispersion could be regenerated by the addition of N-bromosuccinimide (NBS). After this regeneration process the Au NPs-PEGPU matrix showed excellent efficiency without any aggregation, leaching or degradation. The reusability of the catalyst for 28 cycles yielding a total turnover number of 3220 and turn over frequency of 0.152 s^{-1} is demonstrated.

1. Introduction

Nanoparticles (NPs) are being used in a wide range of applications, such as catalysis [1–3], biomedicine [4], sensors [5–7] and optoelectronics [4,8–10], due to their unique electronic properties and high surface to volume ratio. In fact, the catalytic activity of some systems gets enhanced remarkably upon decreasing the NP size. However, issues like aggregation, non-dispersibility of NPs in the desired solvent (especially in aqueous media) are big impediments in the path to realize the full potential of NPs as catalysts. The best way to overcome these barriers is to immobilize them on a support.

Polymer matrices could be the prominent candidates for incorporating such metal NPs, where the well defined spatial

* Corresponding author. Tel.: +91 20 25902013; fax: +91 20 25902636.
E-mail address: pl.bhagavatula@ncl.res.in (B.L.V. Prasad).

0927-7757/$ – see front matter © 2012 Elsevier B.V. All rights reserved.
http://dx.doi.org/10.1016/j.colsurfa.2012.08.026

xradia®

3D X-ray Microscopy for Research and Industry

We congratulate the winners of our 2012 *"Coolest Thing You've Never Seen"* Image Contest!

Non-destructive imaging · Highest resolution · Best contrast · Resolution at a distance

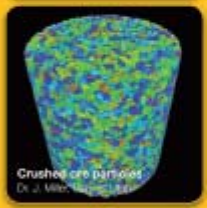

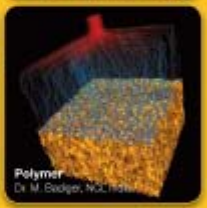

VersaXRM and UltraXRM

Sub-micron and nanoscale 3D X-ray microscopy

Scan this QR code to view the research details for each of these images, or visit **info.xradia.com/XradiaImageContest2012_Top12Winners.html**

Xradia, Inc. 4385 Hopyard Road, Pleasanton, CA 94588
T: +1.925.701.3600 F: +1.925.730.4852 info@xradia.com **www.xradia.com**

Volume 21 Number 2 2013 March

Microscopy TODAY

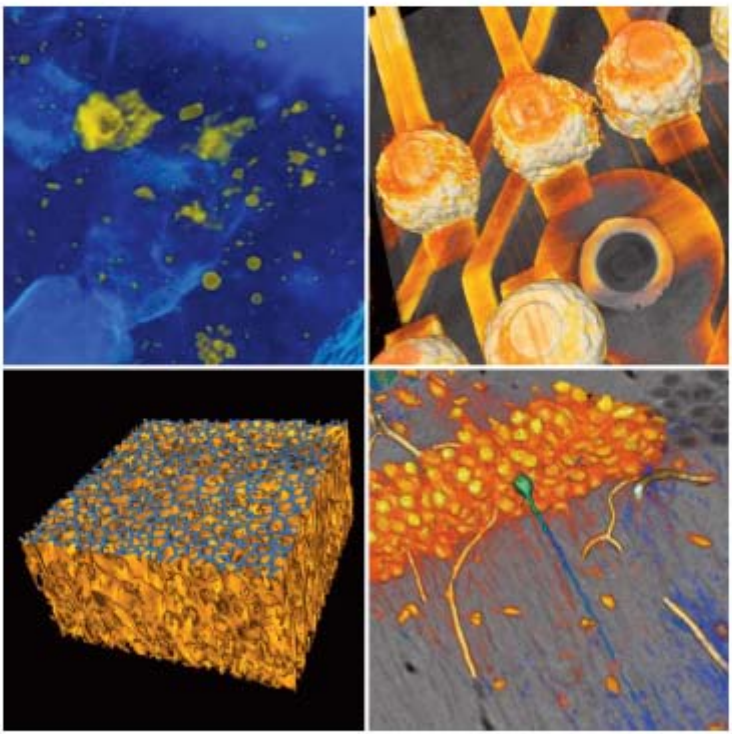

MSA Microscopy Society of America

www.microscopy-today.com

CAMBRIDGE UNIVERSITY PRESS

AMERICAS

MICROSCOPY AND ANALYSIS

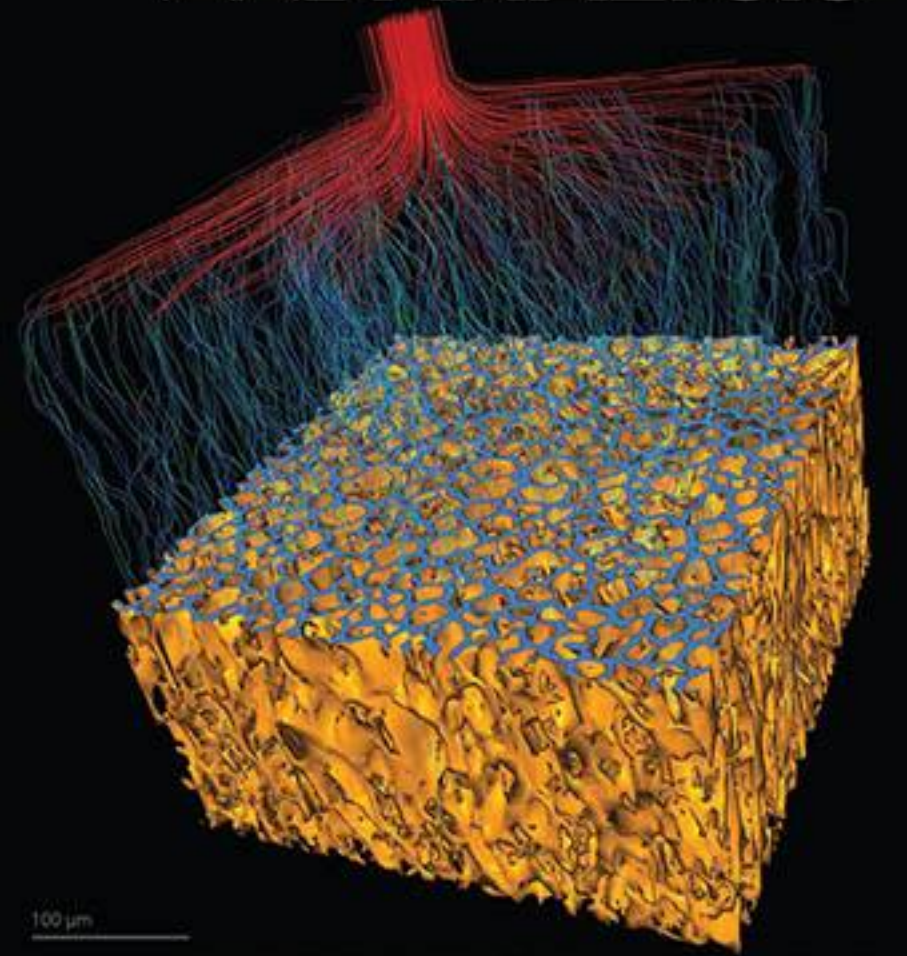

DIRECTORY 2014

Research Article

Received: 6 August 2014 Revised: 00 0000 Accepted article published: 2 September 2014 Published online in Wiley Online Library: 22 September 2014

(wileyonlinelibrary.com) DOI 10.1002/pi.4802

Porous poly(ethylene glycol)–polyurethane hydrogels as potential biomaterials

Anumon V Divakaran, Arun Torris AT, Ashish K Lele and Manohar V Badiger*

Abstract

We report the synthesis of porous poly(ethylene glycol)–polyurethane (PEG-PU) hydrogels using PEG-4000 as a soft segment and 4,4′-methylenebis(cyclohexylisocyanate) as a hard segment. The degree of swelling in the hydrogels could be controlled by varying the amount of crosslinking agent, namely 1,2,6-hexanetriol. Structural characterization of the hydrogels was performed using solid-state ^{13}C NMR and Fourier transform infrared spectroscopy. Wide-angle X-ray diffraction studies revealed the existence of crystalline domains of PEG and small-angle X-ray scattering studies showed the presence of lamellar microstructures. For generating a porous structure in the hydrogels, cryogenic treatment with lyophilization was used. Scanning electron microscopy and three-dimensional micro-computed tomography imaging of the hydrogels indicated the presence of interconnected pores. The mechanical strength of the hydrogels and xerogels was measured using dynamic mechanical analysis. The observed dynamic storage moduli (E') for the equilibrium swollen and dry gels were found to be 0.15 and 4.2 MPa, respectively. Interestingly, the porous PEG-PU xerogel also showed E' of 5.6 MPa indicating a similar mechanical strength upon incorporating porosity into the gel matrix. Finally, preliminary cytocompatibility studies showed the ability of cells to proliferate in the hydrogels. These gels show promise for applications as scaffolds and implants in tissue engineering.

Supporting information may be found in the online version of this article.

Keywords: hydrogels; poly(ethylene glycol); polyurethane; porosity; permeability

INTRODUCTION

Hydrogels have emerged as promising materials for engineering scaffolds and implants because of their biocompatibility, hydrophilicity and similarities to native extracellular matrix.[1–4] However, precise control of hydrogel properties such as porosity remains a challenge. The porosity and the pore architecture play a significant role in cell survival, proliferation and nutrient diffusion to cells.[5,6]

Hydrogels are three-dimensional networks of hydrophilic polymers with high water absorption capacity. Depending on the degree of crosslinking and hydrophilicity of the network, the water content can range from *ca* 20% to thousands of times their dry weight like, for example, in superabsorbent polymers.[7–9] A variety of hydrogels, naturally occurring and synthetic, biodegradable and non-biodegradable, have been used in tissue engineering applications. The naturally occurring hydrogels include collagen[10–12] and collagen–alginate gels.[13] The synthetic hydrogels include poly(glycolic acid) and poly(L-lactic acid) or their composite mixtures.[14] Some non-biodegradable polymers such as polytetrafluoroethylene,[15] polymethacrylate[16] and hydroxyl apatite/Dacron composites[17] have also been studied for tissue engineering applications. An excellent review of natural and synthetic hydrogels for tissue engineering applications is that by Lee and Mooney.[18]

Hydrogels can be chemically crosslinked with covalent bonding or physically crosslinked with non-covalent interactions such as molecular entanglements and/or secondary forces that include ionic, hydrogen-bonding or hydrophobic interactions.[19,20] Most of the hydrogels used or proposed in tissue engineering exhibit weak mechanical strength and are unsuitable for application under load. The fracture energy of typical hydrogels falls in the range 10^{-1}–10^{0} J m^{-2}, which is much smaller than the fracture energy of usual rubbers.[21] Therefore, major research efforts are underway in designing and developing novel hydrogels with improved mechanical properties. These include double network gels,[22] nanocomposite gels,[23] slide ring gels and topological gels.[24] Recently, Sun *et al.*[25] reported highly stretchable and tough hydrogels made by the combination of alginates and polyacrylamides. The toughness was explained by recoverable energy-dissipating mechanisms.

Besides good mechanical strength, the porosity of hydrogels also plays an important role in designing scaffolds and implants for tissue engineering. The scaffold allows cells to enter it, proliferate and secrete their own extracellular matrix, leading to a complete and natural tissue replacement in the long run. The porosity, pore size and pore structure of the scaffold are vital for nutrient supply of cells. Various techniques have been used to fabricate porous scaffolds which include porogen leaching,[26–28] phase separation,[29] emulsion freeze-drying,[30,31] solvent evaporation,[32,33] gas forming,[34] etc. We used cryogenic treatment followed by lyophilization to fabricate scaffolds in our work.

In the present article, we report the synthesis of porous poly(ethylene glycol)–polyurethane (PEG-PU) hydrogels using

* *Correspondence Manohar V. Badiger, Polymer Science and Engineering Division, CSIR – National Chemical Laboratory, Dr Homi Bhabha Road, Pune 411008, India. E-mail: mv.badiger@ncl.res.in*

Polymer Science and Engineering Division, CSIR – National Chemical Laboratory, Dr Homi Bhabha Road, Pune 411008, India

CHEMISTRY OF MATERIALS

Article

pubs.acs.org/cm

Mechanically Tunable Curcumin Incorporated Polyurethane Hydrogels as Potential Biomaterials

Anumon V. Divakaran,[†] Lal B. Azad,[†] Sachin S. Surwase,[‡] Arun Torris A. T.,[†] and Manohar V. Badiger*[,†]

[†]Polymer Science and Engineering Division and [‡]Physical and Material Chemistry Division, CSIR−National Chemical Laboratory, Dr. Homi Bhabha Road, Pune 411008, India

Supporting Information

ABSTRACT: We report here on the one-pot synthesis and characterization of curcumin incorporated polyethylene glycol−polyurethane (PU-CUR) hydrogels using PEG-4000, 4, 4′-methylenebis (cyclohexyl isocyanate), curcumin in the presence of a cross-linker, 1,2,6 hexanetriol (HT). Besides the physical entrapment, curcumin also provides a partial cross-linking in the 3-D structure of the hydrogel. The degree of swelling in hydrogels could be controlled by varying the amount of HT as well as curcumin. The structural characterization of hydrogels was performed using Fourier transform infrared spectroscopy, high-resolution mass spectrometry, UV and fluorescence spectroscopy. The wide-angle X-ray scattering studies revealed the existence of crystalline domains of PEG, and the small-angle X-ray scattering studies showed the presence of lamellar microstructures. Porous structure in the hydrogel was created by cryogenic treatment and lyophilization. Scanning electron microscopy and microcomputed tomography imaging of hydrogels showed the presence of interconnected pores. The mechanical strength of the hydrogels was measured using a universal testing machine. The observed tensile and breaking compression strengths for the equilibrium swollen gels were found to be in the range of 0.22−0.73 MPa and 1.65−4.6 MPa, respectively. Detailed in vitro biological experiments showed the biocompatibility of gels, cytostatic dosage of curcumin, selective toxicity toward cancer cell lines, and antibacterial property. These gels show promising applications as scaffolds and implants in tissue engineering.

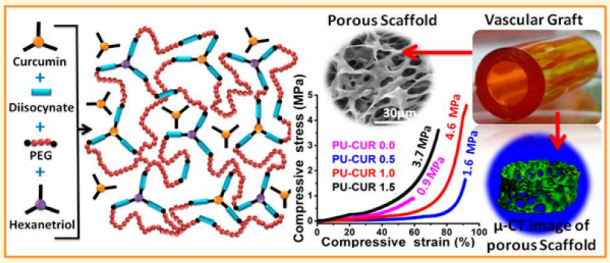

INTRODUCTION

Hydrogels are 3D polymer network structures that are hydrophilic in nature and are capable of absorbing copious amount of water without losing their structural integrity.[1−3] Over the past two decades, hydrogels have received increasing attention from researchers because of their special physicochemical properties such as softness, biocompatibility, stimuli-responsiveness, water permeability, self-healing, etc. They find applications as scaffolds/implants in tissue engineering,[4−6] vehicles for drug delivery,[7,8] synthetic extracellular matrix,[9] sensors,[10] actuators,[11] enzyme immobilization,[12] smart hydrogels,[13] etc. However, a large number of applications of hydrogels are often severely limited by their low mechanical strength due to structural inhomogenity or lack of effective energy dissipation mechanism, and they are unsuitable for applications under load. For example, the fracture energy of a typical hydrogel falls in the range of 0.1−10 J/m^2, which is much smaller than the fracture energy in natural polymers (∼1000 J/m^2) and natural rubber (∼10 000 J/m^2).[14−16] Therefore, major efforts are now devoted to synthesizing hydrogels with improved mechanical properties.[17−22] Novel concepts and strategies that have been developed to make tough hydrogels that are capable of withstanding large deformations include double-network (DN) hydrogel,[23−26] nanocomposite (NC) hydrogels,[27−30] slide-ring hydrogels,[31,32] topological or tetra-PEG (polyethylene glycol) hydrogels,[33−35] etc. In this context, there is a large scope for designing and developing new hydrogels with the combination of good mechanical strength, elongation, and good self-recovery properties. Polyethylene glycol−polyurethane (PEG−PU) based hydrogels represent a class of materials that possess favorable characteristic of PUs along with the ability to mimic soft tissues. In our previous work,[36] we have reported on the porous PEG−PU hydrogels for potential biomedical applications.

In this study, we have incorporated curcumin in the preparation of PU hydrogels. Interestingly the obtained hydrogels showed enhanced mechanical properties in terms of modulus, percent elongation, and recovery. The hydrogels were prepared using PEG-4000 as a soft segment and 4,4′-methylene bis(cyclohexyl isocyanate) (H_{12}MDI) as a hard segment in the presence of a cross-linker, namely 1,2,6-hexanetriol (HT). Curcumin is a 1,7-bis(3-methoxy-4-hydroxy phenyl)-1,6-heptadiene-3,5-diene having a phenolic structure connected by two α,β-unsaturated carbonyl groups. It is well established that curcumin exhibits both antimicrobial and

Received: December 23, 2015
Revised: March 10, 2016
Published: March 10, 2016

DOI: 10.1021/acs.chemmater.5b04964
Chem. Mater. 2016, 28, 2120−2130

Res Chem Intermed
DOI 10.1007/s11164-016-2554-3

Product distribution in hydrogenation of styrene oxide over Pd/chitosan catalyst

Maya Viswanadhan[1] · Aparna Potdar[2] · Anumon Divakaran[1] · Manohar Badiger[1] · Chandrashekhar Rode[2]

Received: 21 December 2015 / Accepted: 18 April 2016

Abstract Palladium-decorated chitosan catalyst was synthesized by an impregnation method by varying the Pd loading in the range of 1–6 %, and was evaluated for the regioselective hydrogenation of styrene oxide. In order to correlate the chemical and textural properties with the catalytic activity, all the prepared catalysts were characterized by techniques such as Fourier transform infrared spectroscopy, X-ray diffraction, scanning electron microscopy, transmission electron spectroscopy, thermo-gravimetric analysis, temperature-programmed desorption of NH_3, and CO_2 and N_2 physisorption. The synthesized catalysts were utilized for the efficient and regioselective ring opening of styrene oxide by hydrogenation under different conditions. The complete conversion of styrene oxide with 65 % selectivity for 2-phenyl ethanol and 33 % for 1-phenyl ethanol were obtained using 4 % Pd/CS catalyst at 70 °C temperature and 3 MPa pressure. The mechanism for the regio selective ring opening of styrene oxide to 1- and 2-phenyl ethanol was also proposed on the basis of properties of the catalyst support, catalytic activity and selectivity. These results indicated that the catalytic activity and selectivity of the catalysts were affected by the nature of support. Further, the basic properties of the support play an important role in the selectivity of the styrene oxide hydrogenation reaction.

Electronic supplementary material The online version of this article (doi:10.1007/s11164-016-2554-3) contains supplementary material, which is available to authorized users.

✉ Chandrashekhar Rode
cv.rode@ncl.res.in

[1] Polymer Science and Engineering Division, CSIR - National Chemical Laboratory, Pune, Maharashtra 411008, India

[2] Chemical Engineering and Process Development Division, CSIR - National Chemical Laboratory, Pune, Maharashtra 411008, India

Published online: 02 May 2016